UNIVERSITY OF CAPE TOWN

MOMENT - ROTATION CHARACTERISTICS OF BOLTED BEAM - TO - COLUMN ALUMINIUM CONNECTIONS

BY: VANDY FRENCH

SUPERVISED BY: PROFESSOR A ZINGONI

DEPARTMENT OF CIVIL ENGINEERING,

UNIVERSITY OF CAPE TOWN

RONDEBOSCH 7701

CAPE TOWN

This thesis is submitted in partial fulfillment of the requirements for the award of the Master of Science Degree in Engineering at the University of Cape Town

September 2009

Declaration

I know the meaning of plagiarism and declare that all the work in this document except that for which intellectual property is acknowledged and referenced accordingly is mine.

Acknowledgement

I would like to register my deep appreciation and profound gratitude to the Department of Civil Engineering, University of Cape Town for the financial and moral support rendered to me in the pursuit of my academic goals.

The guidance, advice and motivation rendered by my supervisor Professor Alphose Zingoni proved invaluable and I am greatly honored to have worked with you and benefit from your vast experience.

To the staff and colleagues at the Department of Civil Engineering for your friendship and encouragement throughout my postgraduate program, I am most grateful.

To Mr. Munda Rogers and Mr. Abdul Bairoh, you are truly a beacon of strength.

The National Research Fund and the Chancellors Challenge Fund proved to be quite a godsend without which this work would have been impossible.

To my family and especially my wife Bernadette and Daughters Nyambe and Nyanda, you are the driving force in my life. Thoughts of you always lifts my spirit.

ABSTRACT

Structural aluminum provides a unique option to engineers by virtue of both its unique strength to weight ratio and its well known corrosion resistance properties. The development of the Eurocode 9 provides an insight to the design of aluminum structures based on results from various researchers worldwide. However the area of connections remains very sparse with regards to research material as compared to steel as provided by Eurocode 3 part 1-8. This work involves the analysis of the performance of aluminum end plate beam – column connections with regards moment rotation behavior as well as the main connection classification criteria, strength, stiffness and ductility. A parametric study is done with the use of the non- linear finite elements program ADINA in which the effects of connection geometry is observed under incremental loading.

LIST OF FIGURES

LIST OF TABLES

Table of Contents

CHAPTER 1

INTRODUCTION

1.1 Background

Aluminum has not been widely used as a structural material in the construction industry when compared to steel. The need for further research in this domain is vital as it possesses certain unique qualities which can render it useful in certain design requirements by virtue of its properties.

1.2 Applications of Structural Aluminum

Aluminum has found use in the design and fabrication of non- structural finishes e.g. windows, doors and guard rails, but is yet to be adopted as a dominant structural material in the construction industry except for special cases. This becomes evident when comparing existing Aluminum codes to steel design codes with regards to details. Of interest in this material is the Eurocode 3, Part 1-8 (The Design of Joints) {16} which deals with steel joints quite extensively whereas the Eurocode 9 (Design of Aluminum Structures) {15} does not provide as much detail on the subject. Notwithstanding, aluminum members have been utilized as structural components of temporary structures for specified purposes taking into consideration the relative light weight of this metal and the resulting ease of transportation and erection costs. Frames specially fabricated with aluminum alloys have found application as scaffolding for easy erection and dismantling of soffit support for the casting of reinforced concrete slabs due to its light weight and therefore simple erection procedures. Aluminum alloys have also been useful in the construction of temporary bridges on diversion works across rivers in highway construction projects where it is desirable for a sustained flow of traffic to be maintained or where inaccessibility makes it cumbersome for the transportation of vital assembly components. An example of this is the access bridge at Knockquhassen, Stranraer, Scotland (1992) as cited by (F.M. Mazzolani 1995) {13}. The advantage of its comparatively light weight can again be made use of to release the pressure on hoisting equipment and even airlifting to allow for a relatively simple erection process. Due to the fact that structural steel is comparatively much more susceptible to corrosion especially

in the marine environment where it is rendered exposed to relatively high concentrations of chlorides, aluminum alloys have been found to be of superior long term cost effectiveness in the construction of various types of structures in the marine environment with minimal maintenance costs associated with corrosion protection. Helli-decks, platforms and various structures on offshore oil rigs Fig 1.1 are sometimes constructed with aluminum to take advantage of the relative corrosion resistance of the metal when compared to steel.

Fig 1.1: Aluminum Helli deck under Construction on Off Shore Facility {28}

The retrofitting of structures has gained prominence as a vital component of increasing service life where loss of structural integrity is experienced either due to ageing or natural disasters such as seismic activities. However Aluminum superstructures have been proven to be of great advantage in replacing concrete or steel during retrofitting especially when loss of sub structural integrity demands reduced dead loads. The Corbin Suspension bridge in Huntingdon Pennsylvania is an example of such Fig 1.2.

Fig 1.2: Aluminum Bridge Deck, Corbin Bridge Huntingdon, Pa. {29}

1.3 Properties of Aluminum

Aluminum constitutes about 8% of the earth's crust, the principle ore from which it is obtained being bauxite {17}. It has a weight of 2700Kg/m^3 compared to 7800 Kg/m^3 for steel and a Young's Modulus E of 69000Mpa {17} which accounts for about a third of that of steel 210000Mpa and as such various alloys of aluminum have been utilized in the construction of ships superstructure and aircraft shells taking advantage of this unique strength to weight characteristic. The stress strain idealization of aluminum is often generated using the Ramberg-Osgood relationship which captures the material behavior quite accurately.

The thermal expansion of aluminum is twice the value of steel and therefore due consideration must be made in this regard where seasonal variation in temperature are substantial. The alloying of aluminum develops added strength to the metal although this could result in reduced corrosive resistance. An idea of the design requirements and actual conditions of exposure is necessary in selecting a suitable alloy for the design of structural elements. There is a tendency of welded aluminum joints to experience reduced strength from the original material due to compression and tension stresses developed in the heat affected zone (HAZ). The high ductility and low shear strength of aluminum has prompted researchers to investigate and discover substantial energy dissipation characteristics in aluminum stiffened shear panels which have been adopted in various designs for enhanced seismic protection{18}. Table 1.1 shows the series of alloys.

Alloy Series (code)	**Main Alloying Constituents**
1xxx	≥ 99% of Aluminium
2xxx	Copper
3xxx	Manganese
4xxx	Silicon
5xxx	Magnesium
6xxx	Magnesium and Silicon
7xxx	Zinc , Magnesium and /or Copper

Table 1.1: Major Constituent Elements for Aluminum Alloys

The variation of mechanical properties with the alloy type and treatment procedure can be so wide ranging that it is crucial for the end use to be properly verified to match the material properties so that the correct alloy is chosen to good effects. Up to 500Mpa tensile strength can be attained with the 7000 series (AlZnMgCu). They are however characterized by reduced corrosion resistance and weld ability. The same alloy series with reduced copper percentage (ALZnMg) records strengths of 200Mpa with good corrosion resistance and self tempering properties which render post weld strengths nearly equal to the original tensile strength close to the HAZ. Aluminum alloys tend to increase in strength and ductility when subjected to sub zero temperature conditions unlike steel which becomes brittle under these same conditions.

The 6082 alloy is selected for this work due to its known high strength and suitability for use in the construction of load carrying structures and bolted connections {13}. It is also quite suitable for anodizing to attain enhanced corrosion resistance especially in marine environments. The principle constituents of the 6082 alloy are magnesium and silicon. Other trace elements are as seen in the percentages given in Table1.2. The tensile strength of the 6082 alloy however decreases at temperatures above 100 C. Therefore care must be taken to avoid these conditions or on the contrary, adequate design considerations taken into account.

Alloy	***Percentages***								**Other**	
	Si	**Fe**	**Cu**	**Mn**	**Mg**	**Cr**	**Zn**	**Ti**	**Each**	**Total**
6082	0.7 – 1.3	0.5	0.10	0.4 – 1.0	0.6 – 1.0	0.25	0.2	0.1	0.05	0.15

Table 1.2: Element Composition of 6082 Aluminum Alloy

1.4 Methodology

With the emergence of aluminum in the construction industry and its inclusion into the Eurocodes {15} and the American Standards {19}, it is but fitting that the necessary attention is focused on its connections as this forms a vital component of structural assemblies and frames.

The main thrust of the research is to study the effects of geometry on the behavior and failure patterns of a selected parametric array of connections. Models are developed with the use of FEM software package ADINA to predict the dominant failure mode due to incremental loading. Modeling involves the setting up of class 2 beam to column cantilever assemblages with the column restrained at the top and bottom ends and chosen with substantial stiffness relative to the beam so that minimal rotation is observed at the column flanges and web at the point of connection through web panel shear and flange buckling. The assemblages are connected with a combination of different jointing techniques including extended end plates and flush end plates combined with steel and aluminum bolts. Loading is positioned at the tip of the cantilever beam and rotation observed for each load step whilst the connection is observed for any evidence of distress. The welds in these assemblies are not modeled, however the relevant HAZ's are monitored during loading. The rotational restraints offered by these connections are monitored whilst areas of high stress and strain are observed for failure. The ductility, strength and stiffness are monitored and compared with existing joint classification systems to see how the different variables affect overall connection performance The results are analyzed with reference to the relevant design codes and conclusions forwarded.

1.5 Plan of Development

Chapter One (Introduction) deals with introductory material with regards Aluminum and provides a general outline of the research with the objective and plan of action of the work laid out clearly.

Chapter Two (Literature Review) provides information and references of previous work on bolted steel and aluminum joints, and some joint classification systems. Some Fatigue

and seismic considerations investigated so far are discussed. Information on design criteria and calculations associated with the design of bolted connections are also provided with reference to associated research work.

Chapter Three (Finite Element Modeling) reviews the framework of the software utilized in this work ADINA, and outlines the techniques used in generating the models in terms of geometry, mesh generation and contact algorithm amongst others.

Chapter Four (Finite Element Model Validation) describes details of Finite Element calibration models used to validate the authenticity of the modeling technique utilized in this work based on previous experiments by other researchers.

Chapter Five (Numerical Modeling Results) provides results obtained from Finite Element Modeling.

Chapter Six (Discussion of Results) involves the analysis of the data obtained from the modeling results and provides an insight to failure modes and individual connection component responses under loading.

Chapter Seven (Conclusions and Recommendations) summarizes the conclusions and recommendations on data made available by the finite element analysis results and provides a classification of investigated parameters.

CHAPTER 2

LITERATURE REVIEW

2.1 Significance of Beam - Column Connections on Structures

Connections are a significant component of framed structures and they represent the means by which various structural elements are assembled. The strength, stiffness and ductility of joints have a direct consequence on the way a framed structure will behave. Furthermore, the relative stiffness of connections is a fundamental determinant as to how the internal forces and moments on adjacent members of the frame are distributed. It is therefore important that connections are better understood and that continuous research is focused on this area. The behavior of steel bolted connections has received a lot of attention from researchers all over the world with a lot of progress being made towards the understanding of the characteristics of various jointing techniques utilized in the construction industry. Not much attention has been focused on the behavior of aluminum connections. Knowledge derived from such investigations can be used to provide the necessary confidence in the use of aluminum as a structural material. Conservative frame analyses methods normally assume that connections are either fixed or pinned. However the real behavior lies between these two conditions. It is thus useful that more accurate analysis of joints is established to facilitate estimates of frame behavior that agrees well with actual conditions on the structure and reduce cost. The importance of joints on framed structures cannot be underestimated as connections with insufficient strength and rigidity can cause a structure with even the most robust elements to fail prematurely under service loads. Limited information is available in the aluminum connections area, as such, the review will dwell largely on studies carried out on steel connections and with a view to assess the performance of these jointing techniques on aluminum end plate connections. Research work done on bolted aluminum lap joints to investigate the fatigue, bolt tightening effects and bearing strength represents to a large extent , the scope of investigations done on aluminum connections to date. These will also be discussed widely.

2.2 Implications of Connection Geometry on Bolted Beam-Column Connection Performance

2.2.1 Simple Connections

Simple connections are generally characterized by low stiffness's and substantial rotation capacities. Moment rotation curves depicting the various boundaries for simple, semi rigid and rigid connections have been developed by various researchers in establishing classification systems for beam to column joints {1}{2}. These connection types have been deemed to match closely with design analysis of frames with joints designated and analyzed to be pinned. Some common varieties of fabricated simple connections include the following;

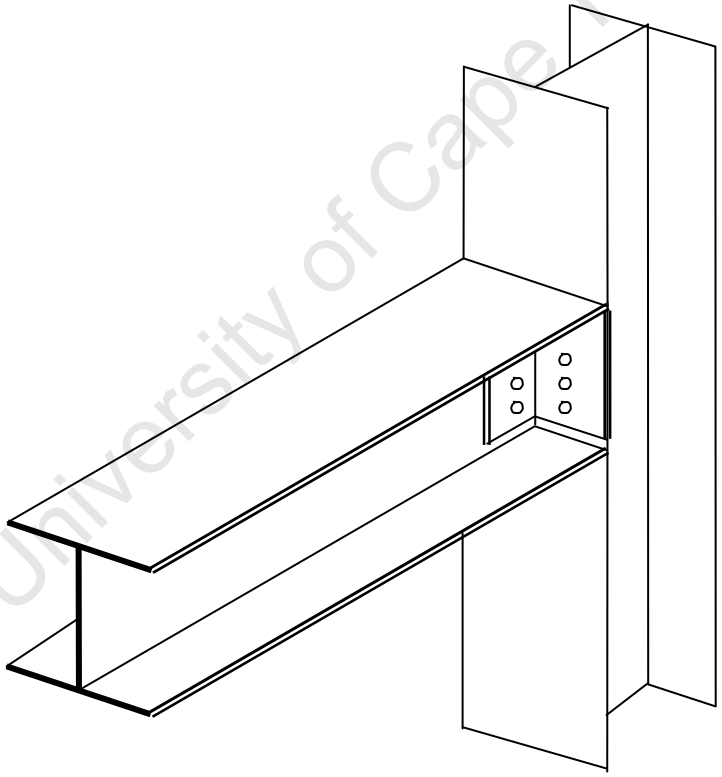

Fig 2.1: Double Angle Cleats

Double angle cleats are basically angles connected to supported beam webs by means of bolts in assembly workshops as shown in Fig 2.1. These beam assemblies are then transported to site and bolted on to columns through prepared clearance holes corresponding to those on the angle cleats. They generally lack the strength of end plate

connections of similar nature and joint slip and angle deformation are the principal determinants of the rotational capacity {3}. Double Angle Cleats offer negligible moment capacities. To optimize the characteristics as simple joints, angle cleat thickness should be as small as possible whilst bolt gauges must be kept high.

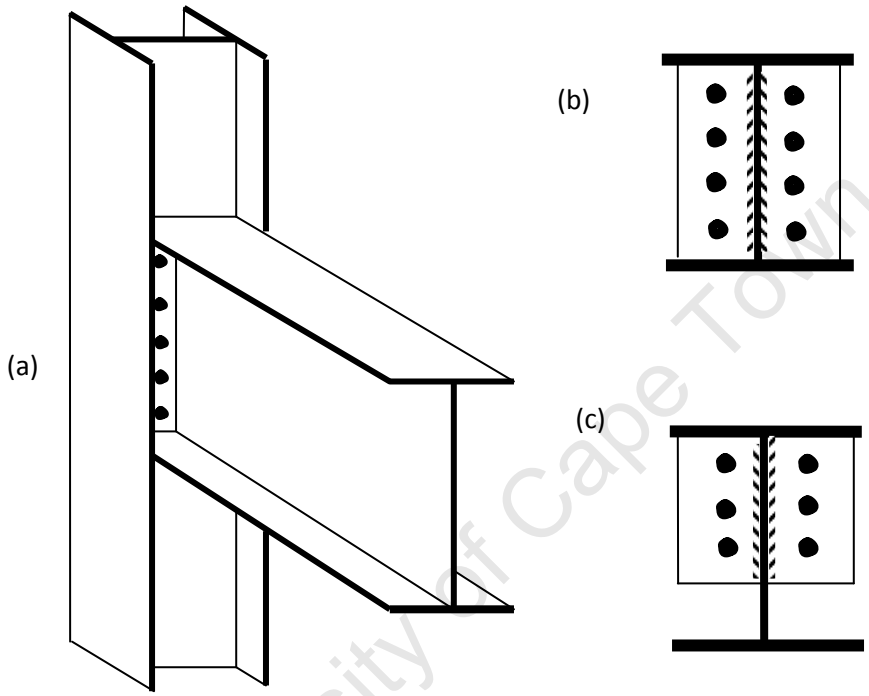

Fig 2.2: Flexible End Plate

Flexible end plates generally consist of end plates welded to the ends of supported beams as preparation at a work shop with fitted pre bored bolt holes as seen on Fig 2.2(a). The assembly is then taken to site and hoisted into position and bolted in place. There are two types of flexible end plate connections and these described as follows.

Partial depth end plates are assembled as seen on Fig 2.2(c) and are normally welded using 6, 8 or 10mm plates. The plate is welded to the web of the supported beam only, whilst the flanges and top parts of the end plates are avoided completely {3}.There is a tendency for some amount of curvature to be experienced on the end plate during welding especially when using thinner plates. However this anomaly is normally corrected after erection and tightening of the end plate assembly to the column by bolting.

Full depth end plates are those that extend the entire depth of the beam as shown on Fig 2.2(b). The plates are welded to the flange of the beam and in some instances this may render the joint to be less flexible than required for design purposes which will move it further to the semi rigid or rigid category. In these instances, care must be taken to ensure that the thickness of the plates utilized is kept to a minimum to ensure that the shear capacity of the joint is less than that of the beam and adequate joint flexibility is thereby preserved.

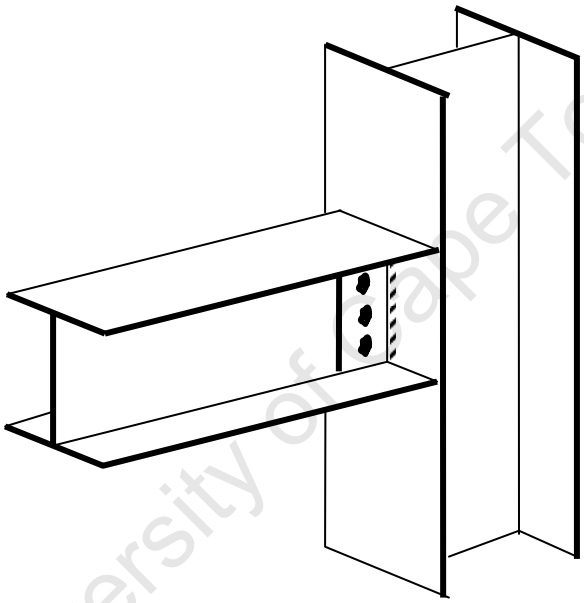

Fig 2.3: Fin Plate Connection

Fin plates are connection arrangements with plates welded on to the supporting column with prepared bolt holes in place. The supporting beam is then hoisted in place and the welded fin plates are bolted on to the web of the beam as shown in Fig 2.3. Its main advantage lies in the fact that it can accommodate connections on opposite sides of a column minor axis quite conveniently without the problem of shared bolts. The rotation is offered primarily by bolt-hole deformation on the fin plate or on the web of the supported beam. Rotation can also result from the shear deformation experienced by the bolts themselves {3}. In instances where it is desirous for the beam to frame into the web of the supporting column , great difficulty is experienced with securing access to the bolt holes for tightening with spanners. This may tempt the designer to increase the length of

the fin plate. However, if adequate calculations and design cannot justify this, it is best avoided.

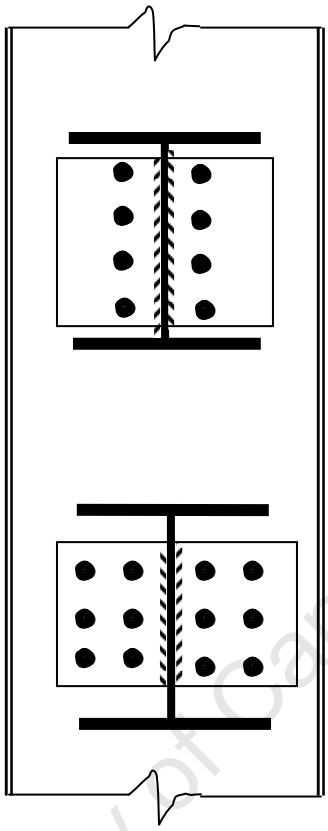

Fig 2.4: Header Plate Connection

Header plate connections comprise of plates welded on to either side of the web of the supported beam as shown on Fig 2.4. The assembly is then bolted on to the supporting column {4}. If the supported member is a beam then it is worthwhile to note that the supporting beam must not be as deep as the supported beam or else top and bottom notches will have to be introduced to allow for the necessary clearance.

2.2.2 Moment Resistant Connections

Moment connections are characterized by rigid connections with minimal rotational capacities and high strengths .In the past, they have been designed primarily to have high strengths with minimal consideration for other parameters. There is currently an understanding that stiffness and ductility are worthy of serious consideration as well {6}. The rotational stiffness and rotational capacity of moment connections are very important

to consider, as the capability to withstand inherent bending moment, shear force and axial forces alone are not always adequate in analysis and design with respect to actual performance{1}{6}. Moment connections and indeed all joints are classified largely by the moment rotation characteristics that they exhibit when subject to loads. Various graphs of Moment versus rotation have been developed to depict the boundaries between different classes of joints {1} {2}. A few examples of moment connections are figs 2.5 & 2.6

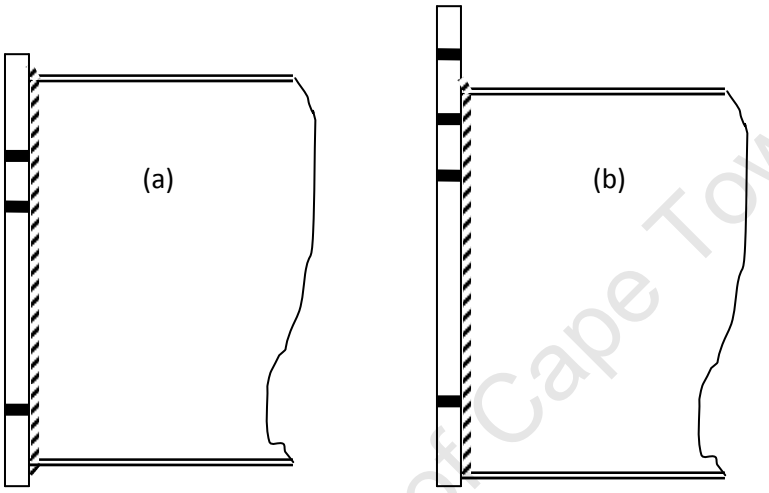

Fig 2.5: Bolted Flush (a) and One Way Extended End Plate Connection (b) {6}

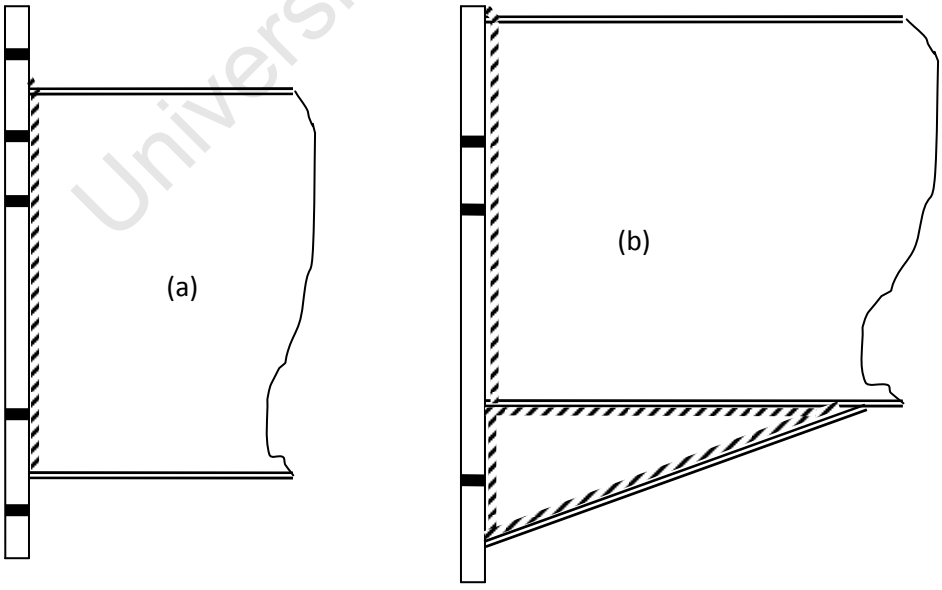

Fig 2.6: End Plate Extended Both Ways (a), End Plate with Mini Haunch (b) {6}

The fabrication of bolted end plate connections takes different forms depending on the objective of the designer. Bolted end plate connections are built with plates welded on to the flange and web of the supported beam .The end plates are then drilled to create bolt holes and bolted on to the supporting column. The mechanism by which these joints operate is such that the bolt tension and compression force at the bottom flange form couples which provide the resisting moment to the applied force on the member. As such the bolts at the top most part of the end plate experience the largest tensile force whereas those closer to the bottom offer the lowest. The centre of rotation is usually very close and most times assumed to be at the centre of the bottom flange of the supported beam. The selection of the various connected members of a moment resistant connection must be done with great consideration to avoid the need for strengthening of the column for additional web shear resistance which in almost all cases can prove expensive. If however this cannot be avoided sufficient measures must be taken to increase the shear capacity of the column web to prevent premature failure. Fig 2.5 shows flush and extended end plate connections. Flush end plate connections are usually built with the end plate terminating at the compression and tension flanges of the beam respectively fig 2.5(a). However, for a more robust weld to be created on the flanges, the plate is usually extended by a few more millimeters to accommodate welds on the outside of the flanges as well. In instances where the additional moment capacity is required, an additional row of bolts is inserted above the tension flange of the beam on an extended portion of the end plate to augment the bolts in tension fig 2.5(b). End Plate connections extended both ways Fig 2.6 (a) provides scope for additional rows of bolts to be placed both above and below the tension and compression flanges of the beam thereby increasing the shear capacity by the combined shear capacity of the bolts and bolt holes. In instances were the end plate needs to be further stiffened if design calculations reveal that it will attain its plastic moment capacity prematurely, the introduction of stiffeners as shown in fig 2.6 (b) serves to improve on moment connection performance whilst also curtailing the rotational capacity of the system. This system is used mostly where it is desirous to attain the full moment capacity of the connected beam.

There is very little information on aluminum beam to column connections. However the behavior of steel beam to column connections has received a lot of attention over the

years. Kulak et al 1997 {22}, Krishnamurthy N, (1978) {23} are among a host of research material that formed the basis of the AISC design codes {24} at the time. The idealization of the tension part of the steel connection as T-stubs has received a lot of attention depicting the failure modes and factors influencing their behavior (Zoetemeijer P, 1974). This idealization has also been investigated using aluminum T-stubs which will be discussed as well {18}. One of the more recent materials available is the work done on steel connections by S.M Coelho et al.

2.2.3 Research by A. M. Coelho et al

Due to the fact that deformation demands on material are particularly high at connections, the need to investigate the performance of high strength materials on bolted connections prompted this research by (A. M. Coelho et al 2007) with an emphasis on end plate bolts located at the tension area of the connection. Geometry, end plate thickness to bolt diameter ratio, end plate and bolt ductility, plate to bolt resistance ratio and weld quality have been mentioned in some previous research by (R. Zandonini et al 1988) and (P. Zoetermeijer 1990) as cited by (A. M. Coelho et al 2007) as principal factors influencing the failure mechanism of such assemblages.

Combinations of seven flush (F1EP & F2EP) and extended end plate connections (EEP) with different plate thicknesses and bolt specifications where investigated with the combination as seen on Table 2.1.

	Column		**Beam**		**E/Plate**		**Bolt**	
	Section	Grade	Section	Grade	$t_{ep}(mm)$	Grade	$\emptyset_b(mm)$	Grade
F1EP_15_2	HE300M	S355	HE320A	S355	14.75	S690	24	12.9
F2EP_15_2	HE300M	S355	HE320A	S355	14.64	S690	24	12.9
EEP_15_2	HE300M	S355	HE320A	S355	14.62	S690	24	12.9
F1EP_10_2	HE300M	S355	HE320A	S355	10.15	S690	24	12.9
F2EP_10_2	HE300M	S355	HE320A	S355	10.25	S690	24	12.9
EEP_10_2a	HE300M	S355	HE320A	S355	10.10	S690	24	12.9
EEP_10_2b	HE300M	S355	HE320A	S355	10.10	S690	24	8.8

Table 2.1 Test Specimen Details {14}

Columns of HE300M were selected with HE320A beams to ensure near rigid behavior of the columns. The (F2EP) specimens were welded in a manner designed on the assumption that outer welds between the beam flange and end plate transfers no load which lead to the increase of the force carried by the inner weld by a factor to account for the eccentricities of forces on both the flange and the weld.

The geometry of the beam – column assemblage connection as tested is seen in fig 2.7. Equipment and instrumentation set up was designed to take readings on Load, Deflection of beam, End plate displacement, strains and Bolt deformations. The beam rotation was calculated through readings from LVDT by the relations eqs 2.1-2.3.

$$\theta_b = \arctan\left(\frac{\delta_{DT1} - \delta_{DT4} - \delta_{b.el(DT1)}}{1150}\right) \ldots\ldots\ldots eq\ 2.1$$

or

$$\theta_b = \arctan\left(\frac{\delta_{DT2} - \delta_{DT4} - \delta_{b.el(DT2)}}{1150}\right) \ldots\ldots\ldots eq\ 2.2)$$

Where

δ_{DTi}= Vertical displacement

$\delta_{b.el(DTi)}$=Beam elastic deflection given by

$$\delta_{b.el(DTi)} = -\frac{P}{E_b I_b}\left(\frac{x_{DTi}^3}{6} - \frac{L_{load} x_{DTi}^2}{2}\right) \ldots\ldots\ldots 2.3$$

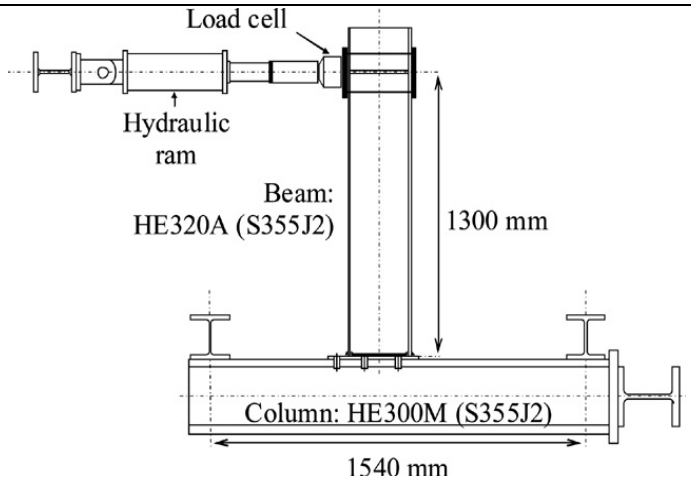

Fig 2.7 Assembly Setup {14}

Some of the conclusions drawn from the results showed that thicker end plates lead to increased moment resistance, initial stiffness and reduced rotation capacity. It was also found that the 12.9 bolts exhibited low ductility thus failed with brittle fracture with low plastic deformation under increased rotation. Bolt failure typified the collapse mode of the 15mm End plate through tensile fracture. In the case of the 10mm End Plates, cracks were observed close to the inner welds for the flush plate whilst the tension flange developed cracks on the extended endplate connection.

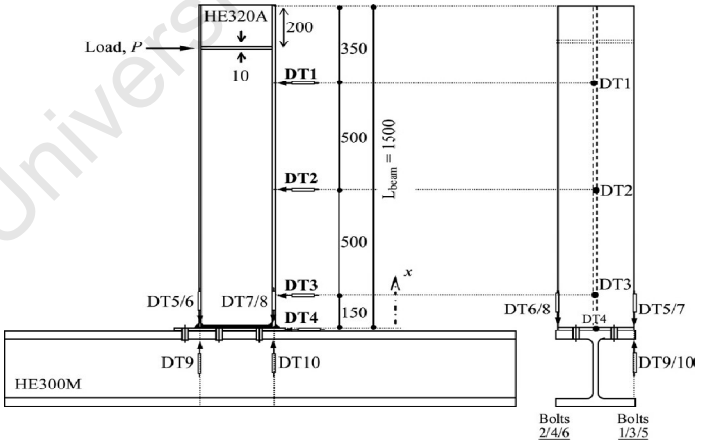

Fig 2.8 Transducer Locations {14}

2.3 Joint Classification Systems

Various classification systems have been proposed aimed at predicting the behavior of beam to column connections. Most simple frame analysis methods classify joints as either fixed or pinned. However in most cases connections demonstrate a semi rigid performance which lies between rigid and flexible configurations. This renders the analysis of connections as pinned or fixed somewhat conservative in some cases, thereby warranting the need for investigations into this particular aspect of connection behavior. Some already existing classification systems highlight a combination of joint stiffness, ductility and strength as their main classification criteria {1}{2}{15}{16}. (Y. Goto et al 1995/1998) examined the boundary between the rigid and semi rigid connections in comparison with the provisions of the Eurocode 3. (R. Hasan et al 1998) developed non linear classification model in terms of a three parameter moment rotation model including initial stiffness, ultimate moment capacity and a shape parameter. The following highlights some of the classification systems used in beam to column connections starting with that proposed in the aluminum code Eurocode 9 {15}.

2.3.1 Joint Classification System According to Eurocode 9 (Design of Aluminum Structures)

The classification of connections according to Eurocode 9 is for a match to be attained between the analysis and structural design of the various elements of the connection. Connection geometry and type should be able to provide results comparable to assumed design assumptions. Their ability to match the structural properties, (rigidity, strength and ductility) of the adjacent members provides a guide as to their categorization which is given as fully connected and partially connected with respect to the connected members' global behavior .

In terms of single behavior, they can also be classified with regards to Rigidity, Strength and Ductility.

In Fully Restoring Connections, the elastic rigidity, ultimate strength and ductility either match or are higher than that of the connected member with the force displacement curve lying above that of the connected member. In these connection categories, the system

behaves as if integrated and the effects of the connection are minimal and therefore ignored.

In Partially Restoring Connections, the elastic rigidity, ultimate strength and ductility of the connection do not match that of the connected member and therefore the force displacement diagram will partly fall below the curve of the member. In these instances the effects of the joints are not to be discarded as their behavior has an influence on the way the structure should be analyzed. Fig 2.9 shows the curves of connection/member behavior.

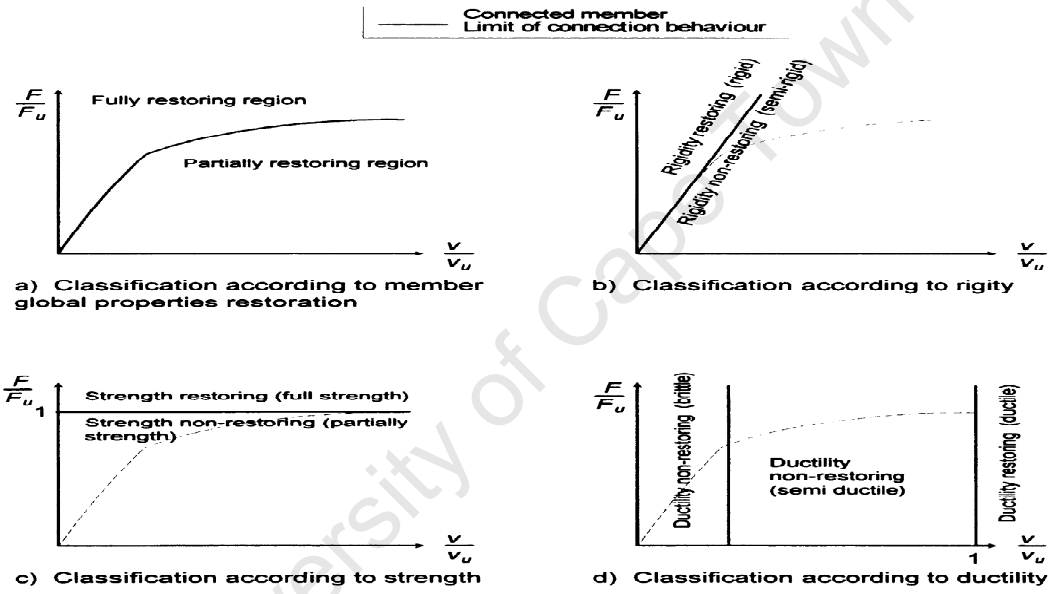

Fig 2.9 Eurocode 9 Classification of Connections{15}

Connections are classified with respect to rigidity as (Rigid) Rigidity restoring connections or (Semi-Rigid) Rigidity Non- restoring connections. These depend on the ability of the connection to restore the initial stiffness of the connected member notwithstanding strength and ductility.

Connections are classified with respect to strength as (Full Strength) Strength restoring connections or (Partial Strength) Strength Non restoring connections. The ability to

achieve the ultimate strength of the connected member regardless of the ductility and rigidity parameters is considered.

Connections are classified with respect to Ductility as (Ductile) Ductility restoring connections or (Semi Ductile or Brittle) Ductility non restoring connections.

Combination of the different scenarios leads to different practical cases as seen on Fig 2.10.

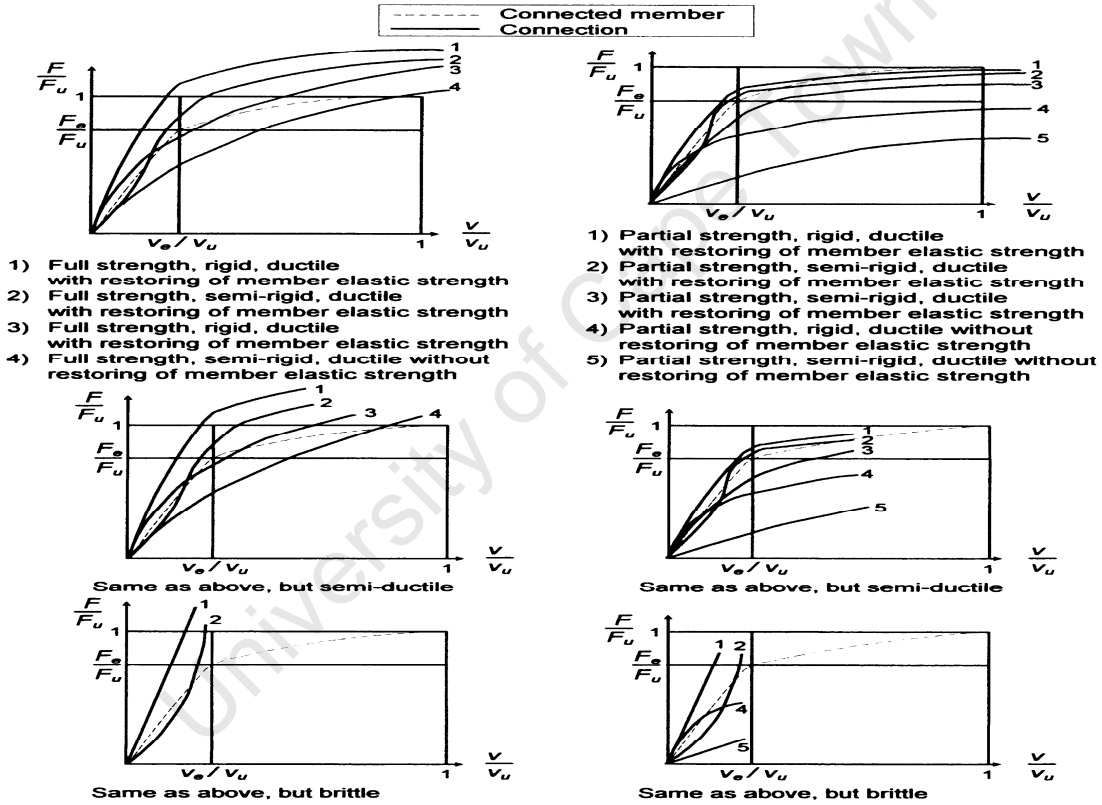

Fig 2.10 Practical cases of Connection Behavior EC 9{15}

Frame structure connections are categorized as nominally pinned and built in connections. Nominally pinned connections generally allow axial and shear loads to be transmitted whilst bending moments are rendered insignificant. The required rotation to

allow full plastic hinge to develop on the member must be satisfied. Built in members allow both axial and shear forces to be transmitted alongside bending moments as well.

2.3.2 Joint Classification System by Bjorhovde et al

Bjorhovde et al 1990 developed a non dimensional classification system taking note of strength, stiffness and ductility criteria. The system takes into account the relationship between reference lengths for beam elements and connection systems. The various rotational and beam slope responses under loading are grouped into semi rigid, rigid and flexible categories depicting their flexural behavior. Fig 2.11 is an illustration of the classification system with the M - Ǿ curves linearized into the three main categories.

Where the x and y axes are represented by eqs 2.4-2.6

$$\overline{M} = \frac{M}{M_p} \dots\dots eq\ 2.4 \qquad \overline{\emptyset} = \frac{\emptyset}{\emptyset_p} \dots\dots eq\ 2.5 \qquad \emptyset_p = \frac{M_p}{EI/_{5d}} \dots\dots eq\ 2.6$$

Reference lengths were identified that provide the initial stiffness's of the member that match the connection stiffness. For the rigid, semi-rigid and flexible connections these are given as 2d, 5d and 10d respectively where d represents the depth of the beam. On the basis of data sets evaluation by (Kishi and Chen 1986), Bjorhovde et al {1} provided the boundary between rigid and semi rigid connections to be 2d and that between semi rigid and flexible to be 10d.

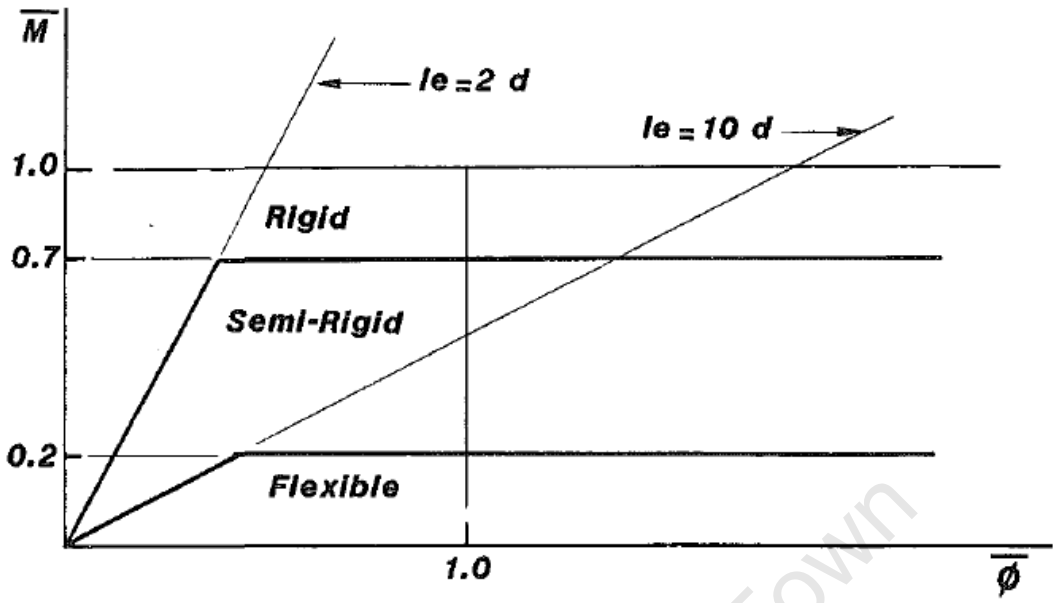

Fig 2.11 Bjohovde Classification of Connections {1}

With regards the ultimate strength classification criterion, values of $0.2M_p$ and $0.7M_p$ were deduced to be the relevant boundaries for the flexible to semi rigid range and the semi rigid to rigid range respectively as illustrated in Fig 2.11.

Bjohovde et al {1} presented the non dimensional ductility of the connection as directly proportional to the ratio of M_u to M_p and inversely proportional to the connections initial stiffness.

2.3.3 Joint Classification System by Nethercot et al

A classification system was developed by Nethercot et al 1998 which took the stiffness and the strength of beam to column connections into consideration simultaneously. It categorized connections based on this system into fully connected, partially connected, pin connected and non structural connections. He characterized these categories as in the case of the fully connected connections to have high strength and stiffness, partially connected connections to have reasonable strength and stiffness and pin connected connections to have low strength and stiffness. Those that fail to embrace the above characteristics were placed in the non structural category. The justification for this classification system among others was based on the EC 3 and the Bjohovde {1} classification systems being not always compatible with results from conventional

pinned and rigid frame analysis calculations for connections classified as rigid and pinned respectively in these two systems.

The Nethercot classification system took consideration of both serviceability and ultimate limit states for the various connection categories for which the single span sub frame shown in Fig 2.12 was used as the reference structure. The ultimate limit state part of the classification system is discussed in the following.

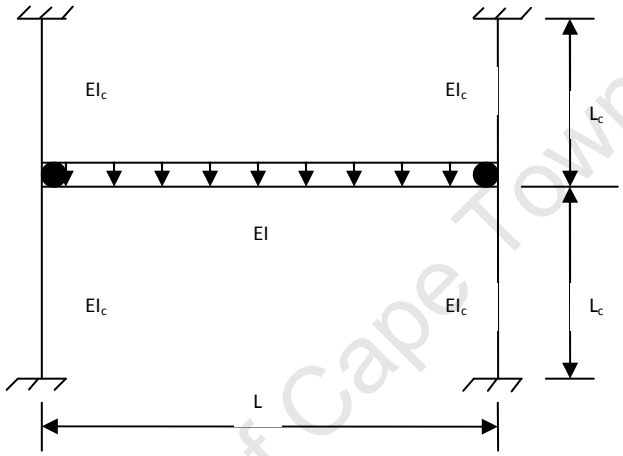

Fig 2.12 Single Span Sub frame from {2}

The criteria for the connection in the Fully Connected category require that the moment capacity of the connection should be greater than or equal to that of the connected beam moment capacity, and that the stiffness of the connection should be high enough to enable the connection to develop full moment capacity. For this the connection stiffness must not be less than K given as follows eq 2.7.

$$K = \frac{38\alpha}{(2+\alpha)}\frac{EI_b}{L_b} \ldots\ldots\ldots eq\ 2.7$$

Where α *and* K_c are given by eq 2.8 - 2.9;

$$\alpha = \frac{K_c}{EI/_L} \ldots\ldots\ldots eq\ 2.8$$

$$K_c = \frac{8EI_c}{L_c} \ldots\ldots\ldots eq\ 2.9$$

The classification of connections into the Pinned category by Nethercot et al is based on the assumption that the stiffness and the moment capacity of the connection should be less than 25% of that calculated with the frame connections assumed to be rigid by conventional frame analysis. With this analysis the connection stiffness must not exceed K Given by eq 2.10;

$$K = \frac{0.67\alpha}{(2+\alpha)} \frac{EI_b}{L_b} \ldots\ldots\ldots eq\ 2.10$$

This will only hold if the connection has sufficient rotation capacity with the given stiffness to be able to fulfill this classification requirement. Thus the rotation capacity must not be less than $\Theta_{r,pin}$ for the connection to fulfill the requirements where $\Theta_{r,pin}$ is given by eq 2.11;

$$\Theta_{r,pin=} \left[0.344 + 0.561 \left[\frac{M_{d,b} - M_{y,b}}{M_{p,b} - M_{y,b}}\right]^2\right] \frac{M_{d,b}L}{EI} \ldots\ldots\ldots eq\ 2.11$$

Where

$M_{d,b}$ is the design moment of the span

$M_{y,b}$ is the yield moment capacity of the beam

$M_{p,b}$ is the ultimate moment capacity of the beam span.

Connections in the Partially Connected Connections Category represent those that fail to fulfill the requirements of the above two but have substantial rotation capacity to qualify them to be classified in the partially connected category. The required minimum rotation $\Theta_{r,pin}$ in this case is given by eq 2.12;

$$\Theta_{r,pin=}\left[0.344+0.212\frac{M_{d,c}}{M_{d,b}}+0.561\left[\frac{M_{d,b-}M_{y,b}}{M_{p,b}-M_{y,b}}\right]^2\frac{1}{\sqrt{1+{M_{d,c}}/{M_{d,b}}}}\right]\frac{M_{d,b}L}{EI}..eq\ 2.12$$

Where

$M_{d,c}$ is the design moment of the connection whilst all the other parameters remain the same.

Connections falling in the Non Structural Connections_Category are those that fail to fulfill any of the above conditions such that they tend to lack the requisite ductility and therefore rotation capacity to attain the design condition.

2.3.4 Joint Classification System by Eurocode 3

The classification of joints according to the Eurocode 3 like many other classification systems establishes a relationship between the properties of the connection and that of the connected structural members. It uses this relationship as a basis for the comparison of connection attributes and predicted behavior under global frame analysis. Unlike the Bjorhovde classification scheme, the Eurocode 3 system does not make use of the reference length concept thereby leaving the designer to classify connections based on his own unique situations in terms of beam spans L especially when dealing with the stiffness criterion.

Connections are classified according to stiffness as one of the three given below.

- Rigid
- Semi-Rigid
- Nominally Pinned

Rigid connections are those that exhibit high enough stiffness for the entire system to be analyzed as a continuous one without considering the influence of the connection.

Nominally pinned connections are defined as those that do not develop significant moments to affect the analyses of the structure whilst transmitting internal forces and demonstrating substantial rotation capacities.

Semi- Rigid connections account for those that fail to meet the criteria of the rigid and nominally pinned boundaries.

The governing factor of the stiffness classification in this scheme is the initial stiffness $S_{j,ini}$ which is defined as the slope of the moment rotation curve on the elastic part of the non-linear relationship with classification boundaries given by eq 2.13-2.15;

$S_{j,ini} \geq \frac{k_b E I_b}{L_b} \ldots\ldots\ldots eq\ 2.13$ Rigid Criterion (Zone 1)

$\frac{0.5 E I_b}{L_b} < S_{j,ini} < \frac{k_b E I_b}{L_b} \ldots\ldots\ldots eq\ 2.14$ Semi Rigid Criterion (Zone 2)

$S_{j,ini} \leq \frac{0.5 E I_b}{L_b} \ldots\ldots\ldots eq\ 2.15$ Nominally pinned Criterion (Zone 3)

Where,

$k_b = 8$ when the frame under consideration is well braced such that

horizontal displacements are reduced by 80% or more.

$k_b = 25$ under other bracing circumstances.

I_b= Second moment of area of beam

L_b= Span of beams, between centers of columns

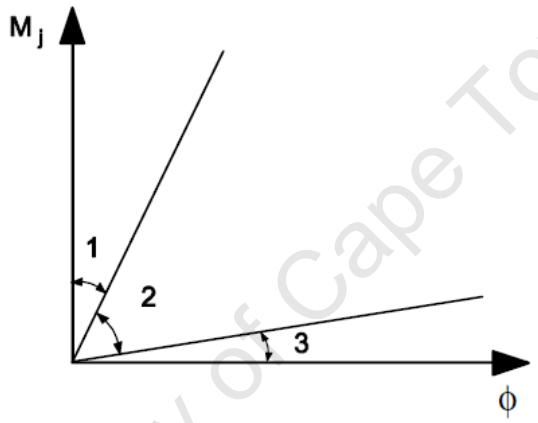

Fig 2.13 Stiffness Boundaries {16}

Connections are classified according to strength in Eurocode 3 by the measure of their capacity to match the moment capacity of the connected member. Three classification designations are provided,

- Full strength
- Partial strength
- Nominally pinned

Full strength connections are those that match or exceed the designed moment capacity of the connected members.

Partial strength connections are those that fail to meet the criteria of both nominally pinned connections and full strength connections.

Nominally pinned connections are characterized by their ability of transmitting internal forces without developing significant moments that affect the analysis and behavior of the structure.

In the case of the strength classification, the plastic moment capacity of the connected member $M_{b,pl,Rd}$ is the governing parameter upon which the classification is based. Thus, the joint design moment resistance $M_{j,Rd}$is classified based on the following eq 2.16-2.18;

$M_{j,Rd} \geq M_{b,pl,Rd} \ldots\ldots\ldots eq\ 2.16$ Full strength

$0.25M_{b,pl,Rd} < M_{j,Rd} < M_{b,pl,Rd} \ldots\ldots\ldots eq\ 2.17$ Partial Strength

$M_{j,Rd} < 0.25M_{b,pl,Rd} \ldots\ldots\ldots eq\ 2.18$ Nominally Pinned

The advantage of the Bjorhovde classification scheme is that its reference length concept allows the connection to be classified even without knowing the lengths of the members. With regards to the EC 3 classification, an idea of the proportions of the frame or connection will have to be at hand before the necessary calculations regarding classification are carried out. The Nethercot classification scheme could prove to be even more accurate in frames whose geometry is closely related to that upon which the scheme is based. In terms of the strength criterion, the EC 3 is much stricter in the determination of the boundary between full strength and Partial strength being equivalent or exceeding the full plastic moment of the connected beam. The EC 9 scheme also places emphasis on the comparison of the connection behavior and beam properties. However in terms of stiffness, the classification will prove to be dependent on the member lengths as in the EC 3.

2.4 Seismic Considerations

The behavior of steel beam to column joints under seismic conditions has captured the interest of researchers the world over and especially in earthquake prone areas of the world due to catastrophic joint failure of structures during severe earthquakes. The onset of cyclic loading conditions presents extra demands on the structural performance of the joints in such a way that certain conditions had to be researched and devised to improve on the cyclic behavior of these joints as these affect the global frame behavior. An example of such work in this area (EP Popov et al 2002) is presented here.

In a bid to improve on the behavior of conventional seismic resistant connections after they demonstrated certain weaknesses during the 1994 North ridge earth quake in los Angeles, California, (Whitaker et al 2000) at the Pacific Earth quake Engineering Research Centre (PEER) sited by (EP Popov et al 2002) carried out extensive research in the area with a view to improve on the performance of these connections. The research focused on cover plate and flange plate connections which sought to remove the plastic hinge from the locality of the column face. As a follow up to this research, (EP Popov et al 2002) sought to improve on the efficiency of this connection type by introducing enhanced reliability and installation costs. The fabrication is in many ways similar to the end plate connection, but in this case it is much more easily compatible to beams of larger weight and dimensions. Boundary parameter values of special moment resisting frames that separate ductile and brittle conditions as far as connections are concerned have been proposed by (JA Swanson et al 2000) as cited by (EP Popov et al 2002) to be 0.03 radians plastic rotation when subject to plastic loading with a 20% subsequent reduction in flexural strength. These were proposed after the Earthquake at Northridge. The research aimed at providing a moment resistant bolted connection with substantial ductility in seismic conditions which required minimal welding and was done in two stages. The high strength bolts that were to be used in the fabrication were tested in the first step and then the second stage consisted of testing of two specimen types as seen on the Fig 2.14. In the experimentation involved in the first part of the test, the A 490 1- ¼ in. bolts were tested at the shank and the thread with specialized equipment built for this purpose during which failure was observed at the threaded region. The ductility was also

tested in another form of experimentation with a constant diameter specimen obtained from the A 490 bolt. It was observed during the experiments that the material demonstrated outstanding ductility and the ultimate stress of 1033Mpa specified was clarified.

W36-150 grade 50 members were used as beams and W14-283 grade 150 as columns in the fabrication of this connection with A 490 bolts.W40-264 grade 50 members were cut through the web to form T stubs which were then used to build single sided beam to column connection assemblies. The stems of the t stubs were welded to the flange of the beams and then given a pre-stress by bolting of the A 490 bolts on to the top and bottom flange of the beam. The pre-stressed T – stub – beam assemblage was then attached to the column by bolting the T stub flanges on to the column Flange as well as bolting the shear tab of the column on to the beam web as shown in fig 2.14. The difference between the two specimens in this second part of the test was in the stem of the T stubs. The first specimen had a rectangular stem on either flange of the beam whilst the second specimen was given a u - shaped geometry attached on both flanges of the beam. Calculations for the design of these connections were in accordance with (G.L Kulak et al 1987) and (AISC Manual of Steel Construction Vol. 1 1995a) as cited by (EP Popov et al 2002)

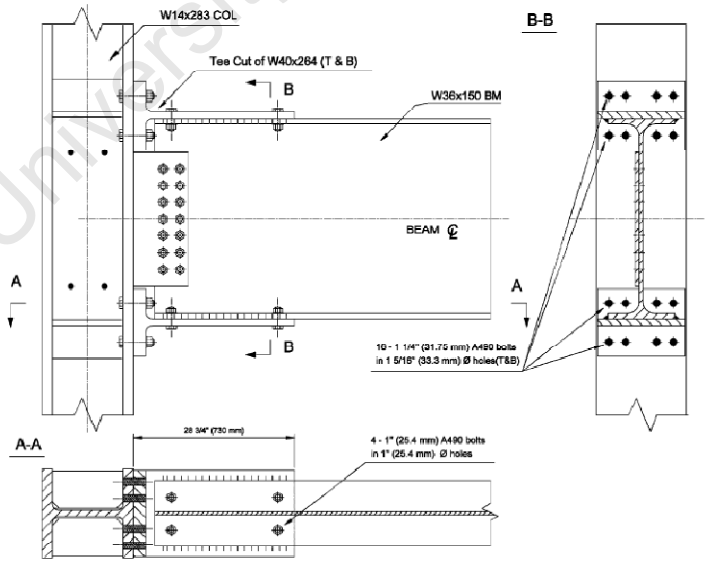

Fig 2.14 Connection Details {8}

Testing of the specimens was done by using horizontal and vertical frames as support for the connection assembly with W14 x311 segments used to provide adequate rotation at the points of connection. A hydraulic actuator attached to the end of the beam of the assembly by means of an end plate and the floor beam served as the loading mechanism. The specifications of the testing mechanism included a ±1558 kN load capacity and ±197mm as the displacement capacity at end of the cantilever beam column connection assembly. Lateral displacement was controlled by a frame built at the end of the 3330mm long cantilever frame which was also free of any axial load on the column.

The results obtained from this work shows that the cyclic loading produced a plastic rotation of 0.0026 radian on specimen 1 without any connection failure. The assemblage requires comparatively minimal welding and easy fabrication. The second specimen was easily disassembled after testing which suggests beam repair and replacement of the T – stubs as a possible remedial measure for structural repair work. The T stub component of the connection assemblage provides low beam deformation. However (EP Popov et al 2002) recommended that further improvement could be achieved in specimen 2 by either increasing the distance of the bolts on the T – stub stem from the column face, or totally discarding them. The additional space required for transporting beams with prepared T – stubs in place could also prove problematic.

2.5 Finite Element Analysis of Aluminum Bolted Joints

The research done by G.De Matteis et al {9} represents one of the closest to the research material on aluminum beam to column connections covered in this work. The idealization of the tension flange area of the connection as an equivalent T-stub is well analyzed and provides an insight of the prying action and failure modes that are characteristic to this zone.

An investigation into the behavior of aluminum T-stub joints was carried out by Matteis G et al {9}. The non linear finite element software ABACUS was used to model the behavior of the T-stubs based on calibration done with the help of available test results on similar experiments carried out on steel T stubs. The research was done to highlight the effects of mechanical properties of aluminum on T stub behavior with emphasis on the

parameters with significant departure from steel. The ABACUS model was developed to simulate aluminum T- stubs subject to tensile forces and was based on experimental results obtained from (O. Bursi et al 1997) as cited by (G De Matties et al 2000). The geometry of the joint as tested is as shown in Fig 2.15. Along with the Finite element model developed.

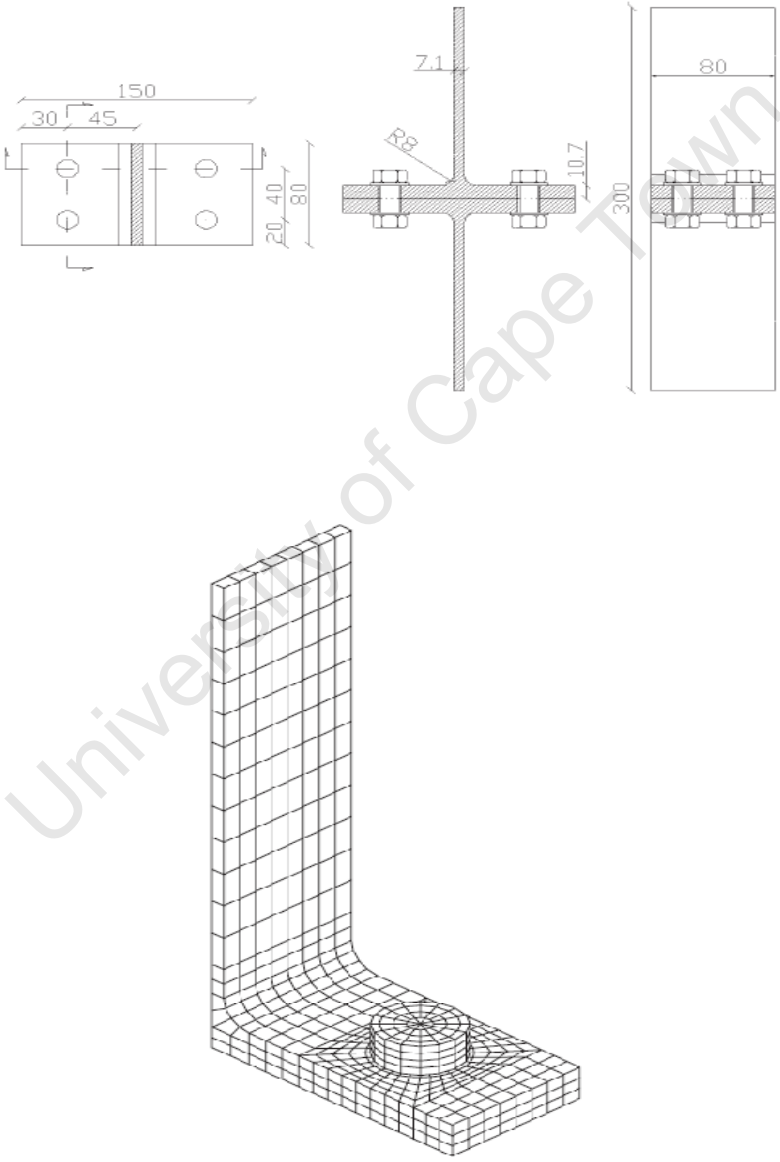

Fig 2.15 T Stub Connection Geometry and Mesh {9}

The model was developed with 3025 nodes and the number of elements added up to 1771 and 7535 degrees of freedom. Boundary conditions were established such that only a quarter of the model was developed representing the global picture and to save computational time. Both the T-stub and the bolts were modeled with 8 node elements whilst bolt threads and washers were neglected. The bolts were however modeled using 10mm depth and 22mm diameter bodies. The developed contact elements utilized in this model consists of isotropic coulomb model with the contact friction between the flange and the rigid surface taken as zero whilst that between the bolt head and the flange surface was given a coefficient of friction of $\mu = 0.3$. A variety of material combinations were adopted in modeling the T- stubs to capture a wide range of failure modes. AW 6082 (T4 and T6) and AW 6061 (T6) were selected for the flange due to good strength, weld ability and corrosion resistant properties. For bolt materials, 5083, (AW 6082 T6) and (AW 7075-T6) were used for aluminum alloy bolts, and steel bolts of 4.6 and 8.8 grades were adopted.

The combination of bolt and flange material used in the analysis is as seen in Table 2.2.

Bolt	*Flange*		
AW 5083	AW 6082 – T4	AW 6061 – T6	AW 6082 – T6
AW 6082 – T6	AW 6082 – T4	AW 6061 – T6	AW 6082 – T6
AW 7075 – T6	AW 6082 – T4	AW 6061 – T6	AW 6082 – T6
Steel Grade 4.6	AW 6082 – T4	AW 6061 – T6	AW 6082 – T6
Steel Grade 8.8	AW 6082 – T4	AW 6061 – T6	AW 6082 – T6

Table 2.2 Flange to Bolt Combinations Considered in Numerical Analysis {9}

Provision was made for adjusted material parameters of true stress and true strain to be force /current area and logarithmic strain respectively due to the large deformations that were these were given by eq 2.19-2.20;

$\varepsilon_{true} = \ln(1 + \epsilon_{nom}) \ldots\ldots\ldots eq\ 2.19$

$\sigma_{true} = \sigma_{nom}(1 + \varepsilon_{nom}) \ldots\ldots\ldots eq\ 2.20$

Inelastic behavior of aluminum alloys was interpreted using the model forwarded by (Berstad T et al 1994) as cited by (G De Matties et al 2000) given as eq 2.21-2.22;

For $\sigma \leq \sigma_0\ ,\ \ \sigma = E\varepsilon \ldots\ldots\ldots eq\ 2.21$

For $\sigma > \sigma_0\ ,\ \ \sigma = \sigma_0 + \alpha\left[1 - exp\left(-\gamma\varepsilon_p\right)\right] \ldots\ldots\ldots eq\ 2.22$

Where

σ_0 = proportionality limit stress conventionally accepted as the elastic limit strength $f_{0.2}$

α = Magnitude of strain hardening

γ = Shape of the strain hardening curve

The plastic stain ε_p is given by eq 2.23;

$\varepsilon_p = \varepsilon - \frac{\sigma}{E} \ldots\ldots\ldots eq\ 2.23$

With ε being the total stain at σ which is the current stress

A value of 10 was adopted for γ as developed by (L. Moen et al 1999) and cited by (G De Matties et al 2000) whereas values for α which depend on the category of aluminum alloy in question are as seen on Table 2.3.

Aluminum Alloy	$f_{0.2}$ (N/mm^2)	f_{ult} N/mm^2	α N/mm^2	$n_{R.O.}$	ε_{ult} (%)
AW 6082 – T6	288	330	80	35	8
AW 6061 – T6	240	300	140	16	6
AW 6082 – T4	162	299	200	8	12

Table 2.3 Mechanical Properties of Aluminum Flange Material {9}

Where

$f_{0.2}$ = the nominal value of proof stress

f_{ult}= the stress

ε_{ult}= the ultimate elongation

$n_{R.O.}$=Ramberg Osgood value

The validity of the model of inelastic material behavior was corroborated by (G De Matties et al 2000) based on work done by (L. Moen et al 1999). Adopted bolt material as used in the analysis is as seen on Table 2.4.

Aluminum Alloy	$\boldsymbol{f_{0.2}}$ $\boldsymbol{(N/mm^2)}$	$\boldsymbol{f_{ult}}$ $\boldsymbol{N/mm^2}$	$\boldsymbol{\alpha}$ $\boldsymbol{N/mm^2}$	$\boldsymbol{\varepsilon_{ult}}$ (%)
Aluminum Alloy Bolts				
AW 5083	110	265	220	12
AW 6082 – T6	288	330	80	8
AW 7075 - T6	440	510	160	6
Steel Grade	$\boldsymbol{f_{0.2}}$ $\boldsymbol{(N/mm^2)}$	$\boldsymbol{f_{ult}}$ $\boldsymbol{N/mm^2}$		$\boldsymbol{\varepsilon_{ult}}$
Steel Bolts				
4.6	240	400		8
8.8	893	974		6

Table 2.4 Mechanical Properties of Aluminum Bolt Material {9}

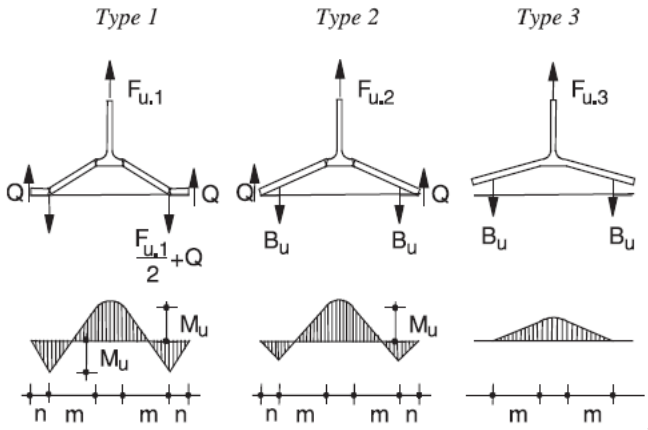

Fig 2.16 T Stub Failure Modes, EC 3 Cited By {9}

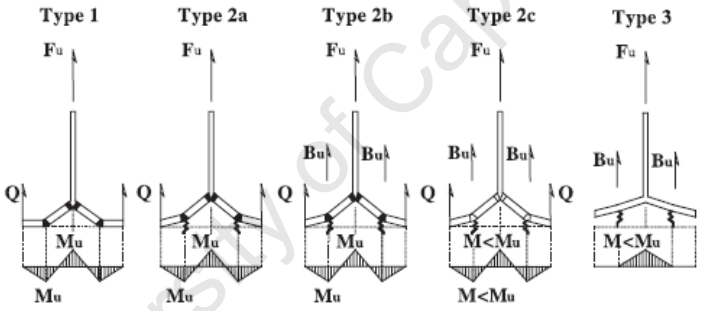

Fig 2.17 Failure Modes of Aluminum T Stubs {9}

This research was the first to analyze aluminum T-Stubs seeking to investigate the effects of mechanical properties on the joint .The investigation found that the failure modes were not easily distinguished amongst each other as compared to steel T- stubs and five different failure mechanisms were identified Fig 2.17 as compared three on an equivalent steel joint Fig 2.16. The importance of taking strain hardening into consideration was made evident on the joints where the plastic deformation of both the flange and bolt contribute towards collapse behavior. The post elastic behavior of aluminum T-stubs was found to be related strongly to strain hardening and ductility properties of the alloys unlike the case of steel connections.

2.6 Fatigue Considerations in Aluminum Bolted Joints

The presence of repeated or cyclic loads on structures precipitates fatigue if the fatigue life of the material is reached under the specified conditions. This generally is characterized by crack development and propagation until subsequent failure. Fatigue failure tends to occur at stress levels lower than those stipulated for the specified static conditions with minimal plastic deformation {13}.Data on Fatigue strength is normally given in terms of S-N diagrams or Wohler curves in which the stress is plotted against number of cycles. Substantial research on aluminum connections to investigating their fatigue characteristics has been done.

2.6.1 Research by P Lasarin et al

A research was carried out by (P Lasarin et al 1996) to ascertain the effects of joint geometry and other technological and environmental parameters on the failure modes of aluminum bolted joints due to fatigue. The tested were carried out with 7020-T6 and 6061-T6 aluminum alloy plates with symmetrical double but joint. Bolts of grade A2-70 and 8.8 were used in different arrangements on over 100 samples with the intention of obtaining different failure modes during experimentation. Geometries for the different bolting arrangements on the different samples were done in conformity with the Italian Standard {11} as cited by (P Lasarin et al 1996){10} with respect to the ratio of transversal inter axis to bolt diameter and the distances from the free edges. Nominal load ratios of R=0 and R=-1 where employed where R $=\sigma_{min}/\sigma_{max}$. The samples were different categories /series of aluminum alloy bolted joints each of which were utilized to develop Wohler curves.

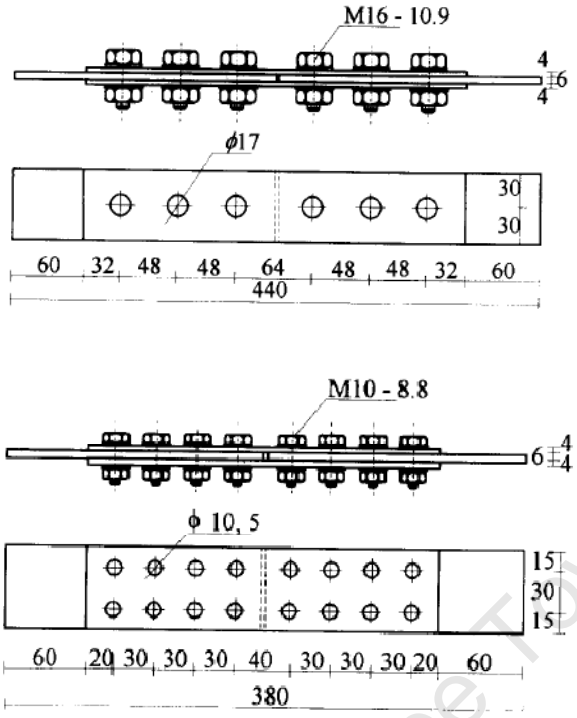

Fig 2.18 Tested Joint Geometries {10}

The data thus acquired during the laboratory work was combined with data obtained from previous research done by another of the authors of this research (Atori et al 1995), to provide information on similar work carried out on the 2024-T4 aluminum alloy. The assemblies were connected by 10.9 steel bolts for the purpose of statistical analysis of the different alloys in question with regards their fatigue behavior. (P Lasarin et al 1996) made reference to previous research work done by (Atori et al 1995) which suggested that the stress amplitudes of friction joints must be considered with the gross transverse section of the plates in question. Observations made by (D Kosteas et al 1993) where it was observed that long life fatigue tests carried out on bolted aluminum alloys that the predominant mode of failure was due to fretting induced cracks that usually occur outside of the weakened area developed by the bolt holes but within the bolt grip. Abrasive forces caused by the dissociation of oxides from the parent alloy during cyclic loading on the metal to metal contact surfaces formed by bolted joints cause fretting which eventually leads to fatigue failure as stated by(P Lasarin et al 1996) citing (D Kosteas et al 1993).

The investigation found that the geometric properties of the joints in terms of number of bolts, size and arrangement had very little or no effect on the fatigue failure of the samples.

With regards to the coefficient of friction being controlled by the presence and absence of sand blasted surfaces, the higher friction coefficient on bearing joints with long service life seems to help due to the friction transfer of loads in spite of low bolt tension. Higher stress levels however precipitate cracking and subsequent reduction of the fatigue life of sand blasted joints relative to the smoother surfaces.

2.6.2 Research by J.M. Minguez et al

This research was aimed at investigating the effect of plate thickness and torque tightening of bolted joints on the fatigue life of single and double lap joints.

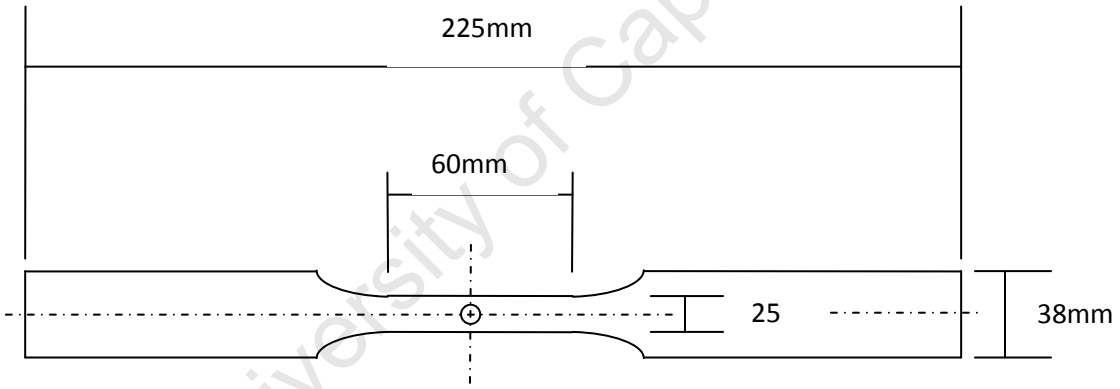

Fig 2.19 Plain Specimen with Drilled Hole {12}

The test were carried out with a 100kN load capacity INSTRON 1332 machine with the specimens being designed according to ASTM E466-82 standards as shown on fig 2.19. Tests where initially done on dog bone specimens with holes drilled at the centre for the purpose of establishing benchmarks for the experiment. The specimens were then split in two and connected by means of double and single lap joints as shown on fig 2.20. 2m and 5mm sheet aircraft specification aluminum alloys BS L165 of T6 temper. The joints were fabricated with 12.9M5 set screws with mild steel washers with fitted ny-lock nuts to

prevent preload relaxation during fatigue test. Splice plates where drilled to 4.9mm diameter to match set screw shank diameter. Torque loading on all nuts was applied using a torque wrench with RS Stock No. 547-379 to ensure uniformity during testing.

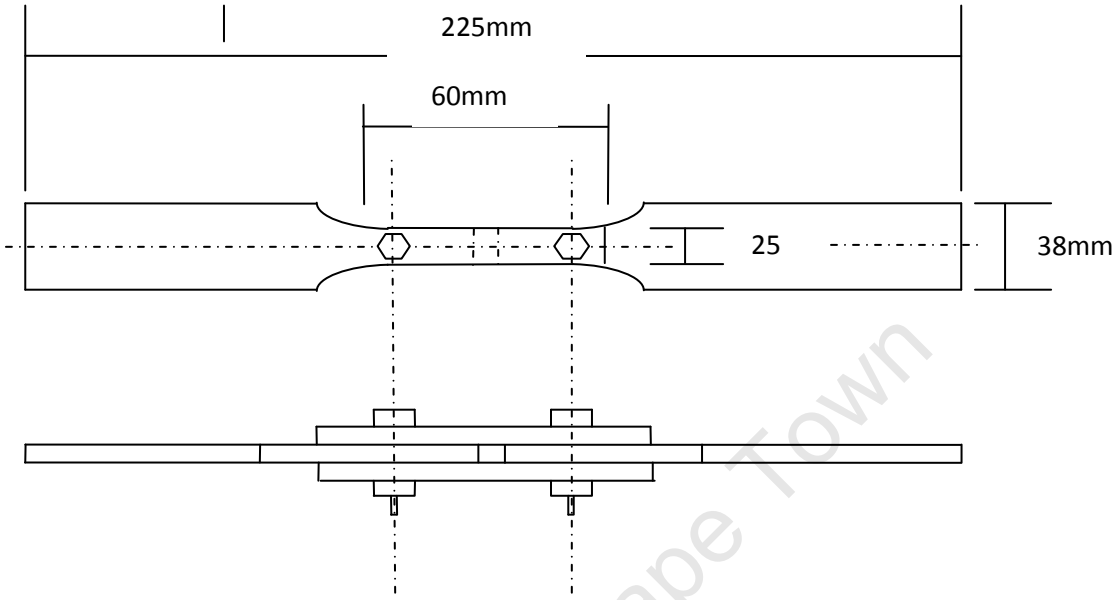

Fig 2.20 Double Lap Joint Specimen {12}

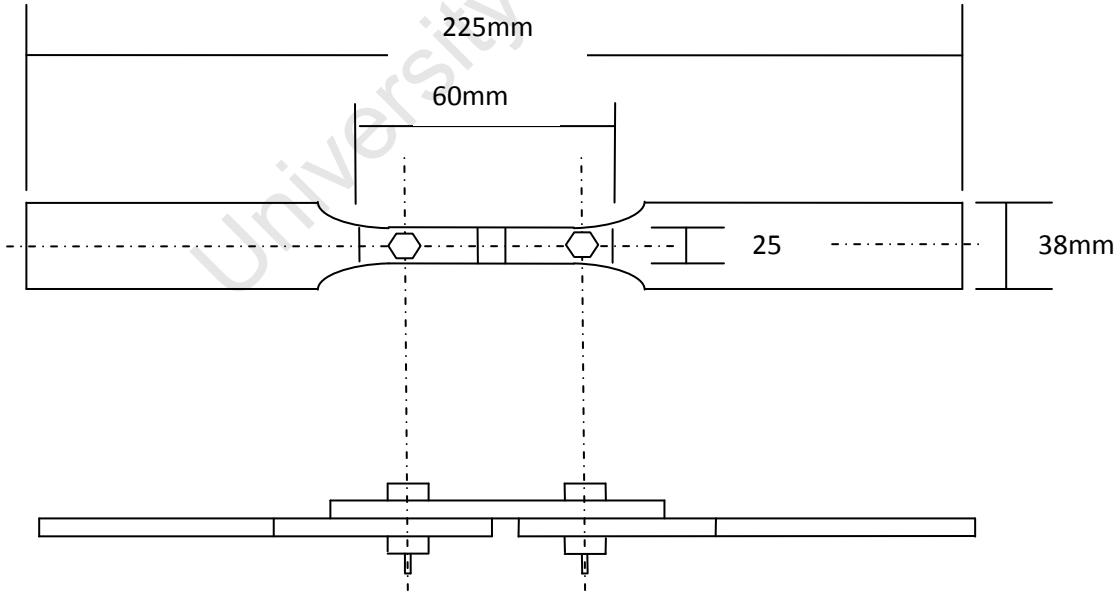

Fig 2.21 Single Lap Joint {12}

A frequency of 20Hz was maintained on the alternating stress purely in tension by applying the minimum stress as small and positive.

The results obtained from this work demonstrated that torque tightening of the bolted joints improved on the friction contact between plates and thereby reduces or removes the bearing of bolts against bolt holes. Thus the concentration of stress is greatly reduced as shear is transmitted through friction over a larger area of the connection thereby increasing fatigue life. It was noted that in these scenarios, a thicker plate will perform better under tighter bolt torque due to a gentler stress distribution.

2.7 Design Considerations for Bolted Aluminum Connections

The arrangement of bolts on a connection in terms of the end spacing and the thickness of the plate along with the diameter of the shank of the bolt itself play a very important role in the fabrication and assembly of bolted joints. Plate buckling, bolt failure and corrosion are among the key failure issues that are to be contended with in ensuring that the geometry of the system is such that it fulfills the design requirements of the expected service loads.

2.8 Bolt Material Properties

The bolting of aluminum plates can be done by aluminum bolts, steel bolts (mild or high strength) or stainless steel bolts. The choice of bolts is entirely dependent on the design and environmental conditions or a combination of both. Where it is desirous to achieve a high frictional contact between plates, it is advisable that high strength bolts are used so that the necessary tensile and shear stresses are well accounted for by the bolt material. In instances of severe corrosion environment where high strength bolts can be avoided, aluminum bolts can then be made use of. The various materials usually used to fabricate aluminum bolts are seen in Table 2.5.

Designation	*Condition*
2024	T4
5083	O
5056A	O
6082	T6
6061	T6
7075	T73

Table 2.5 Aluminum Alloy Bolt Material from {13}

Ideally, the shank of the bolt usually consists of threaded and unthreaded parts. The thickness of the plate material should normally be equal to the length of the unthreaded shank material for optimum results {13}. Where the fabrication of friction joints is required by design it is often standard practice to make use of either mild/high strength steel or stainless steel as the case may be. In the case of the use of mild or high strength steel, it is always necessary to provide some form of corrosion protection on the bolts in order not to compromise the overall corrosion resistance of the joint as the choice of aluminum for the structure in the first place in most cases is due to its enhanced corrosion resistance. In these scenarios the bolts can be galvanized or coated with a protective paint as a remedy. Table 2.6 shows the various steel bolt grades.

Steel Bolts	***Screw***	***Nut***
Standard	4.6	A4
	5.6	5D
	6.6	5S
High Strength	8.8	6S
	10.9	8G
Stainless	X8CND1712	
	X8CNNb1811	
	X15CN1808	

Table 2.6 Steel Bolt Materials from {13}

2.9 Bolt Arrangements

The arrangement of bolts on a connection system has undergone some research {20} from which design codes have been developed to guide engineers in the design and fabrication of aluminum joints {15} and {19}. The need to arrange bolted connections in a manner that avoids premature failure is crucial as several key failure patterns can emerge.

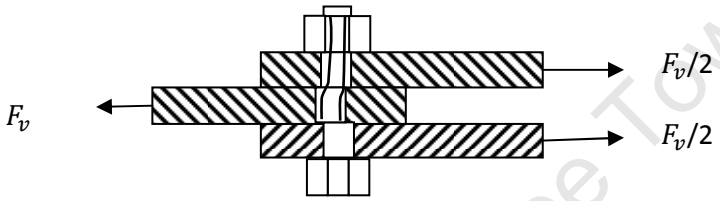

Fig 2.22 Elementary loaded connection from {13}

Consider a simplified bolted connection as shown in fig 2.22. Initially when the load applied is increased gradually from zero, the frictional forces between the plate materials offer the initial resistance to joint slip and are therefore responsible for bearing the load. As the load is increased gradually, it gets to the point where it is equal to the frictional resistance being offered by the plates in contact. At this point, any further increment of load renders the connection to slippage at which bearing between the bolt shank and the bolt holes becomes the dominant resisting factor of the applied load. Subsequent increase in load will then cause joint failure due to the lesser of several possible modes depending on the plate material properties (bearing resistance), bolt arrangement (Edge distances) and the bolt material properties (Bearing or shear resistance){13}. The dominant failure patterns in bolted connections in terms of localized failure are shown on fig 2.23. The section (a) shows failure of the bolt shank in bearing. Failure can also lead to bolt hole deformation as is seen on (b). Plate material could also be ruptured by shear failure (c).

Tension failure of the plate material (d) which causes fracture perpendicular to the line of action of the force is also among possible failures.

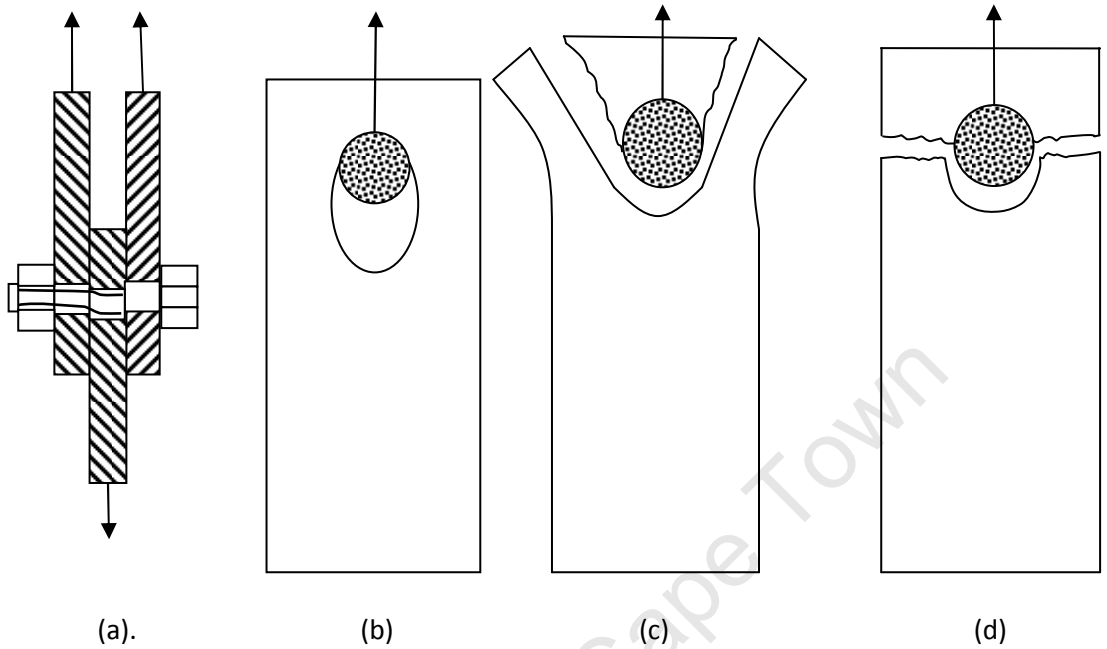

Fig 2.23 Connection failure patterns from {13}

2.9.1 Eurocode 9 Provisions

The Eurocode 9{15} specifies that the minimum distance between the centre of the bolt hole to the adjacent end of the connected plate along the direction of the load should be normally twice the Diameter of the hole $2d_0$.

d_0 is the diameter of the bolt hole.

In situations where a distance of $2d_0$ is not attainable, then a minimum of $1.2d_0$ is provided by Eurocode 9{15} with the proviso that bearing stress is reduced in such a way that the ultimate limit state design bearing force $F_{v,Ed}$ does not exceed the following eq 2.24-2.25;

$F_{b,Ed} = \frac{2.5\alpha f_u dt}{\gamma_{Mb}} \ldots\ldots\ldots eq\ 2.24$

Where α is the least of

$\frac{e_1}{3d_0}; \frac{p_1}{3d_0} - \frac{1}{4}; \frac{f_{ub}}{f_u}$ or 1……eq 2.25

Where

$F_{b,Ed}$ =the design bearing resistance

f_u = ultimate strength of plate material

d = Bolt diameter

t = Thickness of plate

γ_{Mb} = factor of safety of bolted connections

e_1 = Distance between bolt centers and plate end in load direction

p_1 = Distance between bolt centers in load direction

f_{ub} = Ultimate Bolt strength

End distance can be increased up to $3d_o$ with no reduction of the bearing capacity. Eurocode 9{15} further recommends that edge distances between centers of bolt holes to the end of plate perpendicular to the direction of the load $e_2$should not be less than 1.5 d_0

Maximum edge distances are set at 40mm+ 4t in adverse weather or environmental conditions and otherwise the larger of 12t or 150mm to satisfy local buckling requirements.

2.9.2 Research by C.C. Menzemer et al

This research was carried out to investigate the bearing strength of three aluminum alloys through experimental procedures to observe their behavior when subjected to tensile loads. The three alloys utilized in this process are Aluminum Associated Designation,

5052-H32, 5454-H34 and 3003-H16. The research was designed to verify the bearing strength design provisions of the Aluminum Design Manual prior to the 2000 version as this was deemed to be too conservative by (C.C. Menzemer et al 2002){20}. The 1994 version of the Aluminum Design Manual was based on the experimental provisions for determining bearing according to the ASTM Test Method 238 which specifies pin loading on holes. (C.C. Menzemer et al 2002){20} brought out the deficiency in accurate simulation of the actual bolting conditions by pointing out the absence of the effect of bolt clamping on the plate and the plate to plate contact clamping effects both of which have potential influence on the bearing failure of the bolt holes. In this regard the experiments where set up taking both of these parameters into consideration.

100mm by 300mm samples where cut out of the plate materials by means of a band saw with bolt holes placed at a distance of four times the diameter of the bolt shank from the edge. A combination of variables were used which included the bolt diameter, the plate thickness, Aluminum alloy material, effects of bolt washers, plate confinement configuration and the level of torque tightness on the bolt material. 19mm diameter bolts were used on the 6.25mm thick 5454-H34 plate and the 3.2mm thick 5052-H32 plate. A bolt diameter of 6.25mm was used for the 1.25mm thick 3003-H16 plate and the 2.25mm thick 5052-H32 plate. Bolt hole tolerances were set at 1.6mm clearance to fulfill design requirements. The arrangements of the testing samples as were utilized are seen on fig.

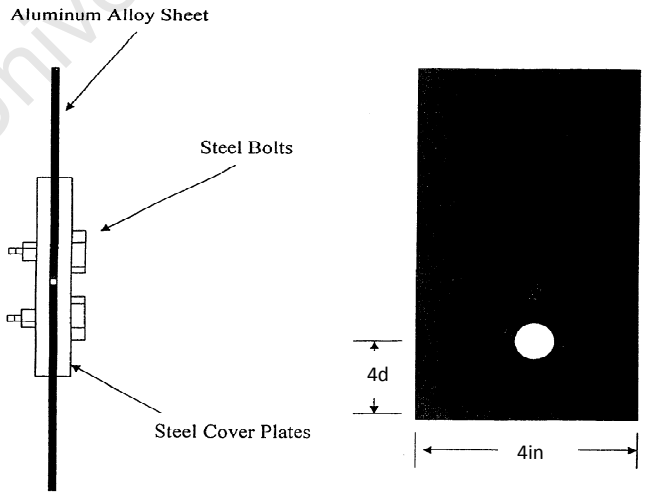

Fig 2.24 Inner Ply Testing Configuration from {20}

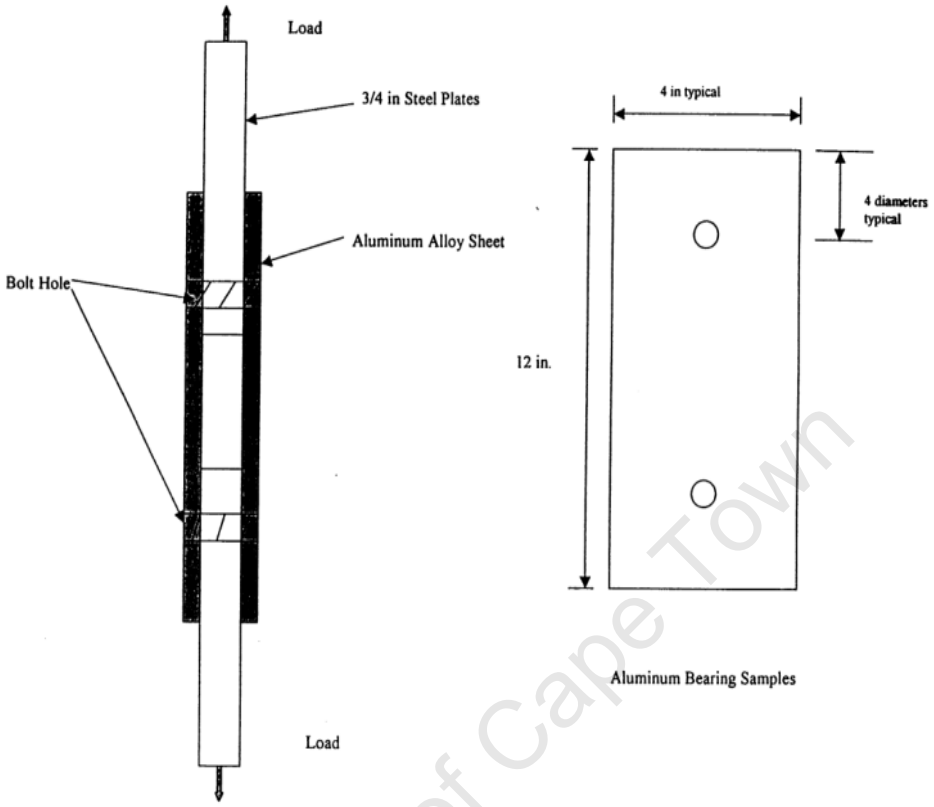

Fig 2.25 Outer Ply Testing Configuration from {20}

Different torque tightened preloads were used for the various confinement specimens to investigate their behavioral response to bearing stresses. Aluminum plates that were bolted on either side of the steel plate as shown on fig 2.25 with loose fitted bolts were classified on the lower bound due to expected performance whilst those that were confined within the two flanking steel plate and snug tightened were classified on the upper bound level. The samples were loaded in tension in a Warner-Swassey Universal Testing Machine and all bolt holes were measured with a micrometer screw gauge prior to testing. After the testing procedure, the bolt elongation was again measured on each sample.

The results of the tests indicated that the samples that where configured with the inner ply arrangement withstood higher bearing stresses compared to samples that were fitted with loosely attached bolts. It was also discovered that bolt hole deformation under tensile

loading was minimized by the clamping action of the outer steel plates pressure applied by torque tightening of the bolts. Samples that were configured with the outer ply arrangement had higher bearing resistance with tighter snug fitted bolts as compared to those that were fitted with loosely fitted bolts.

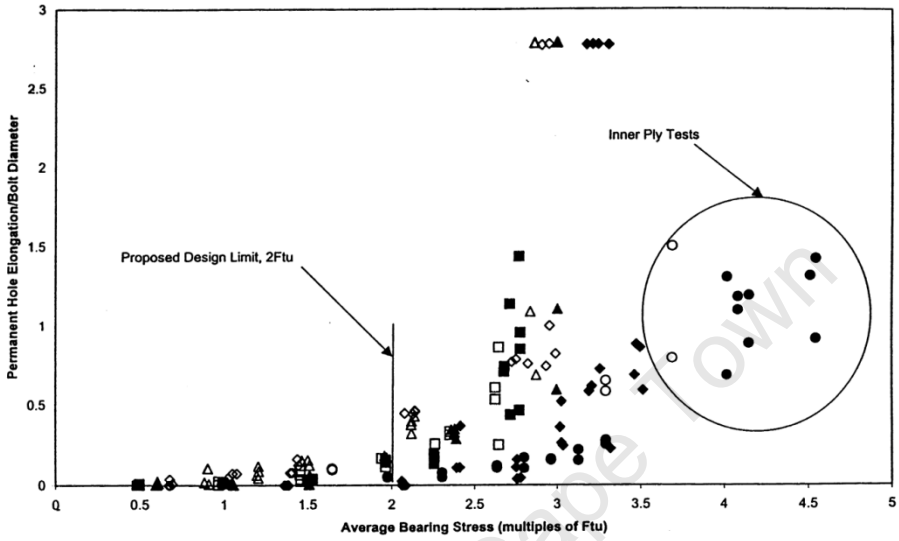

Fig 2.26 Bearing Test Summary from {20}

2.10 Design Considerations for End Plate Connections

End plate connections resist moments by setting up couples that are developed by tensile forces on bolts located above the bottom flange of the beam coupled with bearing resistance being offered by the bottom flange. The centre of rotation is normally located at or around the centre of the bottom flange of the beam, and the bolts that are located at the top most part of the connection normally carry the higher tensile stress {6}. In some other cases, bolts that are located near a stiff section of the connection normally attract higher tensile stresses.

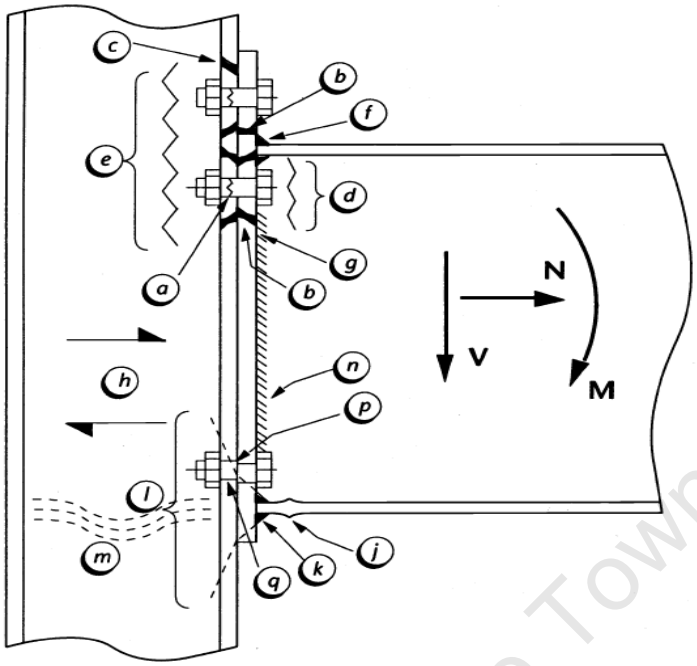

Fig 2.27 Forces in End Plate Connection from {6}

Several design checks are crucial in carrying out the design of end plate beam to column connections. This is well documented in structural steel design {6} {16}. Although in terms of connection geometry, the resolution of forces with regards to the moment resistance of end plate connections at the joint should basically follow the same principle from simple resolution of couples, not much research is available in this area for aluminum connections to actually carry out thorough design calculations. Aluminum T-stub joints has been critically analyzed by finite element analysis {9} and this can be represented in many respects by the tension flange - end plate joint in an equivalent idealization. The influence of strain – hardening and alloy specifications were among the key parameters investigated with a view of observing the failure modes on aluminum T-stubs. However the effects of plate thickness were not monitored. Steel End plate connection design checks as outlined in {6} are seen on table 2.7 and figure 2.27. The tension checks involved for end plate and column flange bending as well as bolt tension are as follows eq 2.26-2.30;

For complete flange yielding:

$$P_r = \frac{4M_p}{m} \ldots\ldots\ldots eq\ 2.26$$

For combined bolt failure and flange yielding:

$$P_r = \frac{2M_p + n(\sum P_t')}{m+n} \ldots\ldots\ldots eq\ 2.27$$

For bolt failure:

$$P_r = \sum P_t' \ldots\ldots\ldots eq\ 2.28$$

Where M_p the plastic capacity of the end plate/column flange is given by:

$$M_p = \frac{l_{eff} t^2 p_y}{4} \ldots\ldots\ldots eq\ 2.29$$

l_{eff}=Effective length of yield line

t=End plate /column flange thickness

p_y=design strength of End plate/column flange

P_r=Resistance of bolt row /group

P_t'= Bolt resistance capacity in tension under prying action

m= Distance between bolt centre to 20% into column root end/plate weld

n= Effective edge distance.

The effective length of the end plate/column flange yield line l_{eff} depends on the bolt spacing and proximity of the stiffeners or edges and varies according to the yield pattern developed by the plate.

With regards to the checks for the column and beam webs in tension, the resistance of the web for a row of bolts in tension is given by:

$$P_t = L_t t_w p_y \ldots\ldots\ldots eq\ 2.30$$

Where:

L_t= Effective length of the web in tension considering 60 degrees spread from bolt centre.

t_w=Thickness of beam /column web

p_y=design strength of column /beam steel

ZONE	*REFERENCE*	*CHECK*
TENSION	a	Bolt tension
	b	End plate bending
	c	Column flange bending
	d	Beam web tension
	e	Column web tension
	f	Flange to end plate weld
	g	Web to end plate weld
HORIZONTAL SHEAR	h	Column web panel shear
COMPRESSION	j	Flange compression
	k	Beam flange weld
	l	Column web crushing
	m	Column web buckling
VERTICAL SHEAR	n	Web to end plate weld
	p	Bolt shear
	q	Bolt bearing plate/flange

Table 2.7 Design Checks for End - Plate Connection {6}

As a matter of principle, these capacity checks should be done in order to satisfy design requirement for end plate connections {6}.

2.11 Conclusions of Literature Review

The material covered in this review represents the general trend of research in the area of bolted connections along with the relevant codes for both steel and aluminum. It can be easily seen that end plate connections has received a lot of attention with regards steel. However the research done on aluminum connections is largely restricted to lap joints. The effect of torque tightening, bolt arrangement and spacing has received much input which has resulted in existing codes of practice {15} {19}. Menzemer et al (1998) {26} investigated bolted aluminum 5083 alloys to evaluate shear block failure of gusset plates in tension. The bracing of aluminum frames with angles channels and T's also precipitated the research of aluminum tension members by C.C Menzemer et al (2005) {27}. In this work members were loaded in tension and the effects of eccentricity and bolting pattern were studied with both experimental work and some finite element modeling. The conclusions of most of the work on aluminum has resulted in the formulation of specifications regarding edge distances, bolt arrangement patterns and bolt spacing to counter against block shear, bolt hole deformation and bolt shear. The specific areas involving beam to column aluminum connections still remains sparse and warrants investigation.

2.12 Statement of Research, Justification and Aims

The use of aluminum as a structural material is an evolving phenomenon especially in peculiar circumstances warranting the advantage of its unique weight and corrosion resistant properties. The aircraft manufacturing, automobile and railway industries have already extensively made use of this material in this regard with substantial cost effectiveness and efficiency. However, the main jointing techniques utilized in assembling these involve single or double lap joints which have been covered to a substantial extent by research highlighted earlier. However aluminum frames forming parts of offshore oil rig platforms or sewage plant components involve different kinds of connections from these as they might require extruded I sections assembled into beam and column arrangements. Other uses including temporary and retractable bridges such as the Aberdeen harbor in Scotland as cited by Mazzolani F.M. {13} may also require end plate beam to column connections depending on design. The area of steel

connections is generously covered by Eurocode 3 part 1-8 and AISC (Allowable Stress Design Manual) as far as these connections are concerned{16}{24}. However, designing structures involving bolted end plate aluminum connections will prove to be rather conservative as design codes such as Eurocode 9 and Aluminum Design Manual still require input in this direction. This work aims at taking a step towards understanding the moment rotation characteristics of aluminum end plate connections as may be needed for design and use on the types of structures mentioned. The failure modes, strength, stiffness and ductility of the parametric array analyzed forms the focal point of the research.

2.13 Methodology

The base methodology employed in this investigation is Finite Element Modeling. The approach involves the development of bench mark Finite Element Models against previous work done on steel end plate connections. The accuracy of the developed models is ascertained by comparing moment rotation curves generated by actual experimental tests done to prove the veracity of the results. When once the results are accurate enough, the various Finite Element Modeling techniques including element properties, contact algorithm and boundary conditions are applied to the selected parameters in aluminum to observe their rotational capacities strength and stiffness's.

CHAPTER 3

FINITE ELEMENT MODELING

3.1 General Overview of Finite Element Software Package

The finite element software ADINA (Automatic Dynamic Incremental Non linear Analysis) was utilized in the modeling of the different assemblies investigated in this work. The software was developed and is a registered trade mark of K.J Bathe/ ADINA R & D, Inc. It has a variety of elements which are available for users to choose from depending on the analysis being carried out and has been proven to be reliable in linear large displacement, large strain, small displacement large strain and small displacement large strain modeling. The flexibility of this package allows the investigation of many problems such as Eigen value analysis (linearized buckling and frequency analysis), static, implicit and explicit dynamic analysis as well as fracture mechanics.

3.2 Units

Consistency in units is quite important when inputting data, and as such when SI units are utilized, length force and mass are to be entered with the units Meters, Newtons and Kilograms respectively. The models developed in this work were entered with consistent SI units with length in millimeters and force in Newtons. As such, Young Modulus E and stress values f are inputted and read as N/mm^2.

3.3 Geometry

ADINA-M is a special feature available in this package that allows for the creation and modification of a wide variety of solid geometry. It was used in generating the various structural components of the model assembly. Block bodies where first generated with this feature, followed by the creating of several cylindrical bodies for bolt shank and bolt heads. Bolt holes where generated by creating additional cylindrical bodies within the flanges of the column and end plates and then subtracted using the Boolean operator provided in ADINA-M. To strike a balance between computational cost and accuracy, the symmetry of the assemblies was taken advantage of in generating the geometry whereby the model was developed with only half of the geometry on the positive z axis

considered. The necessary boundary conditions were then activated to restrain Z-translation so that all displacements and strains on the half of the model under consideration will be the exact mirror image of the other half. This is of further relevance due to the fact that torsion effects are ignored in this investigation.

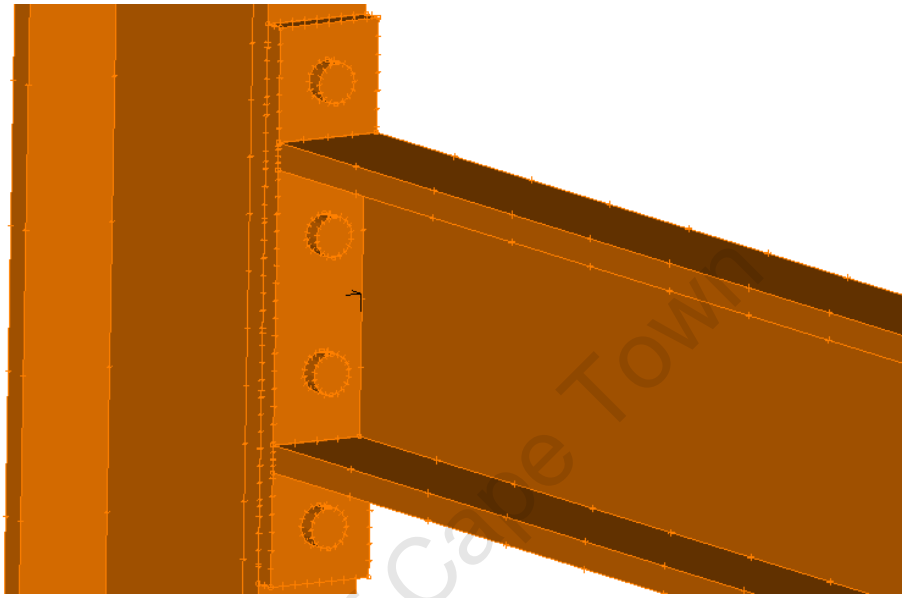

Fig 3.1 Beam – Column Endplate Connection (ADINA)

3.4 Elements Groups

Due to the fact that significant stresses are generated on the bolts during the loading of the assembly and by virtue of the nature of the geometry involved, three dimensional solid elements where used in the analysis being that plane stress and plane strain conditions cannot be assumed in this case. Because of limited computational resources available, eight node elements were made use of in the meshing process which entails reduced integration and far less computational effort. The three dimension solid elements can be used in large displacement, large strain situations effectively and are compatible with the required plastic multilinear material model utilized to investigate the post elastic behavior of the assemblies under incremental loading conditions.

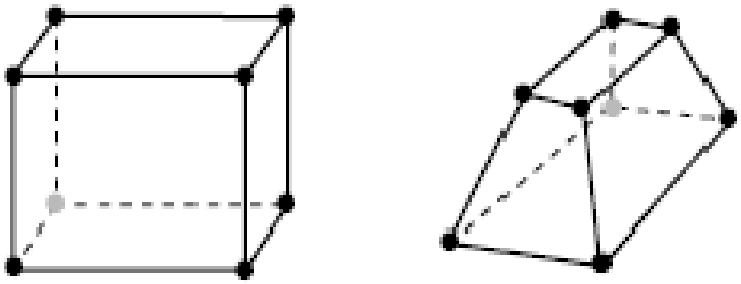

Fig 3.2 Eight Node Elements {30}

Although the use of higher order elements normally yields higher accuracy, the twenty and twenty seven node brick elements are inefficient with contact analysis which subsequently renders tractions at contact segments to be rather inaccurate.

3.5 Non-Linear Material Properties

The plastic multi linear material formulation was adopted, with large displacement and large strain option as the selected kinematic norm for the analysis assumptions considering that substantial stresses were expected especially in the locality of the bolt and bolt-hole areas of the model. Stress strain values were computed by making use of the Ram berg Osgood material stress strain relationship model to develop the curve defining the post elastic behavior of the materials. This material formulation is governed by the Von misses yield condition and adopts an isotropic bilinear /multi linear strain hardening behavior.

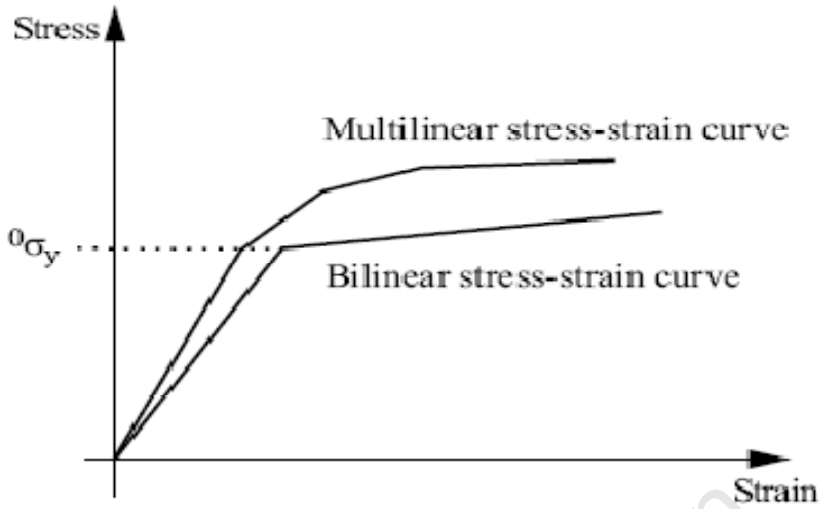

Fig 3.3 Isotropic Bilinear/ Multi-linear Material Idealization {30}

The two principal materials utilized, Aluminum 6082 T6 and Grade 10.9 steel were inputted as seen on table 3.1 along with their poison ratios and young's modulus values.

	Young Modulus (Mpa)	*Proof strength* $f_{0.2}$ *(N/mm²)*	*Ultimate Strength* f_u*(N/mm²)*	*Density (Kg/m³)*	*Ultimate Elongation (%)*
Aluminum 6082 T6	70000	288	330	2700	8
Grade10.9 steel	210000	893	1100	7800	6

Table 3.1 Finite Element Material Data

3.6 Meshing

Due to the relatively complex assembly geometry, the models had to be partitioned using the Boolean operator feature available in ADINA-M so that they can be further simplified to an extent that an acceptable mesh was obtained with the angles subtended by the element edges within acceptable limits. As stated earlier, eight node brick elements were

predominantly used with transition zones being filled with six and fifteen node prisms were the eight node elements are rendered inappropriate.

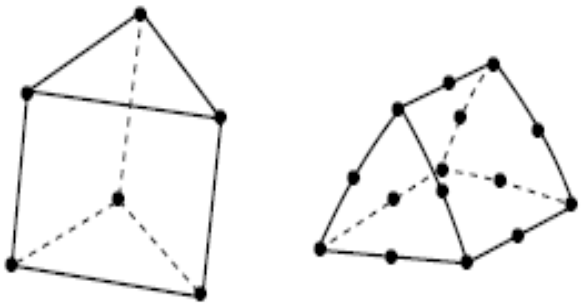

Fig 3.4 Six and Fifteen Node Prism Elements {30}

It is important to note that the meshing process needed to be carried out before the establishment of contact groups and contact surfaces due to the fact that, additional surfaces are auto generated on adjacent bodies which may cause the reordering of the surface numbering system. In order to capture the stress and strain plots accurately, higher mesh densities were generated at areas of high stress e.g. bolts and bolt-holes, whereas much coarser mesh was defined in areas with lower stress gradients.

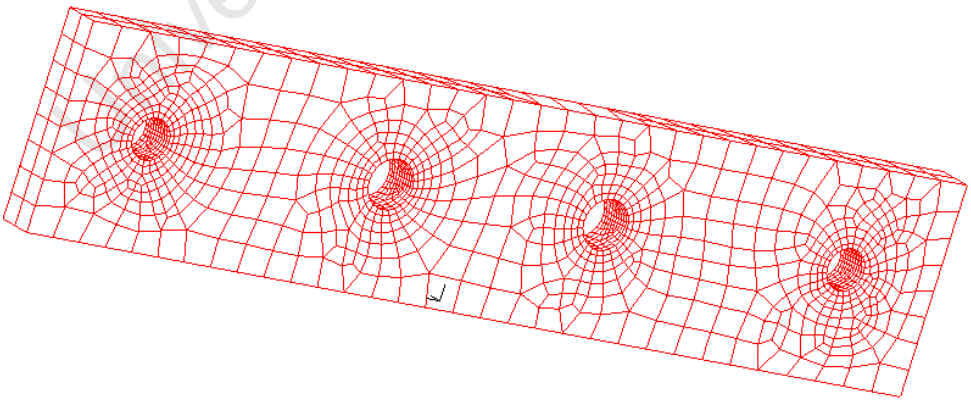

Fig 3.5 Typical End Plate Mesh

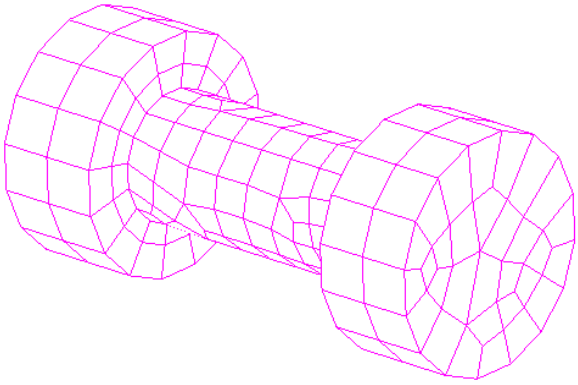

Fig 3.6 Typical Bolt Mesh

This technique also allows for areas of interest to be assessed quite accurately whilst preserving the geometrical properties of the assembly in terms of dimensions and economizing computational effort at the same time.

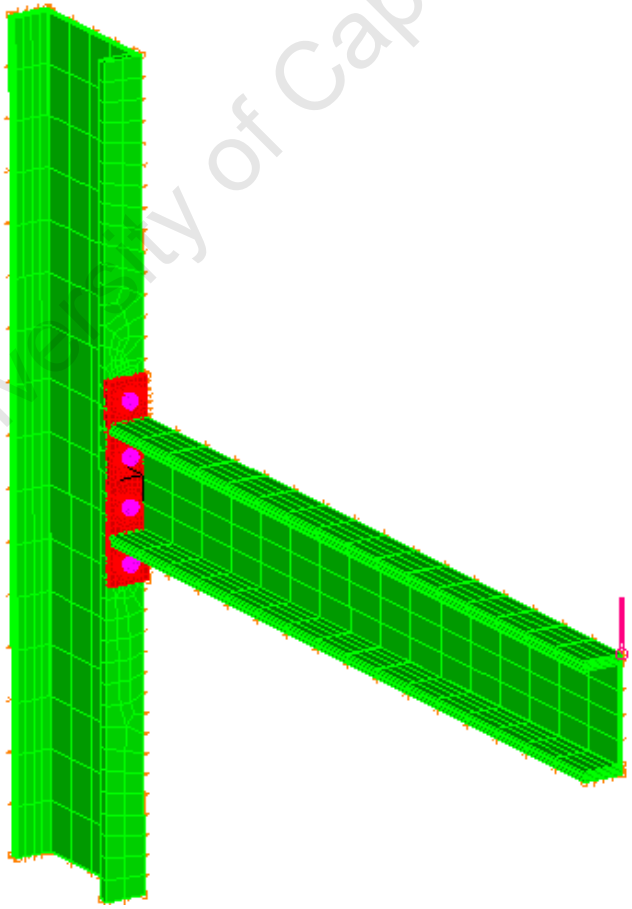

Fig 3.6 Meshed Assembly Showing Colored Element Groups

3.7 Contact Algorithm

The predominance of three D elements in the analysis warranted the use of 3-D contact group as well throughout the modeling process with the default constraint function contact algorithm used being that the effects of friction was neglected to cut down on computational effort. Zero compliance factors were imputed into the modeling data to take account of the lack of interpenetration between contact elements as the aluminum and steel material being analyzed are sufficiently rigid enough to account for this input.

Contact between bolt head and end plates and between bolt heads and column flanges were then defined. A much finer mesh was used to generate the bolt geometry more accurately. As such the bolt heads were taken as the contactor with the end plate and the column flange surfaces considered as the target surface.

3.8 Boundary Conditions and Descretizing of Models

Complete fixity was prescribed for the top and bottom edges of the attached column for x, y and z translation, whilst a new boundary condition was prescribed to limit to zero all translation in the z direction right across the axis of symmetry, the z axis. All rotational degrees of freedom were rendered inactive as specified by the software literature for 3D elements so as reduce computational effort.

3.9 Loading and Time Step Function

An incremental load was established at the extreme tip of the beams away from the joint on the connection assembly by the automatic time step and the time function. This is particularly useful in non- linear analysis as a sudden imposition of full loads can render the model not to converge. Furthermore, if the range of loading condition is known beyond which the model will collapse, then the total load can be partitioned into smaller increments. The solution for the last converged time step corresponding to the final load before collapse can then be observed through post processing.

3.10 Post Processing

All successfully completed runs of ADINA models generate a porthole file that is stored in the temporary folder of the computer. For the solution to be obtained and analyzed through the post processing procedure, this file with extension .por needs to be opened. There is a wide variety of results which can be viewed by the porthole file in the ADINA post processing module the most common being stresses, strains, displacements, traction and reaction at specified nodes or elements depending on the area of interest. Band plots can be generated by which the gradient of the variable of interest to the user can be inspected and the magnitudes verified as such at various points on the assembly. ADINA calculates results through interpolation from integration points to other points/nodes of the element. Adjacent elements connected by a node can be evaluated into one result for stress and strain values through this procedure termed as smoothing. The deformation of the model can also be observed by plotting the deformed mesh. In instances where this is rather small, the mesh plot can be modified by scaling the displacements to good effect.

CHAPTER 4

FINITE ELEMENT MODEL VALIDATION

4.1 Back ground To Previous Experimental Work

For the necessary confidence to be gained in the results of the Finite Elements modeling, models were run based on experimental work done with similar connection geometry. These were done based on the materials utilized by the researchers and the various structural elements used. The selected experimental work was that carried out by (Coelho A, M, and Bijlaard, F, 2006) {14} who investigated the experimental behavior of high strength steel end plate connections. The investigation involved the use of grade S355 steel column and beam material of section HE300M and HE320A respectively. High strength steel end plate material was made use of S690, whilst both grade 12.9 and 8.8 steel bolts of 24 mm diameter M24 were used in the fabrication of the assembly as mentioned in Chapter 2. The moment rotation behavior of the extended end plate connections with end plate thicknesses 10.15 and 14.75mm respectively and grade 12.9 M24 bolts were modeled with ADINA using eight node 3D element and plastic multi-linear material idealization. The geometry of the extended end plate in this research is as seen in Fig 4.1.

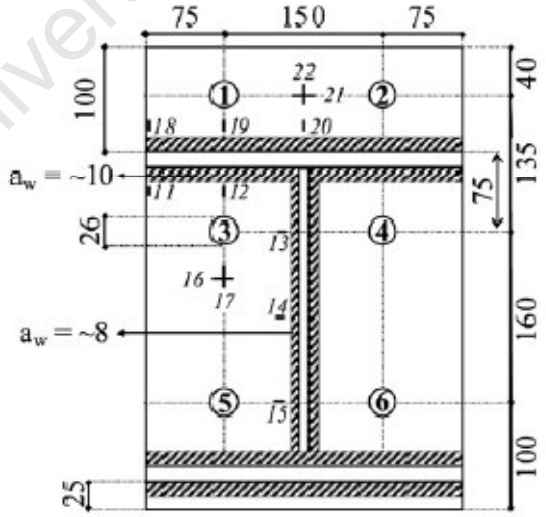

Fig 4.1 Extended End Plate Geometry {14}

The moment rotation curves generated from the results of the experimental work is reproduced here Fig 4.2 for comparison with that obtained from ADINA. Of particular interest are the two parameters which were utilized for the benchmarking process namely EEP-15_2 and EEP_10_2a as defined by (Coelho A, M, and Bijlaard, F) {14}.

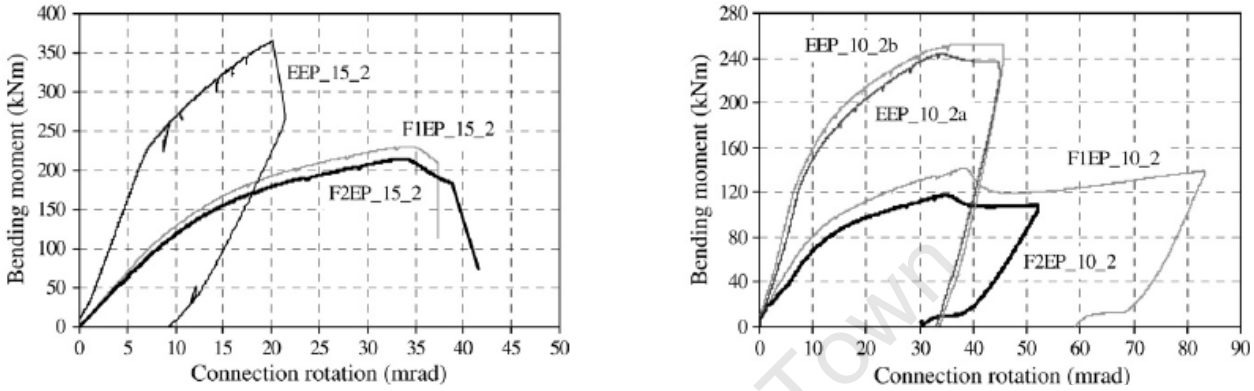

Fig 4.2 Moment Rotation Relationships {14}

The results shows greater stiffness and higher strength from the connections fabricated with the 14.75mm end plate whilst that of the 10.15mm end plate displayed higher ductility.

The failure mode observed for the 14.75mm end plate connection was failure of the bolts on the extended part of the end plate connection above the tension flange, whilst for the 10.15mm extended end plate connection, there was failure of the tension flange in the heat affected zone (HAZ) close to the weld with the end plate.

4.2 Model Calibration with ADINA

The meshed model geometry as generated with ADINA is shown on Fig 4.3. with the loading applied at the tip of the cantilever 1300mm away from the connection as was the case with the experimental work done by (Coelho A, M, and Bijlaard, F, 2006) {14}.

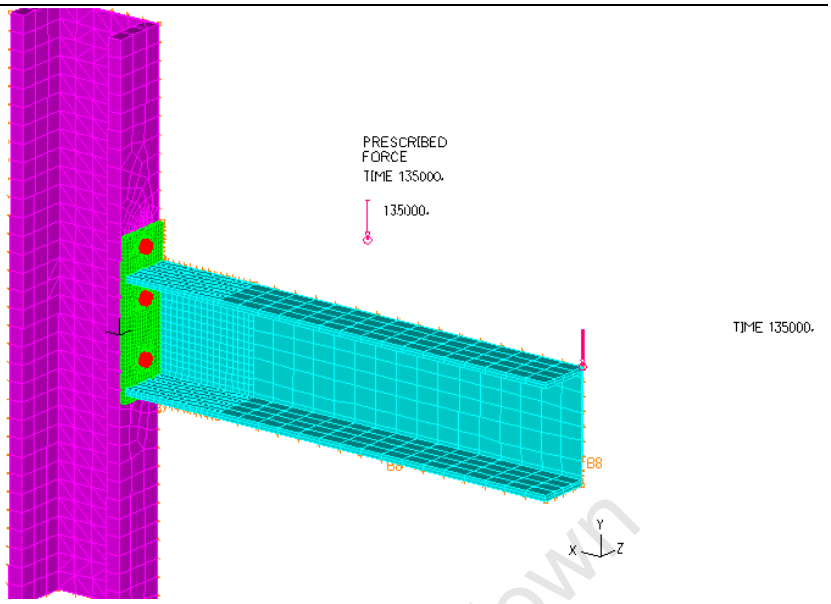

Fig 4.3 Typical Mesh Plot of Calibration Models

Moment rotation plots were developed using the same method as was done in this work which was , subtracting the beam elastic deflection from observed deflections during the incremental loading and calculating rotations in radians through simple trigonometry.The comparison of plots so obtained with that obtained by the research experimental work are produced in Figs 4.4 and 4.5 for comparison.

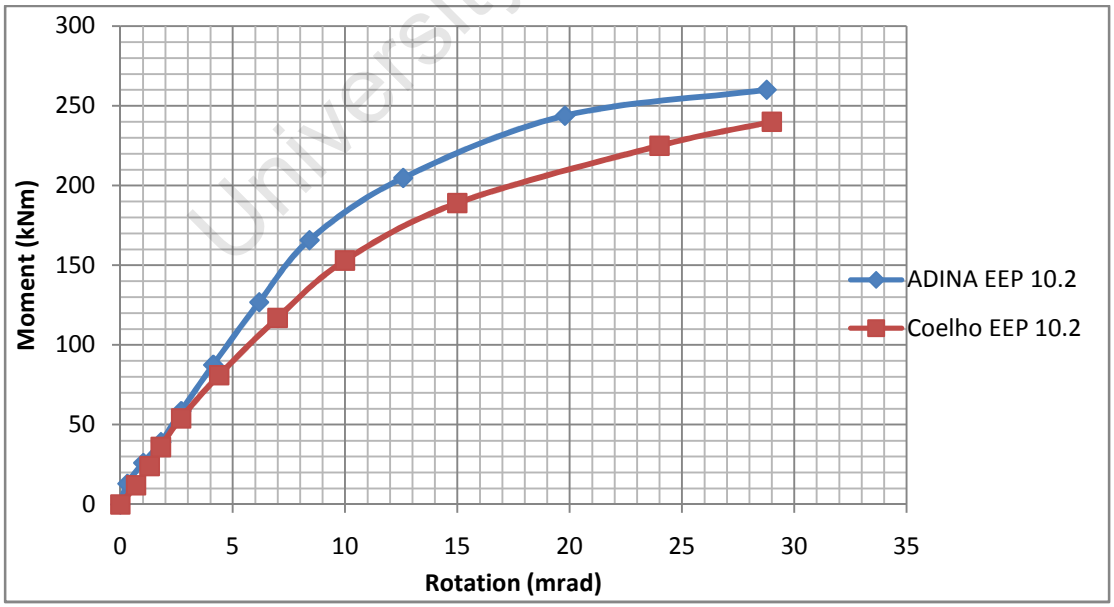

Fig 4.4 Comparison of Moment Rotation Charecteristics 10mm ExtendedEnd Plate

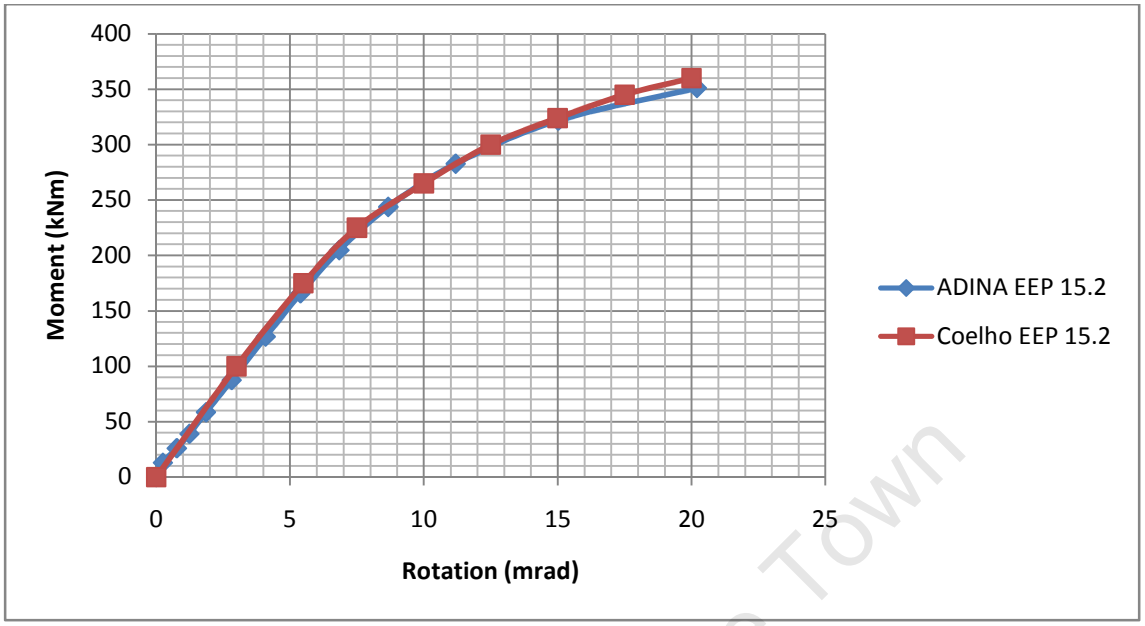

Fig 4.5 Comparison of Moment Rotation Charecteristics 15mm Extended End Plate

It can be seen from the plots that the initial stiffnesses can be calculated from the slope of the curves at the origin quite easily. The initial stiffness on the two parameters are equal and can be attributed almost 100% accuracy as far as the finite Element model is concerned. In terms of the strengths of the connections, The finite element model attained a strength of 240kNm wheras the experimental assembly failed at 260kNm for the 10.15mm extended end plate connection.This represents 92% accuracy. In terms of the ductility of the assembly, a 97% accuracy was achieved with the experimental assembly failing at 29mrad and the ADINA model at 28mrad. A similar pattern was obtained with the 14.75mm thick end plate when compared to the moment rotation curve developed from the experimental results. In addition, the linear and nonlinear parts of the curve followed quite closely with that of the experimental results. Being that the material data was inputed into the ADINA based on the coupon test results as produced by (Coelho A, M, and Bijlaard, F, 2006) {14}, the necessary confidence in the plastic multi linear material model that was utilized in ADINA was obtained based on this correlation.

4.3 Analysis of Failure Patterns

The effects of the welds on the end plate connections with respect to the extent and severity of the (HAZ) were not taken into consideration during the modeling process both for the calibration models and the parametric study on the aluminum end plate connections. However, the behavior of the models was monitored at sensitive areas within the (HAZ). The tension flange/End plate weld is of particular concern for two main reasons. Firstly, this is an area that generates large quantities of stress during the loading process and secondly, HAZ softening accounts for substantial loss of material strength at these points.

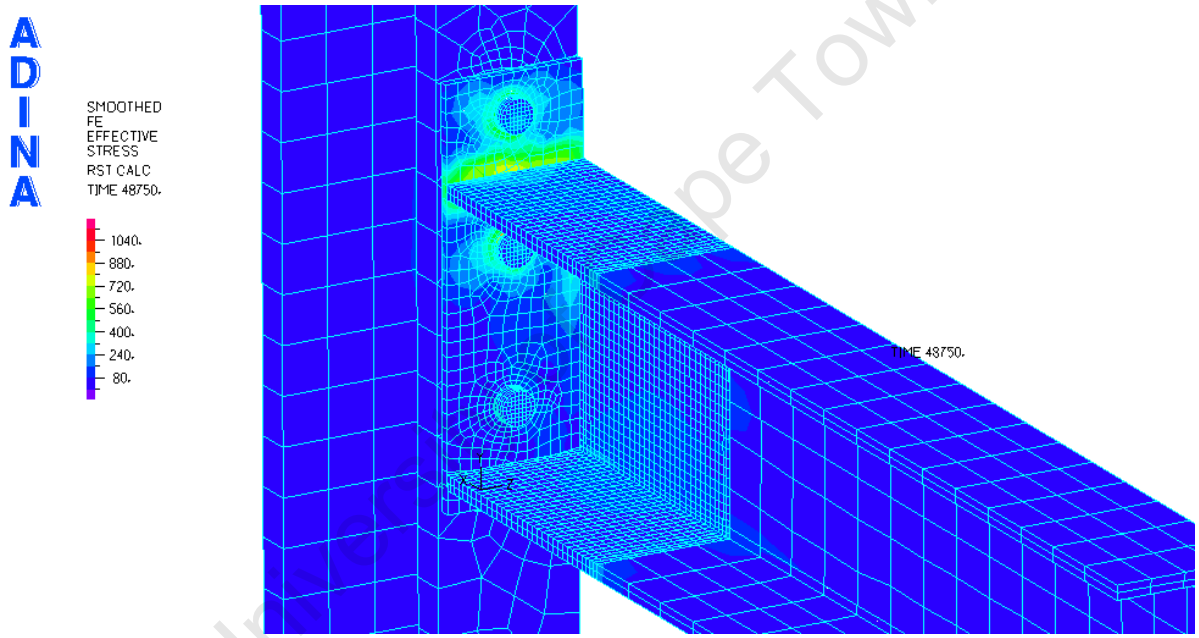

Fig 4.6 Stress Plot For Loaded Assembly

Fig 4.6 shows a plot of the stress across the assembly at a time step representing 126kNm, which is half of the moment capacity of the connection for EEP_10_2a. Already large stresses have developed at the tension flange/endplate intersection as can be seen. The failure mode as reported for this parameter by (Coelho A, M, and Bijlaard, F, 2006) {14} is cracking at this location attributed to reduced material strength due to HAZ softening. Data obtained from the ADINA models show the variation of stress at this location with incremental loading up to failure as shown on Table 4.1 It can be seen

that stresses of 308.5MPa are recorded in the case of the 10.15mm end plate connection at failure whilst the 14.75mm connection records stresses of up to 266.9MPa. Yield strength of 355Mpa was inputted in the plastic bilinear material formulation to account for beam and column materials (S355 Steel)). The failure recorded by the researchers can easily be interpreted by these results as the stresses developed in the 10.15 mm endplate account for 87% of the yield strength of the material. It is thus more likely that HAZ softening on the tension flange at this position would render failure to occur at this stress level as opposed to that recorded on the 14.75mm end plate assembly which only accounts for 75% of the yield stress at failure.

EP_10_2a		**EEP_15_2**	
Moment(kNm)	Stress(MPa)	Moment (kNm)	Stress(MPa)
0	0	0	0
13	14.0	13	10.7
26	36.5	26	26.4
39	60.2	39	40.4
58.5	91.1	58.	60.6
87.5	142.8	87.5	90.6
126.75	221.0	126.75	130.7
165.75	253.4	165.75	171.8
204.75	269.5	204.75	204.0
243.75	291.9	243.75	226.6
260	308.5	282.75	246.2
		321.75	259.7
		351	266.9

Table 4.1 HAZ Stress Moment Variation at Tension Flange/End Plate Intersection

In the case of the variation of bolt stresses with incremental loading, Coelho A, M, and Bijlaard, F, 2006) {14} observed that the 14.75mm end plate connection failed by bolt rupture at the extended end plate section of the assembly. Table 4.2 shows the variation of bolt shank stress with increasing moment up to failure for the two parameters. At failure, the 14.75mm end plate connections attain stresses of op to 1249.22MPa as compared to 1198.05MPa in the case of the 10.15mm end plate connection. It is thus easy to see why the predominant failure mode during experimentation was bolt failure on the thicker end plate.

EEP_10_2a		EEP_15_2	
Moment(kNm)	Stress(MPa)	Moment (kNm)	Stress(MPa)
0	0	0	0
13	11.72	13	10.9
26	48.93	26	134.0
39	219.78	39	255.71
58.5	336.03	58.	388.58
87.5	510.55	87.5	589.93
126.75	738.15	126.75	862.31
165.75	916.16	165.75	1107.11
204.75	946.65	204.75	1204.76
243.75	1176.46	243.75	1211.98
260	1198.05	282.75	1221.43
		321.75	1235.38
		351	1249.22

Table 4.2 Variation of Bolt Shank Stress with Increasing Moment

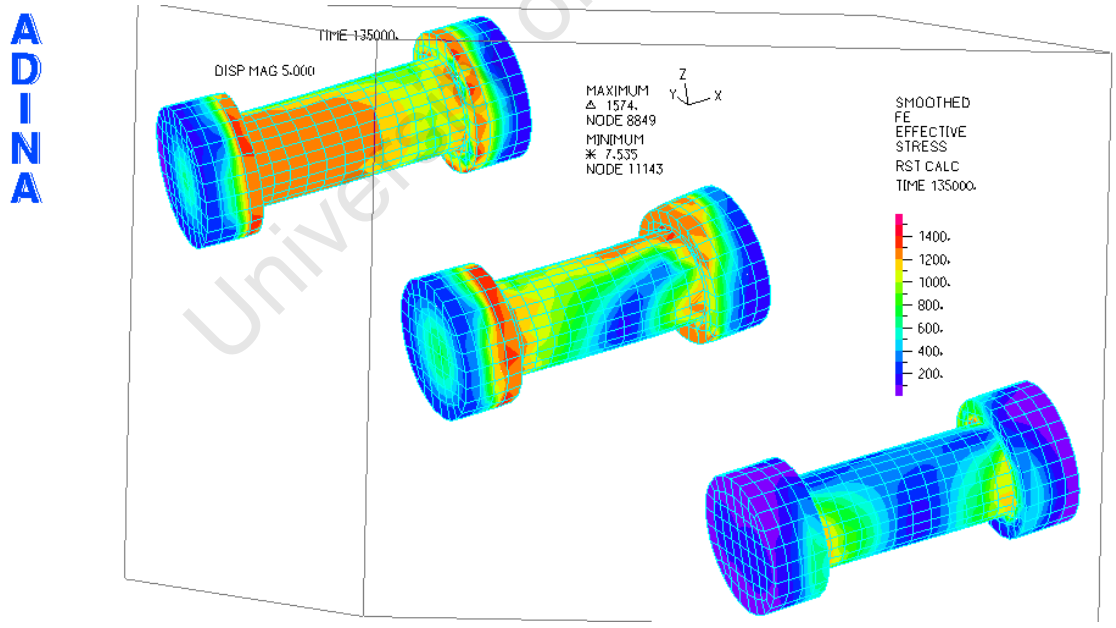

Fig 4.7 Stress Band on Deformed Bolts

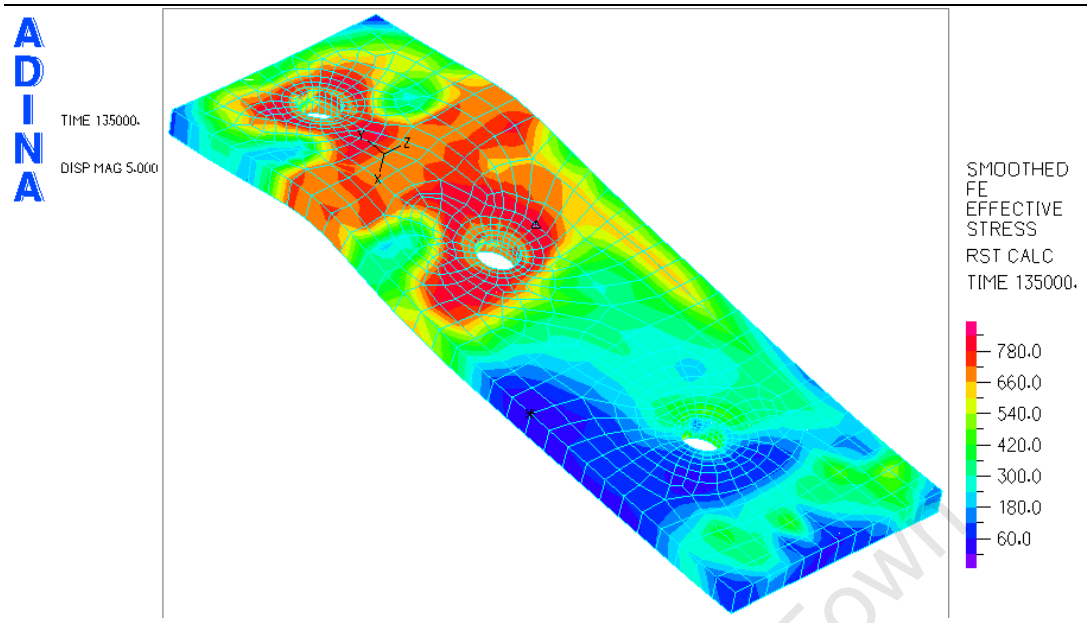

Fig 4.7 Stress Band on Deformed End Plate

Typical End plate and bolt stress bands for the connections are as seen on Figs 4.6 and 4.7 with the deformed configuration magnified through the model depiction function so that they can be better appreciated.

The interpretation of data obtained from the finite element analysis done with ADINA matches very closely to observed connection behavior by the researchers of this work. The necessary confidence going forward can be gained by these results in interpreting similar ones obtained from the Aluminum connection modeling.

CHAPTER 5

NUMERICAL MODELLING RESULTS

5.1 Geometry and Cross - Section Classification

Fig 5.1 shows the geometry of a typical assembly as generated by the Finite Element Models. As can be seen, complete fixity was defined for the top and bottom ends of the columns. The point of application of the load is 1m away from the connection locality thereby creating the requisite lever arm for generating moment. The column depth is substantially greater than that of the beam thereby creating a much stiffer member. All variable components such as end plate, bolts and web stiffeners are as seen labeled.

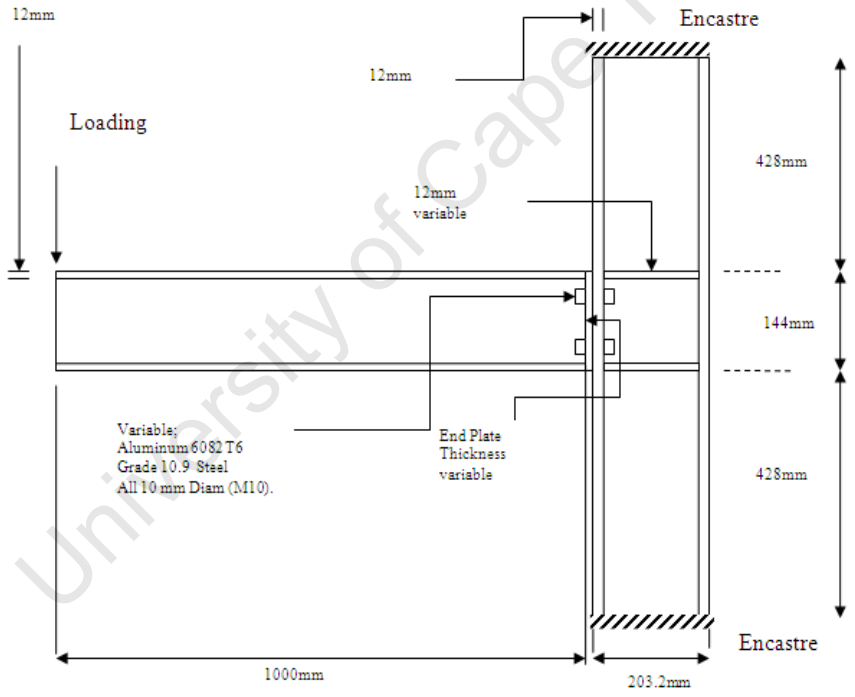

Fig 5.1 Finite Element Model Assembly with Variables

The layout of bolt holes in terms of edge spacing and bolt hole diameter was done in compliance with the provisions of Eurocode 9 such that the spacing is not less than $2.0d_o$ where d_o is the bolt hole diameter and does not exceed $12t$ or 150mm, where t is

the thickness of the thinner outer connected plate. This serves as a control for local buckling requirements. The layout is shown on Fig 5.2.

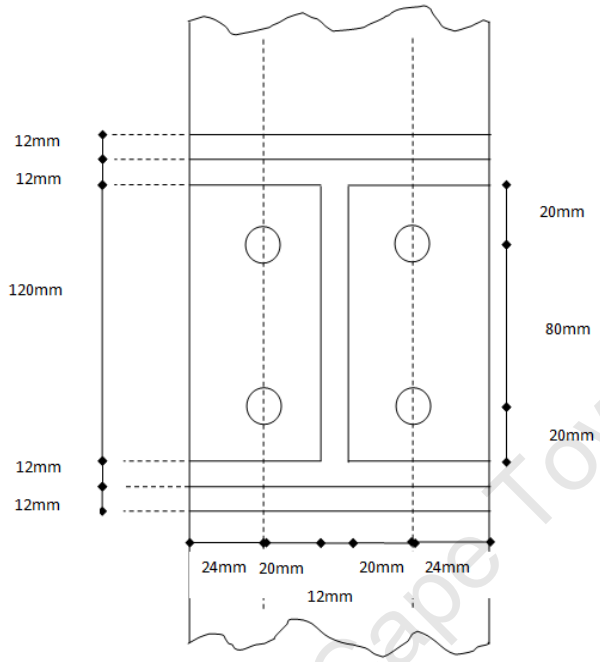

Fig 5.2 Bolting Arrangement for Flush End Plate Connections

Beam and column cross section classification as outlined in Eurocode 9 was carried out to ascertain the susceptibility of the elements to local buckling. This also serves as a basis of determining the ultimate moment of resistance of the beam which is crucial information in accordance with joint classification schemes as connection strength classification, as highlighted in chapter 2 is a measure of the moment resistance of the connection with respect to that of the connected beam. Slenderness parameter values, ß for the beam flange and web are 3.67 and 4 respectively. In the case of the column, the ß values are 3.67 and 5.97 respectively. ε is given by the following relation eq 5.1;

$$\varepsilon = \sqrt{\frac{250}{f_0}} \ldots\ldots\ldots \text{eq } 5.1$$

The cross section classification boundaries as provided by Eurocode 9 being $ß_1$, $ß_2$ and $ß_3$ for internal and outstand elements render both the beam and column members to class 2. This applies as the 6082 T6 alloy is among the heat treated variety, and as such

relevant slenderness parameter boundaries were chosen accordingly. This provides the sections with adequate local buckling resistance such that design can be done without its consideration. This is particularly significant with regards the performance of the beam compression flange very close to the end plate. The ultimate moment of resistance of class 2 members can also be regarded as the plastic moment of resistance of the section given by the relation eq 5.2;

$$M = Zf_d \ldots\ldots\ldots eq\ 5.2$$

Where Z =Plastic Section Modulus

And f_d= Design Value of Strength

5.2 Parametric Combinations

Various combinations of connection geometry were investigated in the parametric study. These include the variation of end plate thickness in the end plate connections, the variation of bolt material and also the effects of web stiffeners in the column section. The effects of utilizing extended end plates are also studied with an additional row of bolts beyond both the tension and compression flanges of the beam.

Parameter	*Plate Material*	*Thickness (mm)*	*Bolt Material*	*Extended End Plate*	*Web Stiffeners*
6mmEP	6082 T6	*6*	Grade10.9 steel	*None*	*None*
8mmEP	6082 T6	*8*	Grade10.9 steel	*None*	*None*
10mmEP	6082 T6	*10*	Grade10.9 steel	*None*	*None*
12mmEP	6082 T6	12	Grade10.9 steel	*None*	*None*
16mmEP	6082 T6	16	Grade10.9 steel	*None*	*None*

Table 5.1 Combination 1 (Effects of Flush End Plate Thickness with Grade 10.9 Steel Bolts and un Stiffened Column Webs)

Parameter	*Plate Material*	*Thickness (mm)*	*Bolt Material*	*Extended End Plate*	*Web Stiffeners*
6mmEPAB	6082 T6	*6*	6082 T6 Aluminum	*None*	*None*
8mmEPAB	6082 T6	*8*	6082 T6 Aluminum	*None*	*None*
10mmEPAB	6082 T6	*10*	6082 T6 Aluminum	*None*	*None*
12mmEPAB	6082 T6	12	6082 T6 Aluminum	*None*	*None*
16mmEPAB	6082 T6	16	6082 T6 Aluminum	*None*	*None*

Table 5.2 Combination 2 (Effects of Aluminum 6082 T6 as Bolt Material)

Parameter	*Plate Material*	*Thickness (mm)*	*Bolt Material*	*Extended End Plate*	*Web Stiffeners*
6mmEPSW	6082 T6	*6*	Grade10.9 steel	*None*	*12mm 6082 T6*
8mmEPSW	6082 T6	*8*	Grade10.9 steel	*None*	*12mm 6082 T6*
10mmEPSW	6082 T6	*10*	Grade10.9 steel	*None*	*12mm 6082 T6*
12mmEPSW	6082 T6	12	Grade10.9 steel	*None*	*12mm 6082 T6*
16mmEPSW	6082 T6	16	Grade10.9 steel	*None*	*12mm 6082 T6*

Table 5.3 Combination 3 (Effects of Aluminum 6082 T6 as Column Web Stiffener Material)

Parameter	*Plate Material*	*Thickness (mm)*	*Bolt Material*	*Extended End Plate*	*Web Stiffeners*
6mmEEP	6082 T6	*6*	Grade10.9 steel	*6mm 6082 T6*	*None*
8mmEEP	6082 T6	*8*	Grade10.9 steel	*8mm 6082 T6*	*None*
10mmEEP	6082 T6	*10*	Grade10.9 steel	*10mm 6082 T6*	*None*
12mmEEP	6082 T6	12	Grade10.9 steel	*12mm 6082 T6*	*None*
16mmEEP	6082 T6	16	Grade10.9 steel	*16mm 6082 T6*	*None*

Table 5.4 Combination 4 (Effects of Extended End Plate with Varying Thicknesses, Grade 10.9 Steel Bolts and un Stiffened Column Webs)

5.3 Moment Rotation Characteristics of Parameters

5.3.1 Combination 1 (EP)

Five different end plate thicknesses were utilized in developing the geometry of the Finite Element model on this parameter Fig 5.3. The results of the load displacement relationship are as given on Table 5.5.

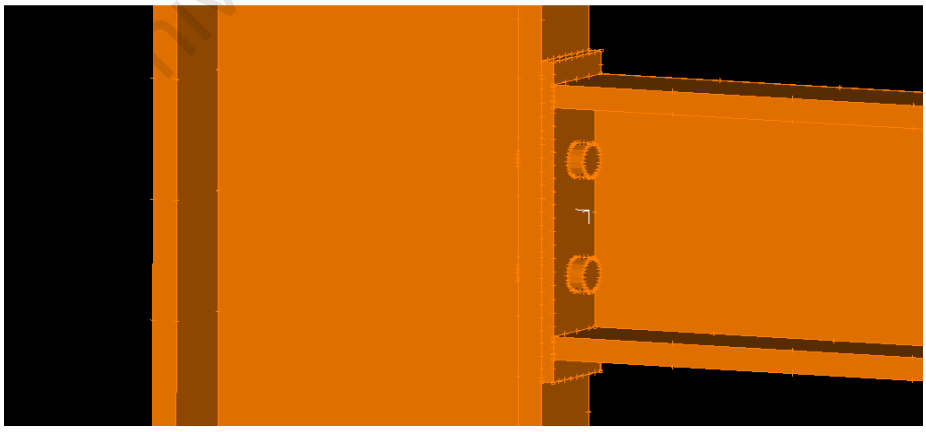

Fig 5.3 Solid Geometry for EP Parameter

6mmEP		8mmEP		10mmEP		12mmEP		16mmEP	
M (kNm)	Θmrad	M (kNm)	Θmrad	M (kNm)	Θmrad	M (kNm)	Θmrad	M (kNm)	Θmrad
0	0	0	0	0	0	0	0	0	0
1	0.71	1	0.71	1	0.64	1	0.58	1	0.49
2	2.39	2	2.19	2	2.08	2	1.70	2	1.23
3	3.61	3	3.35	3	3.17	3	2.59	3	1.86
4.5	5.47	4.5	5.05	4.5	4.76	4.5	3.89	4.5	2.82
6.75	8.82	6.75	7.70	6.75	7.15	6.75	5.84	6.75	4.26
9.75	16.75	9.75	12.21	9.75	10.53	9.75	8.52	9.75	6.28
12.75	36.54	12.75	20.61	12.75	14.62	12.75	11.56	12.75	8.54
15.75	107.17	15.75	41.07	15.75	20.79	15.75	15.48	15.75	11.19
		18.75	99.26	18.75	32.34	18.75	21.61	18.75	14.41
				21.75	102.66	21.75	32.92	21.75	18.37
						24.75	61.57	24.75	23.56
								27.75	30.6
								30.75	41.42

Table 5.5 Moment Rotation Data for EP Parameter

From the Moment – Rotation plots Fig 5.4 the lowest value for connection strength 15.75kNm, was recorded from the 6mmEP model, with a maximum rotation in excess of 100mrad. The 16mmEP parameter recorded the highest strength attaining a moment of 30.75kNm but was however characterized by limited rotation capacity of 41.42mrad. The curves generated by the FEM results were relatively smooth with the elastic and post elastic portions evident. Connection strength and stiffness increased with end plate thickness but however resulted in reduced ductility.

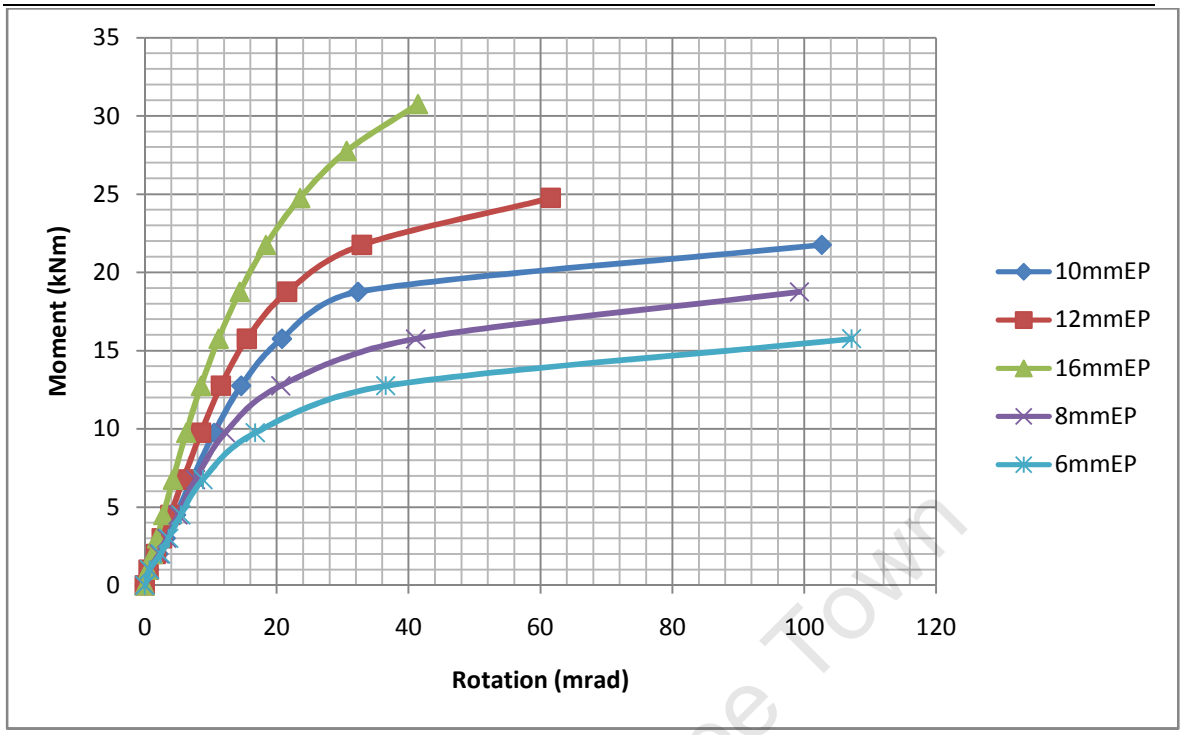

Fig 5.4 Moment – Rotation Curves for EP Parameter

Stress band plots were generated for a typical model within this parameter to show both the buckling configuration and the stress propagation around the area of the connection as shown on Fig 5.5. The stress band plots of the end plate and the bolts can also be seen on Fig 5.6 and 5.7.

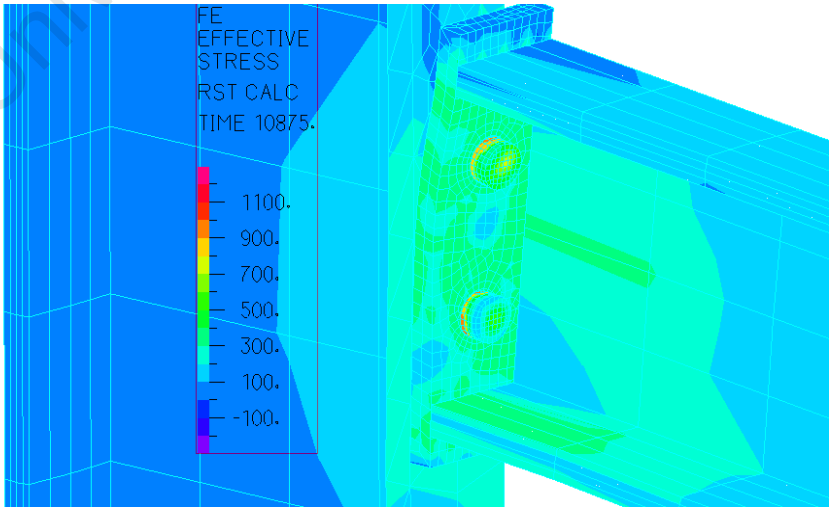

Fig 5.5 Typical Connection Stress Band Plot for EP Parameter

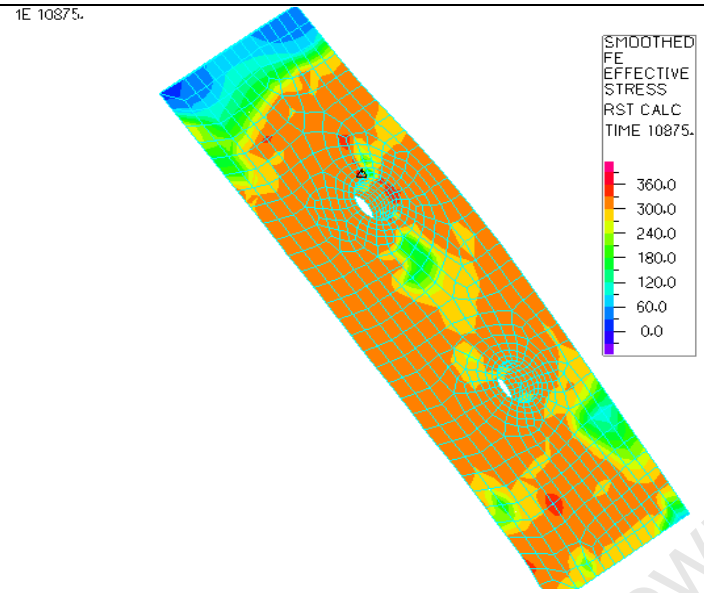

Fig 5.6 Typical Deformed End - Plate Stress Band Plot for EP Parameter

It can be seen from the plots that the bolt closest to the tension flange of the beam developed the greatest magnitude of stress of within the region of 950MPa, whereas the end plate developed stresses within the range of 330MPa with the highest stress recorded at the bolt hole closest to the tension flange.

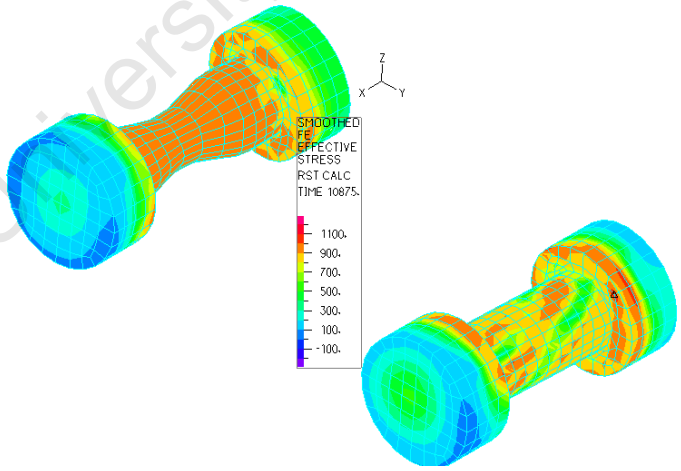

Fig 5.7 Typical Deformed Bolt Stress Band Plot for EP Parameter

5.3.2 Combination 2 (EPAB)

One of the main advantages of aluminum as a structural material as documented by various researchers and by virtue of its material properties is its superior corrosion resistance as compared to steel. It is however noteworthy that aluminum alloys such as 6082 T6, which is the primary material property utilized in this research is characterized by yield strength F_y within the range of 330 MPa. This is well within the yield strength values of some mild steel materials. This parameter investigates the use of aluminum bolts in the same geometrical configuration as in Combination 1. The method utilized in generating the geometry and mesh is the same as in Combination 1and the response is as seen on Table 5.6.

6mmEPAB		**8mmEPAB**		**10mmEPAB**		**12mmEPAB**		**16mmEPAB**	
M (kNm)	Θmrad	M (kNm)	Θmrad	M (kNm)	Θmrad	M (kNm)	Θmrad	M (kNm)	Θmrad
0	0	0	0	0	0	0	0	0	0
0.4	0.586	0.5	0.653	0.5	0.66	0.7	0.78	0.4	0.17
0.9	1.34	1.125	1.54	1.125	1.53	1.57	1.80	0.8	0.45
1.95	2.91	2.438	3.34	2.438	3.32	3.41	3.92	1.2	0.68
3.15	4.75	3.938	5.58	3.938	5.39	5.51	6.73	1.8	1.03
4.35	7.11	5.438	10.02	5.438	7.95	7.61	13.92	2.7	1.54
5.55	11.65	6.938	20.74	6.938	13.32	9.71	37.99	3.9	2.24
6.75	20.87	7.688	32.12	8.418	23.43	10.43	74,65	5.1	2.96
7.35	29.96							6.3	3.73
								7.5	4.55
								8.7	5.44
								9.9	6.41

Table 5.6 Moment Rotation Data for EPAB Parameter

As evident in the table and moment rotation plots, endplate connection with aluminium bolts are characterized by much reduced strengths.

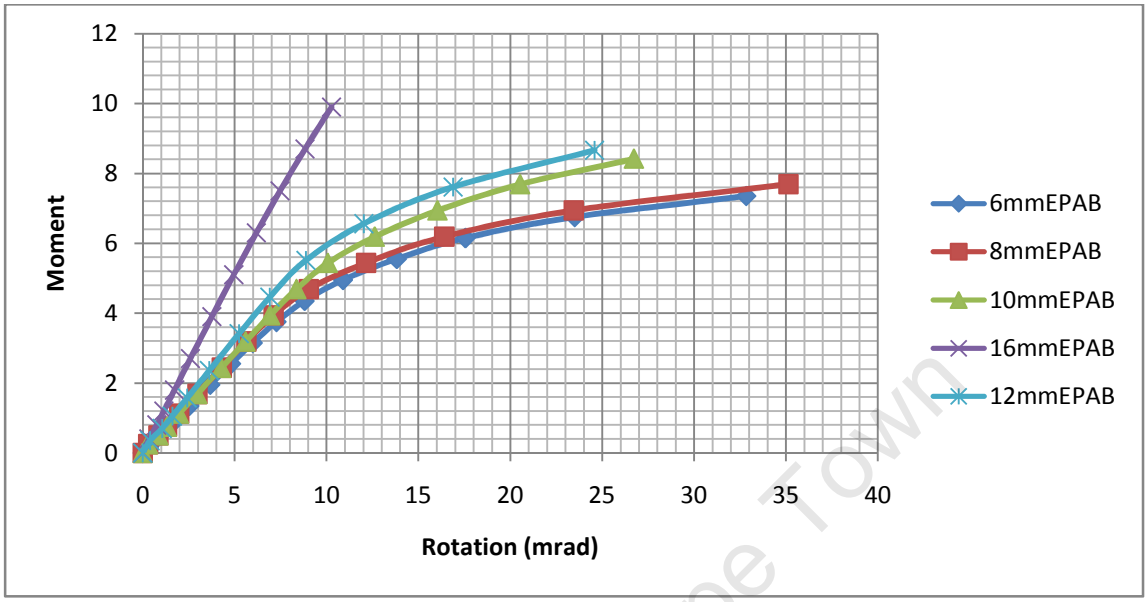

Fig 5.8 Moment – Rotation Curves for EPAB Parameter

Fig 5.8 shows the moment – rotation curves for the EPAB parameter.The connection with the 16mm end plate attained a strength of 9.9kNm prior to failure whilst the 6mm end plate recorded 7.35 as its maximum moment before failure. The relation ship between end plate thickness, connection strength, ductility and stiffness remains the same as in the EP parameters.

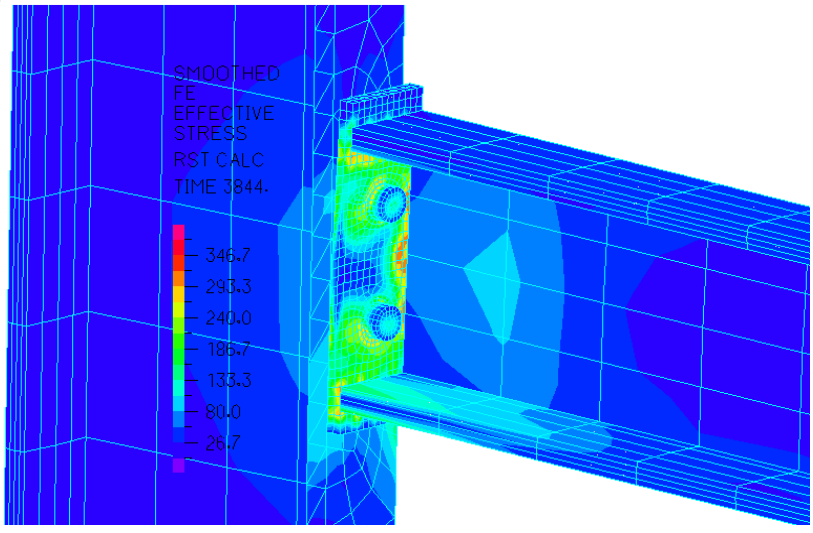

Fig 5.9 Typical Connection Stress Band Plot for EPAB Parameter

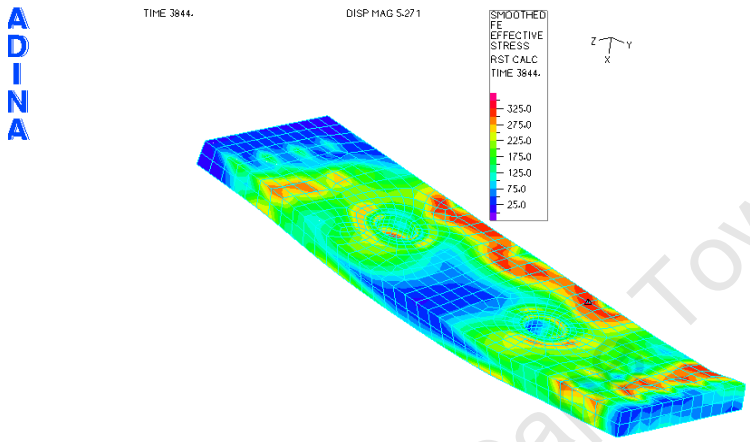

Fig 5.10 Typical Deformed End - Plate Stress Band Plot for EPAB Parameter

The lower yield strength aluminum bolts, failed quite prematurely leaving other components of the connection namely, endplate, column web and flange with comparatively low stresses below their ultimate capacities.A typical band plots of the stress on the endplate, bolts, beam and column webs are as seen on Fig 5.9, 5.10 and 5.11.

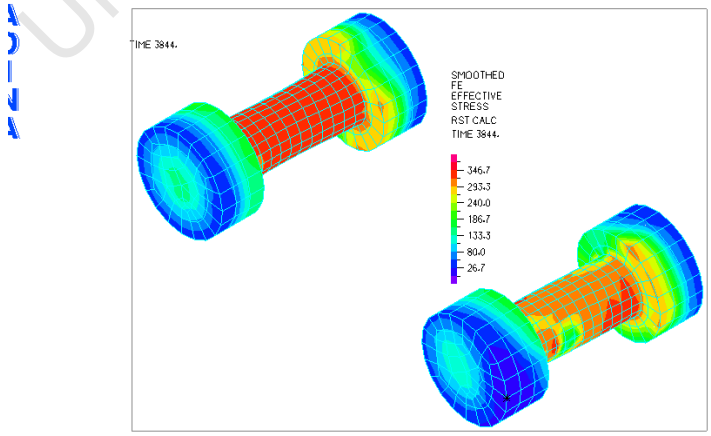

Fig 5.11 Typical Deformed Bolt Stress Band Plot for EPAB Parameter

5.3.3 Combination 3 (EPSW)

12mm Aluminum 6086 T6 tension and compression stiffeners were included into the geometrical configuration Fig 5.12 and the resulting moment rotation characteristics is as seen on Table 5.7**.**

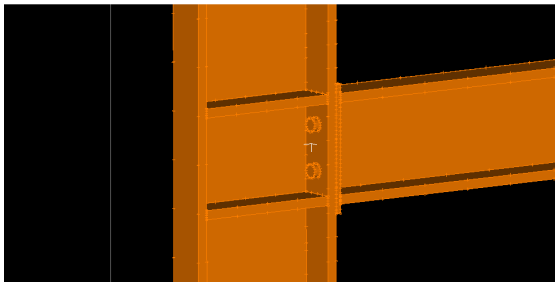

Fig 5.12 Solid Geometry for EPSW Parameter

6mmEPSW		**8mmEPSW**		**10mmEPSW**		**12mmEPSW**		**16mmEPSW**	
M (kNm)	Θmrad	M (kNm)	Θmrad	M (kNm)	Θmrad	M (kNm)	Θmrad	M (kNm)	Θmrad
0	0	0	0	0	0	0	0	0	0
1	0.46	1	0.71	1	0.62	1	0.62	1.5	0.87
2	2.26	2	1.90	2	1.77	2	1.56	3	1.87
3	3.48	3	2.86	3	2.66	3	2.35	4.5	2.82
4.5	5.30	4.5	4.32	4.5	3.99	4.5	3.53	6.73	4.35
6.75	8.73	6.75	6.63	6.75	6.03	6.75	5.30	10.12	6.96
9.75	17.47	9.75	10.38	9.75	8.90	9.75	7.73	14.62	11.41
12.75	40.47	12.75	17.39	12.75	12.57	12.75	10.48	19.12	18.09
15.75	104.67	15.75	33.26	15.75	18.33	15.75	14.13	23.62	29.98
		18.75	75.98	18.75	28.48	18.75	20.35	28.12	53.65
				21.75	59.31	21.75	32.70		
						24.75	69.92		

Table 5.7 Moment Rotation Data for EPSW Parameter

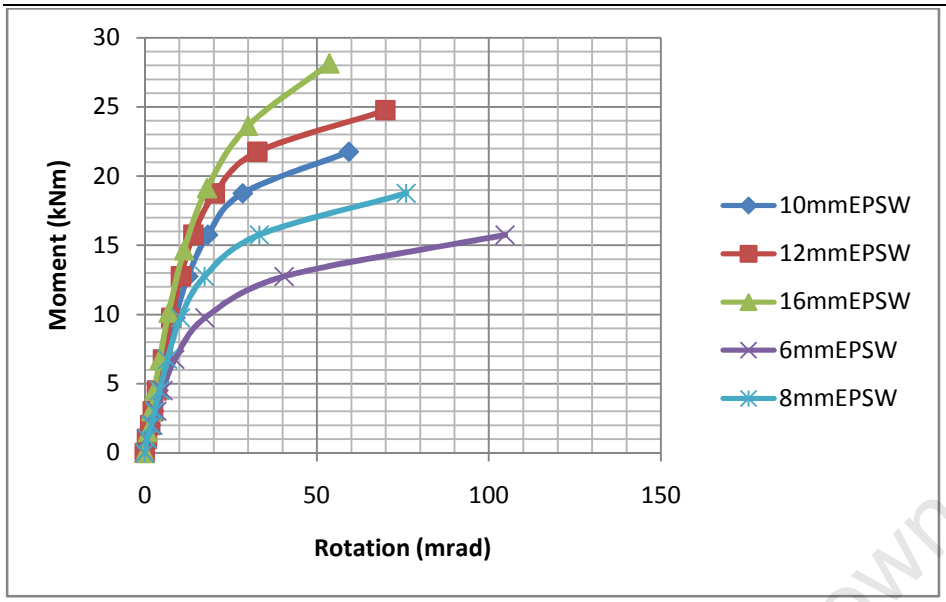

Fig 5.13 Moment – Rotation Curves for EPSW Parameter

The 16mm end plate connection 16mmEPSW attained strength of 28.12kNm in this case, whilst the 6mmEPSW recorded up to 15.75kNm before failure. Furthermore, the same relationship as in the other parameters with regards end plate thickness, strength, ductility and stiffness held sway Fig 5.13.

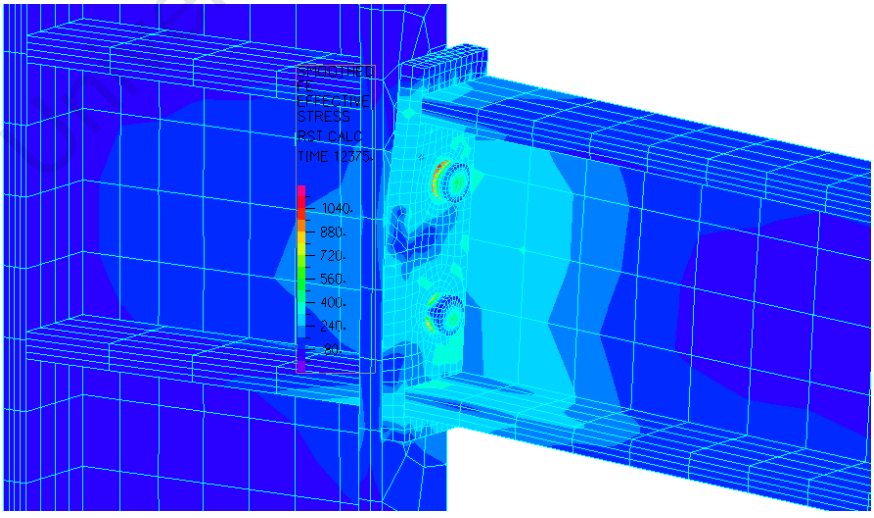

Fig 5.14 Typical Connection Stress Band Plot for EPSW Parameter

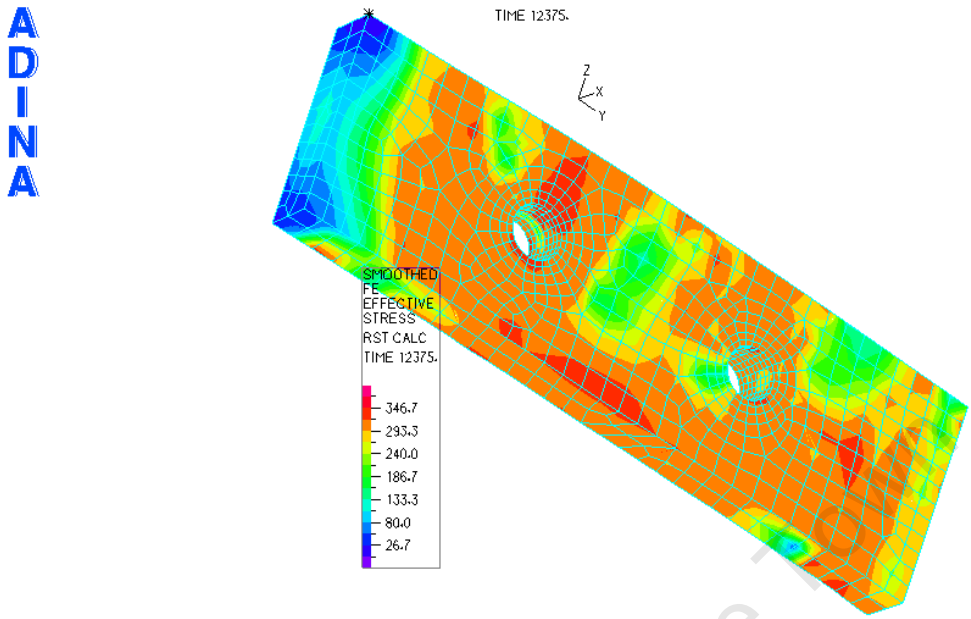

Fig 5.15 Typical Deformed End - Plate Stress Band Plot for EPSW Parameter

As in the EP parameter, the bolt closer to the tension flange developed stresses much faster than the lower bolt and eventually reached its ultimate value causing failure. The entire shank of the highly stressed bolt as shown on Fig 5.16 recorded stress of up to 1040Mpa and beyond at failure as compared to the bolt close to the compression flange.

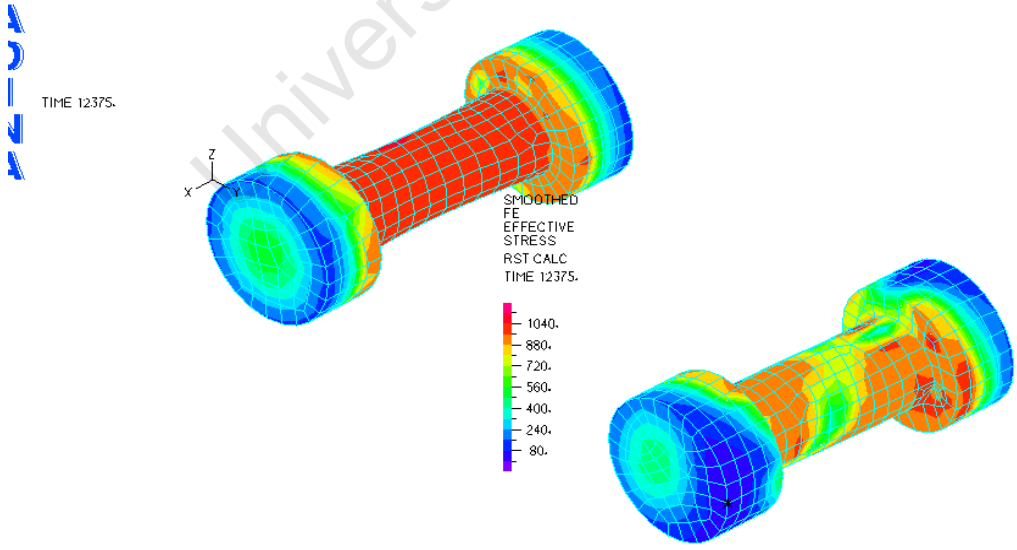

Fig 5.16 Typical Deformed Bolt Stress Band Plot for EPSW Parameter

5.3.4 Combination 4 (EEP)

An additional row of bolts was generated beyond both the tension and compression flanges to see the amount of strength gained in terms of the increase in the moment capacity of the connection. This was done in line with the provisions of Eurocode 9 and Aluminum Design Manual {15} and {19} with regards edge and end spacing Fig 5.17. The resulting stresses developed by the bolts and the end plate as well as the flanges and webs of the connected members of the assembly were again monitored under incremental loading. Table 5.8 shows the resulting moment rotation characteristics of this arrangement.

Fig 5.17 Solid Geometry for EEP Parameter

6mmEEP		8mmEEP		10mmEEP		12mmEEP		16mmEEP	
M (kNm)	Θmrad	M (kNm)	Θmrad	M (kNm)	Θmrad	M (kNm)	Θmrad	M (kNm)	Θmrad
0	0	0	0	0	0	0	0	0	0
1	0.47	1	0.45	1	0.45	1	0.41	1	0.38
2	1.24	2	1.07	2	1.05	2	0.89	2	0.79
3	1.87	3	1.62	3	1.59	3	1.34	3	1.19
4.5	2.81	4.5	2.43	4.5	2.40	4.5	2.01	4.5	1.79
6.75	4.22	6.75	3.65	6.75	3.62	6.75	3.02	6.75	2.68
9.75	6.17	9.75	5.29	9.75	5.24	9.75	4.37	9.75	3.88
12.75	8.42	12.75	7.02	12.75	6.91	12.75	5.72	12.75	5.07
15.75	11.56	15.75	8.97	15.75	8.67	15.75	7.09	15.75	6.28
18.75	16.70	18.75	11.36	18.75	10.64	18.75	8.51	18.75	7.51
21.75	25.08	21.75	14.65	21.75	12.89	21.75	10.09	21.75	8.78
24.75	39.05	24.75	19.83	24.75	15.57	24.75	11.95	24.75	10.13
27.75	57.47	27.75	28.31	27.75	19.01	27.75	14.30	27.75	11.64
		30.75	44.55	30.75	24.11	30.75	17.50	30.75	13.39
				33.75	31.93	33.75	21.97	33.75	15.56
						36.75	28.96	36.75	18.57
								39.75	23.66
								40.00	24.22

Table 5.8 Moment Rotation Data for EEP Parameter

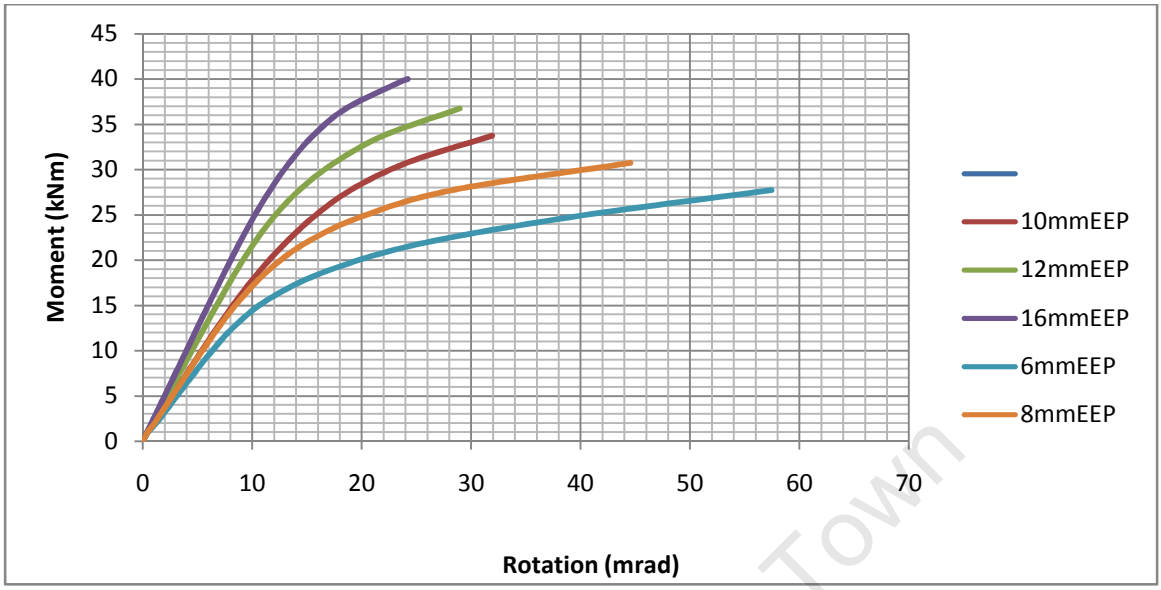

Fig 5.18 Moment – Rotation Curves for EEP Parameter

In this instance as well, the relationship between end plate thickness and connection stiffness, strength and ductility remained the same however with different individual strengths for each parameter as expected. The 16mmEEP parameter recorded strengths of up to 40kNm with a steady decline of strength to 27.75kNm for the6mmEEP connection.

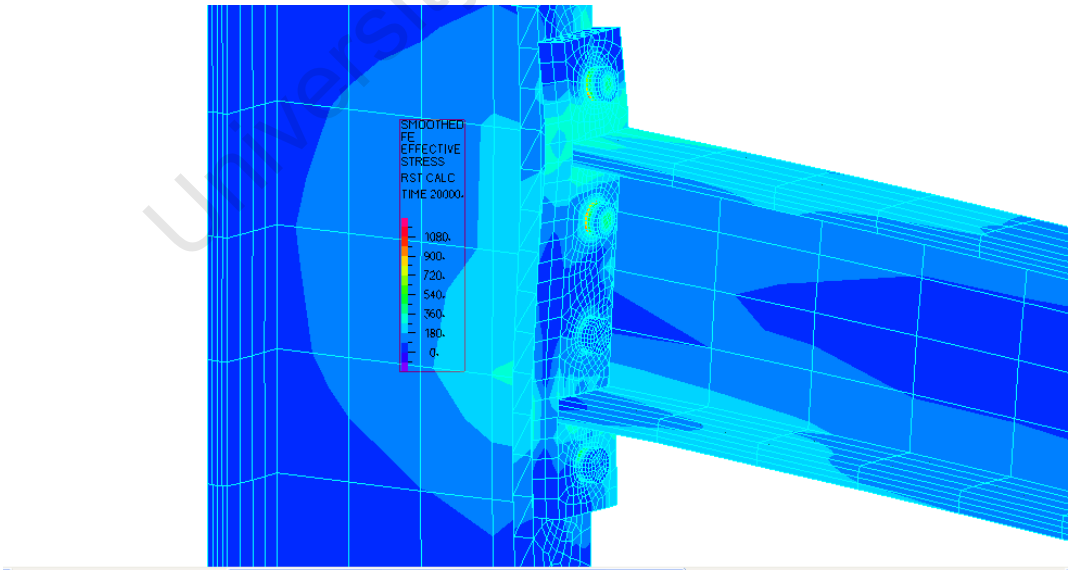

Fig 5.19 Typical Connection Stress Band Plot for EEP Parameter

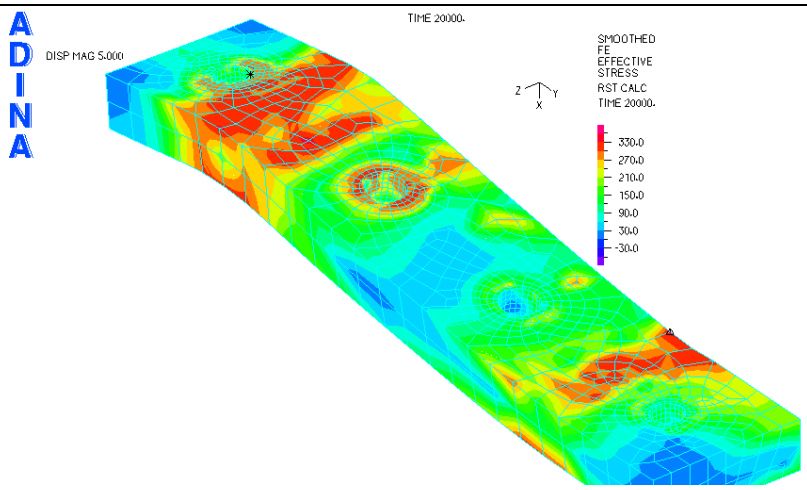

Fig 5.20 Typical Deformed End - Plate Stress Band Plot for EEP Parameter

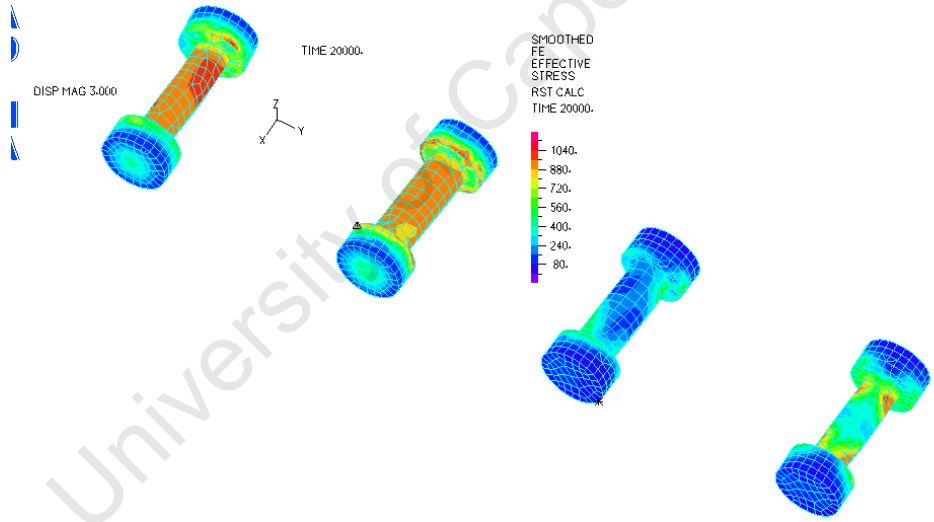

Fig 5.21 Typical Deformed Bolt Stress Band Plot for EEP Parameter

The resulting stress distributions as evident from the generated stress band plots showed high stress concentrations within the locality of the bolt holes, particularly those on either side of the tension flange Fig 5.21. High stress concentrations were also observed at the end plate beam flange intersections for both the tension and compression flanges as seen on Fig 5.20. Since one of the limitations of the research is that the welds have not been modeled, the stress distributions at these points needs to be studied closely with reference

to the effects of the HAZ and consequent loss of strength at the welds. The bolts closer to the tension flange of the beam demonstrated high tensile stresses as expected Fig 5.21.

CHAPTER 6

DISCUSSION OF RESULTS

6.1 The Effect of Geometry on Connection Behavior.

The load deflection curves of the various parameters as outlined in chapter 5 is plotted for each end plate thickness as seen on Figs 6.1 – 6.5. The effect of the geometry of the connections can be seen on each of these plots for the different thicknesses of end plates. There is not much difference between the EP and the EPSW plots from the diagrams. This is expected as the moment of area of the column member is substantially larger than that of the beams thus providing it with a superior stiffness. However, the stresses generated on the column webs for the stiffened members are substantially lower.

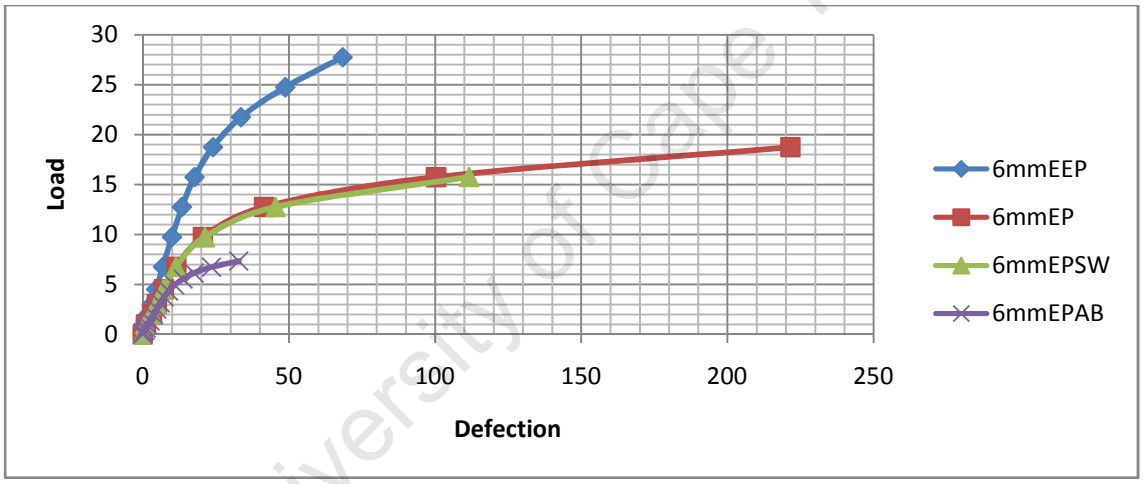

Fig 6.1 Load Deflection Curves For 6mm End Plates

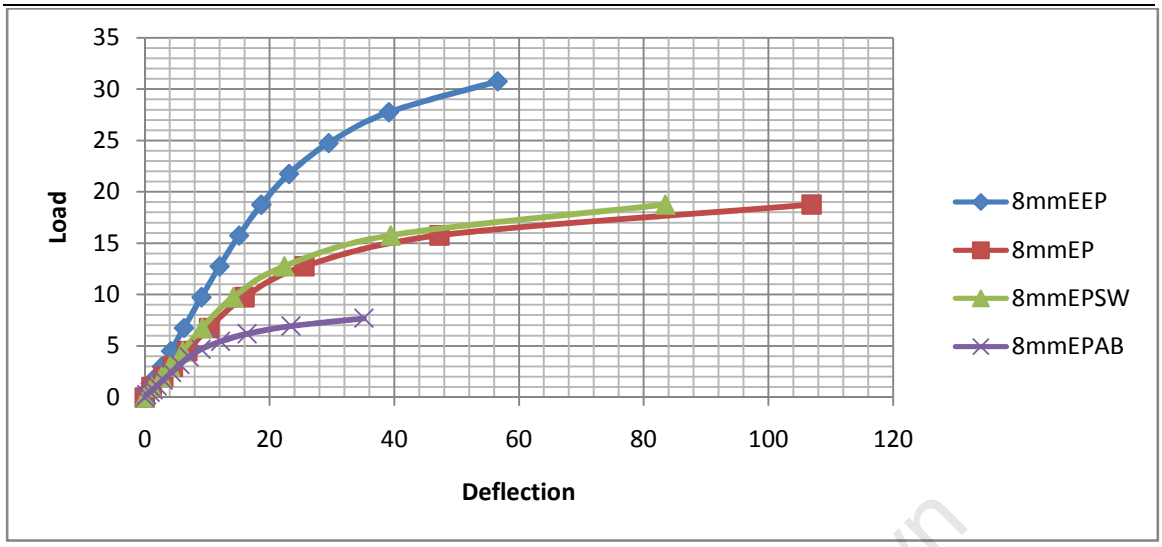

Fig 6.2 Load Deflection Curves For 8mm End Plates

The EEP connections demonstrate higher initial stiffness and strength as compared to the EP, EPSW and EPAB connections. This matches results obtained by earlier research work on steel end plate connections {14}. EP and EPSW connections demonstrate much lower initial stiffness's and strengths whilst EPAB connections are characterized by very low strengths due to premature bolt failure.

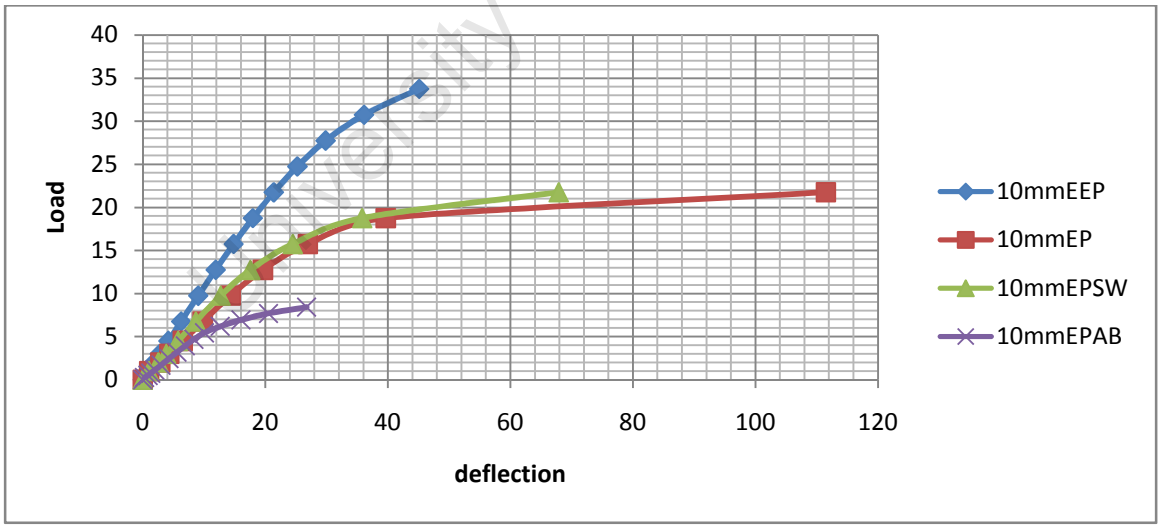

Fig 6.3 Load Deflection Curves For 10mm End Plates

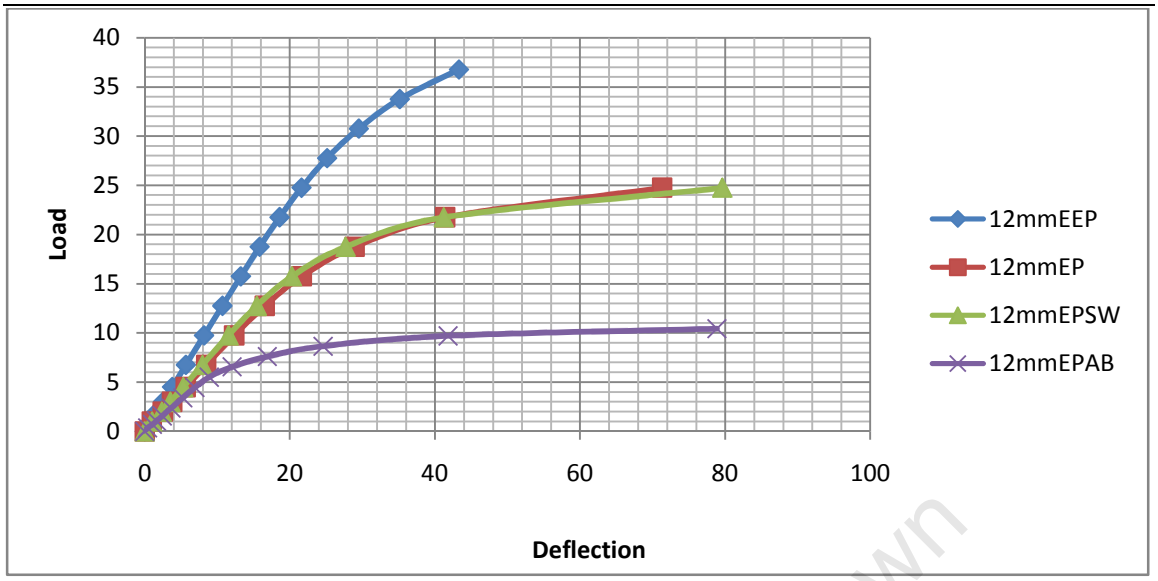

Fig 6.4 Load Deflection Curves For 12mm End Plates

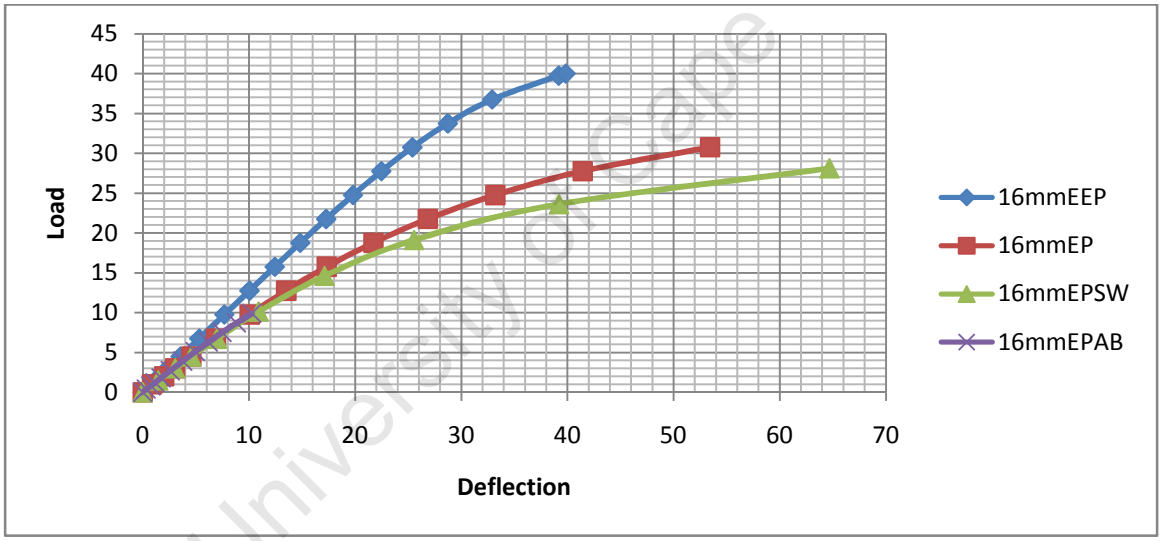

Fig 6.5 Load Deflection Curves For 16mm End Plates

It can clearly be seen that the there is a direct relationship between connection strength, stiffness and ductility as documented by previous research on similarly connected steel end plate connections {14}{23}{25}. Connections with thicker end plates such as the 16mmEP showed much higher strength as characterized by the ultimate moments attained prior to failure. It however exhibited much reduced ductility compared to the thinner end plates 6mmEP. The relationship between initial stiffness and end plate thickness can also be seen by the slope of the moment - rotation curve at the origin of the plots as shown on Figs 5.4, 5.8, 5.13 and 5.18. The plots were derived from data

obtained from the FEM model post processing feature. A nodal point was defined at the tip of the cantilever part of the assembly. A value list of the y-displacement within the response range of the load steps defined in the time function. The values obtained as such were then subtracted from the individual beam elastic deflections within the same response range and the resulting rotation calculated by simple trigonometry. As evident from Fig 6.1 – 6.5, the plots were relatively smooth with the elastic and plastic parts of the curves clearly visible in line with the plastic bilinear material model utilized.

6.2 Equivalent T-Stub Behavior

The deformation pattern of the extended end plate at the point of intersection of the tensile flange of the beam is similar to that of equivalent T stub as researched by G De Matteis et al {9}.

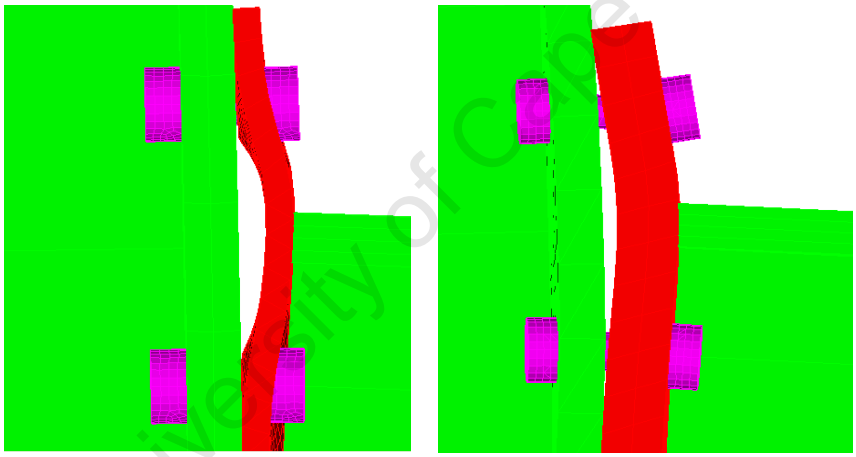

Fig 6.6 Equivalent T-stub Anology for 6mmEEP and 16mmEEP Parameters

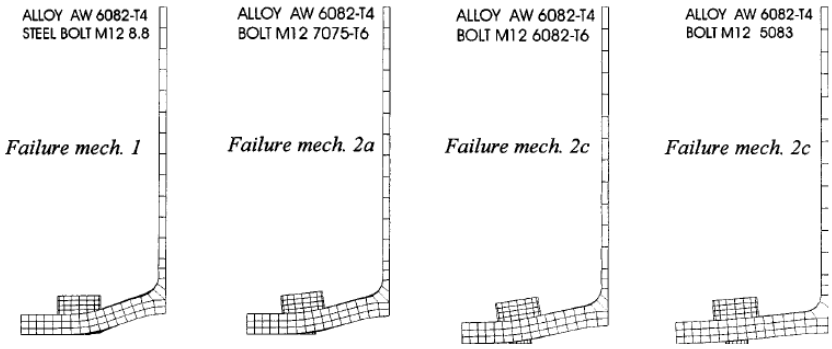

Fig 6.7 Aluminum T- Stub Failure Mechanisms from {9}

It can be observed that the deformation pattern exhibited by the equivalent T-Stub of the 6mmEEP model closely matched that of failure mechanism 1 as documented by {9}, whereas that of the 16mmEEP model tended towards the failure mechanism 2c. This follows from the strength of the bolt material in all cases being grade 10.9 causing a plastic hinge to develop on the thinner plate. In the case of the 16mm plate, the additional rigidity characteristic of the thicker plate coupled with substantial prying force resulted in bolt elongation as seen in Fig 6.6.

6.3 Stress Variations on End Plate and Bolts with Incremental Deformation

An analysis was carried out to monitor the rate of increase in stresses on both the End plate Bolt holes and the bolts. The assemblies with 10mm thick end plates were investigated in this analysis and model points were defined on the mesh element carrying the greater stress based on the band plots generated and output data. The bolt and bolt hole stresses closest to the tension flange of the beam were plotted for the EP, EEP, EPSW and EPAB parameters and shown on Figs 6.8- 6.11.

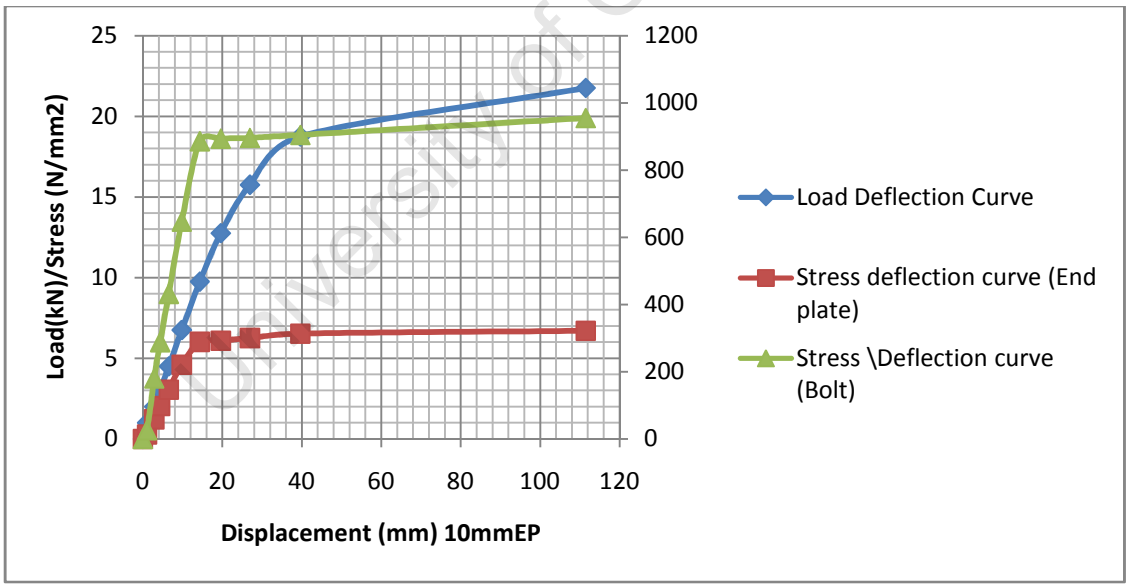

Fig 6.8 Variation of Bolt and End Plate (Bolt Hole) Stress With Displacement (10mmEP)

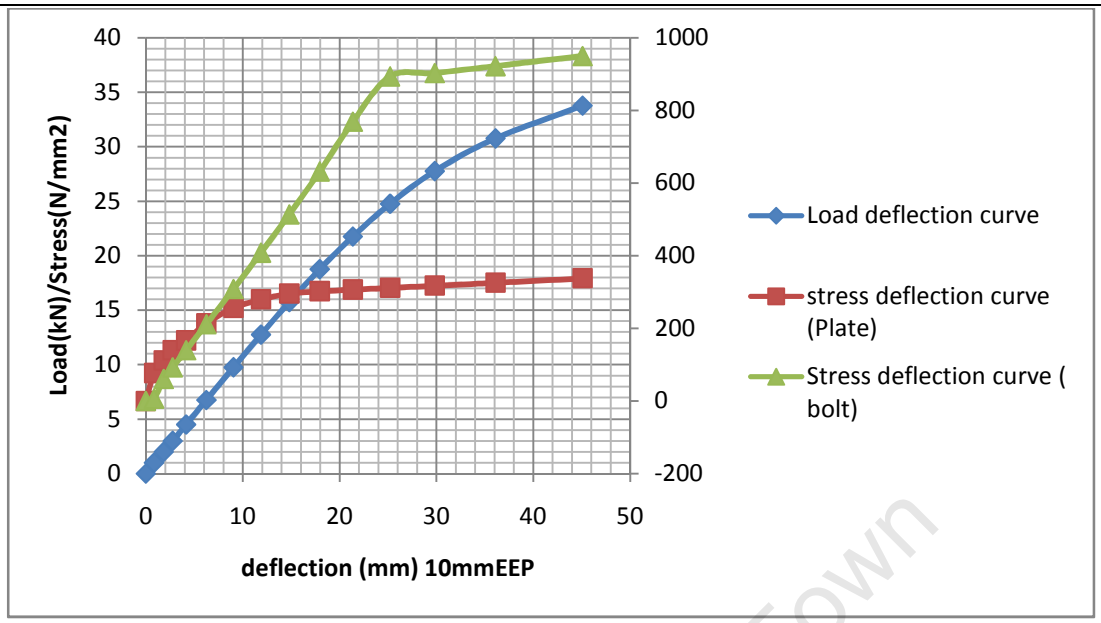

Fig 6.9 Variation of Bolt and End Plate (Bolt Hole) Stress With Displacement (10mmEEP)

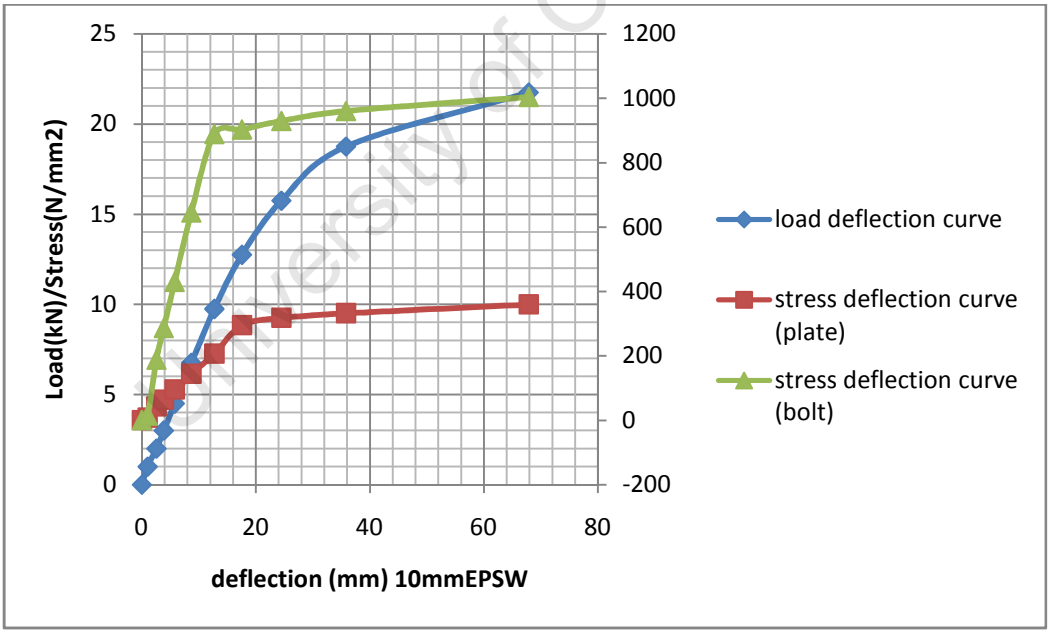

Fig 6.10 Variation of Bolt and End Plate (Bolt Hole) Stress With Displacement (10mmEPSW)

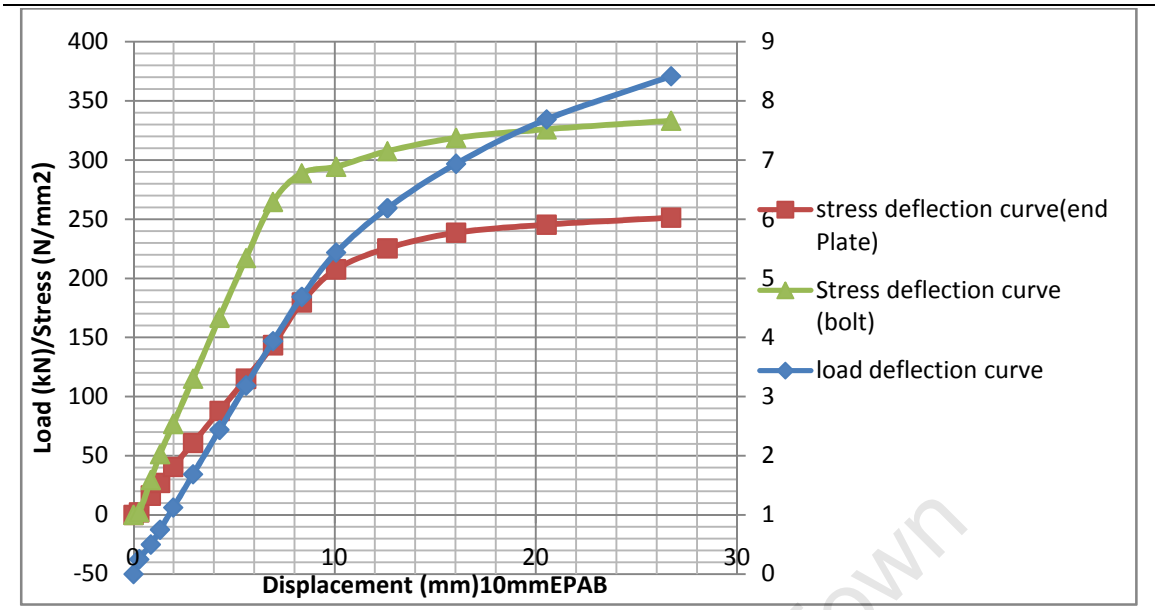

Fig 6.11 Variation of Bolt and End Plate (Bolt Hole) Stress With Displacement (10mmEPAB)

The stress increase in the bolts appears to be much steeper in the EP and SW assemblies as compared to that of the EEP connection. This can be seen from the Fig 6.12 where bolt stress is plotted with deflection. At a deflection of 8mm, stresses in the bolt are in the region of 600MPa whereas for the EEP connection, it takes a deflection of the order of 18mm for 600MPa stress to be generated. In the case of the stress on the end plate bolt holes, the reverse seems to occur as stress are generated much faster in the EEP assembly than in the other two parameters. This could be explained by the presence of an additional row of bolt above the tension flange which actually relieves some of the stress on the bolts immediately below the tension flange. Being that the moment resistance of the joint is generated by couples with the centre of rotation at the compression flange or at the bottom edge of the end plate as the case may be, additional moment capacity is generated by this extra row of bolts which creates a connection with a much larger initial stiffness. The additional bolt row above the tension flange, which can be idealized as an equivalent t-stub, acts to share the tensile force being generated by this flange.

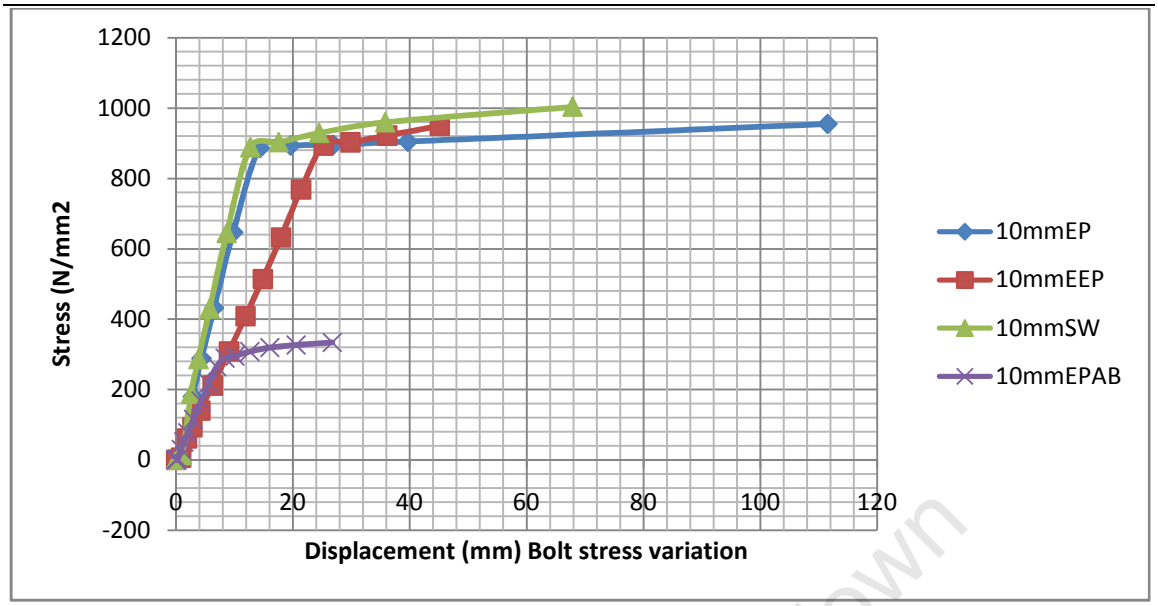

Fig 6.12 Variation of Bolt Stress With Displacement All Parameters (10mm) End Plates

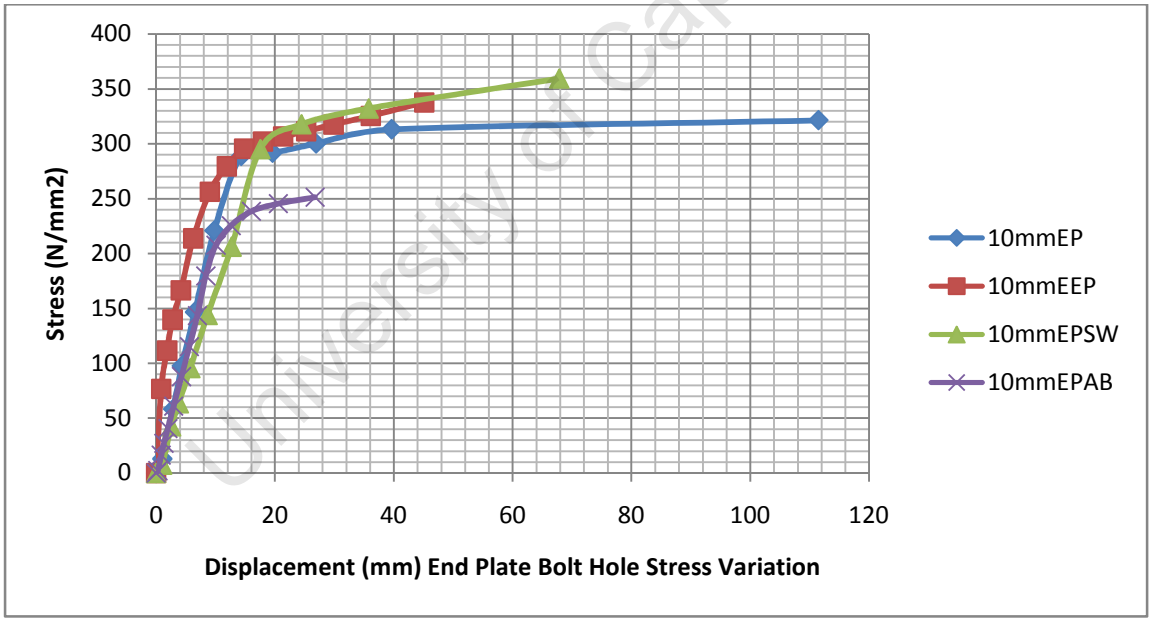

Fig 6.13 Variation of Bolt Hole Stress on End Plate, All Parameters (10mm) End Plates

6.4 Stress Variations on End Plate / Tension Flange Joint

The fabrication of end plate connections primarily involves the welding of the beam element to the designed thickness of end plate, at the edge to be assembled with the column, in beam to column connections. The welding procedure which leads to reduced

material strength in areas of close proximity to the weld (HAZ), and indeed the weld itself is worthy of investigation as it is oftentimes a source of connection failure in end plate connections. Eurocode 9 specifies a heat softening factor ρ_{haz} as 0.65 for 6xxx series aluminum alloys, supplied as extrusions, sheet and plate in the T6 condition for MIG welding, and as 0.5 for TIG welding. Thus characteristic strengths will have to be multiplied by these factors for the actual post welded strength to be obtained. Although the welds and the effects of the heat affected zone (HAZ) were not considered in the modeling process due to the already elaborate bolt modeling process, their effects in areas of high stress which are potential weld locations in fabrication procedures can be evaluated by monitoring the stress levels as the loading process is carried out through the time step feature. As such, the elements connecting the tension flange and the end plate were monitored for stress increments with load and these were recorded for further analysis. Data for the EEP parameter in this respect is seen on Table 6.1. Considering ultimate limit state, the percentage loss of strength at the HAZ for MIG will render the ultimate tensile strength of the alloy (6082 T6) to be reduced from 330MPa to about 214.5MPa. It can be seen as expected that end plate thickness plays an important role in the rate of stress development in the assemblies. There is a marked decrease in the strengths of the connections if the HAZ on the tension flange is to be taken into account. Although the 16mm End plate (16mmEEP) records strengths of up to 40kNm, it could well be the case that if connections of this nature were fabricated and tested, the predominant failure mode will be tensile cracks on the tension flange within close proximity of the weld induced HAZ. Most of the connections recorded 0.65Fy at about 30% of their strengths based on the ADINA results.

P (kN)	HAZ Stress (MPa)				
	6mmEEP	8mmEEP	10mmEEP	12mmEEP	16mmEEP
0	0	0	0	0	0
1	19.75	17.02	21.06	19.74	18.05
2	56.37	38.53	49.31	44.6	38.39
3	85.09	58.12	74.06	67.25	57.73
4.5	127.7	87.16	111.25	100.87	86.6
6.75	187.75	130.82	167.09	151.31	129.89
9.75	239.76	196.53	234.45	204.27	185.57
12.75	259.61	241.63	262.95	243.98	219.96
15.75	278.85	262.14	284.19	263.43	251.11
18.75	292.87	273.47	294.29	272.73	263.82
21.75	309.3	279.67	298.58	283.37	270.9
24.75	319.15	289.43	303.04	295.65	278.38
27.75	326.87	303.42	307.62	301.64	288.36
30.75		316.92	313.2	306.63	294.71
33.75			318.07	311.17	301.53
36.75				316.01	307.85
39.75					313.59
40					314.11

Table 6.1 Stress Increase in T-Stub of EEP parameters

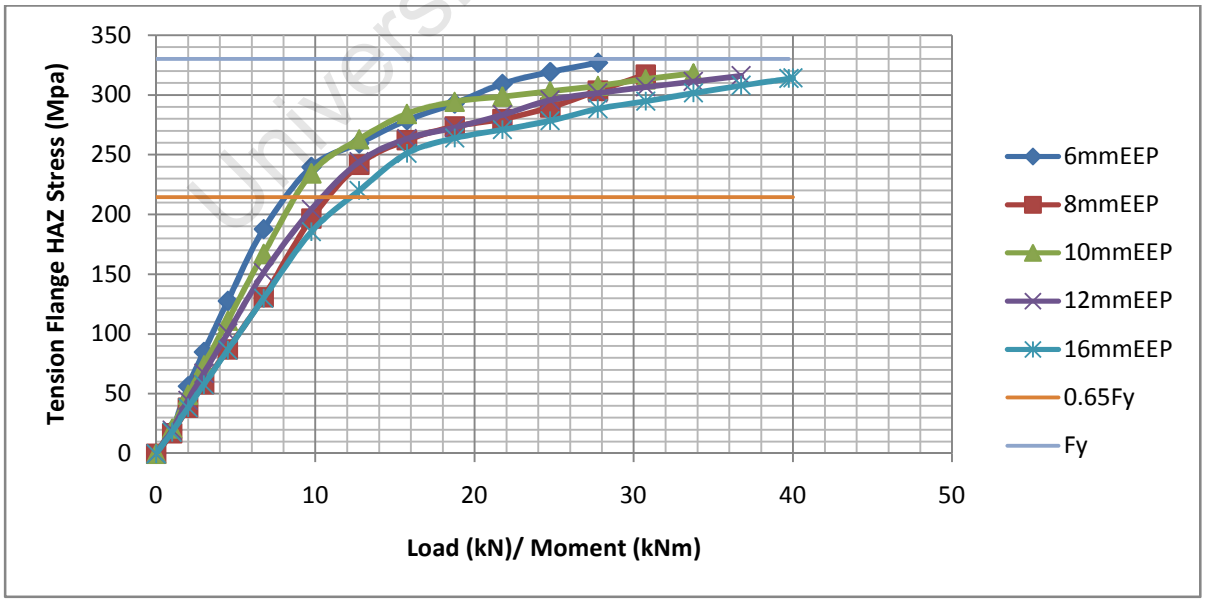

Fig 6.14 Stress Increase in T-Stub of EEP Parameters

CHAPTER 7

CONCLUSIONS AND RECOMMENDATIONS

7.1 Introduction

End plate connections prove to be useful in structural design due to their relative ease of fabrication and erection in practical circumstances. They are mainly utilized where there is a desire for high strength and stiffness to be attained. The design of aluminum end plate connections with enough moment capacity to match that of the connected member proves to be much more delicate than in the case of steel for reasons based on the material properties. Reduced flexural rigidity due to lower young's modulus E renders aluminum beams and frames to be more susceptible to higher deformations under loading. Although the behavior of simple connections is not covered in this work, it is expected that huge demands will not be placed on these connection types as in moment connections due to the fact that they transmit minimal moments in beam to column connections and are mainly characterized by the shear capacity of the attached bolts and bolt hole bearing. Thus the demands on moment connections prove to be greater and require much scrutiny for optimized designs to be achieved capable of satisfying structural requirements.

7.2 Conclusions

The ability of the utilized FEM package ADINA to reproduce moment rotation relationships of beam-column end plate connections based on existing data used in chapter 4 from (Coelho A, M, and Bijlaard, F, 2006) {14} provides substantial confidence going forward in this research area given that the data collected in this work was done with relatively sophisticated equipment compared to that of similar work done much earlier. Although the effects of the heat affected zone HAZ was not considered, the data from stress plots obtained from the models were able to predict possible failures due to HAZ related material inconsistencies on the tension flange of the connected beams. This is particularly useful as endplate connections in reality are a combination of bolted and welded assemblies. As such both of these aspects of the design must be taken into consideration.

The classification as shown in Table 7.1 shows all connections of the EP, EPSW and EPAB in the semi rigid category with regards to the stiffness category. Only the connections with aluminum bolts EPAB fell under the nominally pinned classification with regards to strength. This can be attributed to the untimely bolt failure in these connections with the bolt stresses reaching the yield strength f_y of the alloy 6082 T6 quite early in the loading process. Only the 12mmEEP and the 16mmEEP parameters attained the rigid criterion for stiffness classification, but were not able to develop full strength characterized by the plastic moment of the beam, M_p. The effects of the HAZ monitored for the EEP parameter by extracting stress increments close to the tension flange weld suggests that strength may be curtailed to as little as 30% of the recorded values due to weld failure or tension flange cracking close to the HAZ. Thus the welding process remains the most delicate feature in the fabrication of such connections and the quality will largely determine the capacity to attain the design strength.

7.3 Classification of Connections

The behavior of connections as stated earlier is critical in the analysis of structural systems. Connection failure is oftentimes the cause of loss of structural integrity in a system and as such its importance cannot be overemphasized, and are typically classified by their ability to restore the stiffness, strength and ductility of the connected structural elements. This phenomenon is the framework upon which the various classification systems are based {1}{2}{16}. The connections analyzed using the Finite Element software ADINA have provided data obtained by the moment rotation characteristics through which they can be classified using any of the classification systems that have been proposed. The connections will now be classified comparatively using the Eurocode 3 system with a 3m beam length as a reference.

Connection	Initial stiffness $S_{j,ini}$ (kNm/rad)	Moment Resistance $M_{j,Rd}$ (kNm)	Stiffness Classification	Strength Classification
6mmEEP	2092	28	semi-rigid	partial strength
8mmEEP	2192	31	semi-rigid	partial strength
10mmEEP	2202	34	semi-rigid	partial strength
12mmEEP	2436	37	rigid	partial strength
16mmEEP	2621	39	rigid	partial strength
Connection	**Initial stiffness $S_{j,ini}$ (kNm/rad)**	**Moment Resistance $M_{j,Rd}$ (kNm)**	**Stiffness Classification**	**Strength Classification**
6mmEP	830	16	semi-rigid	partial strength
8mmEP	895	19	semi-rigid	partial strength
10mmEP	946	21	semi-rigid	partial strength
12mmEP	1157	25	semi-rigid	partial strength
16mmEP	1610	30	semi-rigid	partial strength
Connection	**Initial stiffness $S_{j,ini}$ (kNm/rad)**	**Moment Resistance $M_{j,Rd}$ (kNm)**	**Stiffness Classification**	**Strength Classification**
6mmEPAB	682	7.2	semi-rigid	Nominally pinned
8mmEPAB	765	7.6	semi-rigid	Nominally pinned
10mmEPAB	757	8.4	semi-rigid	Nominally pinned
12mmEPAB	869	8.7	semi-rigid	Nominally pinned
16mmEPAB	1741	10	semi-rigid	Nominally pinned
Connection	**Initial stiffness $S_{j,ini}$ (kNm/rad)**	**Moment Resistance $M_{j,Rd}$ (kNm)**	**Stiffness Classification**	**Strength Classification**
6mmEPSW	847	16	semi-rigid	partial strength
8mmEPSW	1046	19	semi-rigid	partial strength
10mmEPSW	1126	22	semi-rigid	partial strength
12mmEPSW	1272	25	semi-rigid	partial strength
16mmEPSW	1600	28	semi-rigid	partial strength

Table 7.1 Connection Classification According To Eurocode 3

7.4 Recommendations

The behavior of 6082 T6 aluminum bolts in these connections renders them un suitable in withstanding the substantial stresses developed, and as such the required strength and stiffness's characteristic of moment connections will be difficult to attain with their use particularly with column web stiffeners. The capacity of the class two 6082 T6 elements to withstand local buckling particularly in the compression flange is further clarified as all connections were restricted to end plate buckling and bolt failure modes. Particular attention must be paid to welding procedures of end plates to limit loss of mechanical properties. End plates thinner than the thickness of the column flange are characterized by less favorable strengths and as such could prove to be unsuitable if high connection strength is desired.

7.5 Future Research

The authenticity of the information obtained in this work can be further corroborated by the implementation of experimental work based on assembly geometry utilized. The area of aluminum connections remains relatively sparse in terms of research material. As such, there are endless possibilities and connection assemblies based on various aluminum sections of other classes available in the market to investigate. These results could provide an insight for designers to achieve optimum performance of aluminum connections based on relationships between geometry and connection stiffness, strength and ductility. The behavior of other classes of beam and column elements are worthy of investigation to document their performance. Simple connections in beam – column aluminum joints are also potential research areas as these have received little attention to date and as such could prove worthwhile.

REFERENCES

1. Bjorhovde, R., Brozetti, J., Colson, A., 1990.A Classification System for Beam to Column Connections. *Journal of Structural Engineering*, 116(11):3059-3076
2. Nethercot, D.A, Li, T.Q, Ahmed, B, 1998. Unified Classification System for Beam-Column Connections. *Journal of Constructional Steel Research*, 45(1): 39-65
3. SCI, BCSA. 2002. Joints in Steel Construction, Simple Connections. P212
4. Jaspart, J.P., Demonceau, J.F., 2008.European Design Recommendations for Simple joints in Steel Structures. *Journal of Constructional Steel Research,*64 822-832
5. BS 5950:Structural Use of Steelwork in Buildings; Part 1 1990
6. SCI, BCSA. 1995. Joints in Steel Construction, Moment Connections. P207/95
7. Swanson J, A, Leon RT. Bolted Steel Connections; Test on T- Stub Components. Journal of Structural Engineering ASCE 2000: 126(1): 50 – 6
8. Popov E. P, Shakhzod M, Takhirov. 2002. Bolted Large Seismic Steel Beam – Column Connections Part 1. *Engineering Structures*, 24 (2002) 1523- 1534
9. De Matteis, G, Mandara, A, Mazzolani, F, M., 2000. T Stub Aluminum Joints: Influence of Behavioral Parameters. *Computers and Structures*, 78 (2000) 311-327
10. Lazzarin, P, Milani, V, Quaresimin, M.1997. Scatter Bands Summarizing the Fatigue Strength of Aluminum Alloy bolted Joints. *International Journal of Fatigue,* Vol. 19.No. 5 pp. 401-407
11. UNI 8634-85."Strutture di leghe di alluminio. Istruzioni per il calcolo e la ascuzione"(in Italian), Milano, Italy 1985
12. Minguez, J, M Vogell, J. 2006.Effect of Toque Tightening on the Fatigue Strength of Bolted Joints. *Engineering Failure Analysis,* 13 (2006) 1410-1421
13. Mazzolani F. M., *Aluminum Alloy Structures*. Chapman & Hall, London 1995
14. Coelho A, M, Bijlaard, F. Experimental Behavior of High Strength Steel End-Plate Connections. *Journal of Constructional Steel Research*. 63 (2007) 1228-1240
15. Eurocode 9, Part 1-1, Design of Aluminum Structures 1999
16. Eurocode 3, Design of Steel Structures. Part 1-8, Design of Joints 1993
17. Malan S.F. Paterson A.E. "Aluminum Design Guide 1" South Africa : AFSA, 1989
18. De Matteis G., Mazzolani F.M, Panico S. "Experimental Tests On Pure Aluminum Shear Panels With Welded Stiffeners" Elsevier 2008

19. Aluminum Design Manual. *Aluminum Association*, Washington, DC, 8th Ed, January 2005

20. Menzemer, C.Ortiz, Morgado, R. Srivatsan, T.S. An investigation Into the Bearing Strength of Three Aluminum Alloys, Material Science and Engineering, A327(2002) 203 – 212

21. Wald F, Sokol Z, Moal M, Mazura V, Muzeau J.P., "Stiffness of Cover Plates With Slotted Holes". Journal of Constructional Steel Research. 60 (2004) 621 – 634

22. Kulak G.L, Fisher J.W, and Struik J. "*Guide to Design Criteria for Bolted and Riveted Joints*".2nd Ed., John Wiley & Sons, Inc., New York.(1987)

23 Krishnamurthy N. "A Fresh Look at Bolted End- Plate behavior and Design" Engineering Journal American institute of steel Construction, 15(2), 39-49.(1978)

24 American Institute of Steel Construction. "Allowable Stress Design Manual of Steel Construction" Chicago Ill. (1989)

25 Zoetemeijer P. A design Method for the Tension zone of Statically Loaded Bolted Beam to Column connections. Heron 1974; 20(1); 1-59.

26 Menzemer C.C,Fei L,Srivatsan T.S."Mechanical Response and Failure of Bolted Connection Elements in Aluminum Alloy 5083" *Journal of Material Engineering and Performance* (1998)

27 May J.E, Menzemer C.C. "Strength of Bolted Aluminum Tension Members" *Journal of Structural Engineering* (2005)

28 http://aluminium-offshore.com/our-business/helideck-support-frames

29 http://www.tfhrc.gov/pubrds/spring97/alum.htm

30 ADINA R&D Inc. "ADINA Theory and Modeling Guide", MA 024725, USA (2008)